Comprehensive Vibration Assessment Program for US-APWR Reactor Internals

Non-Proprietary Version

August 2011

Revision History

Revision	Date	Page	Description
0	December 2007	All	Original issued
1	April 2009	Chapter 1, 3 Appendix A,B,C,D,E	1. To reflect responses to Request for Additional Information No. 206-1576, 1577, 1578 and 1585 Revision 0 2. Composition of Chapter 3 was changed to correspond to the procedure in the validation of the analysis methodology, and add description to respond to the above RAI. 3. Replace the analysis results of the J-APWR SMT and US-APWR Prototype based on re-evaluated forcing functions for FIV and RCP loads. But the conclusion was not changed.
2	August 2011	1	Addition of related DCD section number after the RAI ID numbers reflected in Revision 1.
		2-3	2. Addition of new description about Revision 2 items.
		7	Revise the flow velocities in Table 2.1-1 reflecting the design progress.
		18	Revise Table 3.1.1-1 to reflect the additional use of Single Beam Model for the cross flow loads on upper plenum structures.
		19	Addition of the damping in Fig.3.1.1-1
		20-21	Revise the typical error of natural frequencies between the benchmark analysis and measured data based on Rev.2 results. Addition of the description about the bias errors and uncertainties.
		22	Natural frequencies in the benchmark analysis are revised from Rev.1 model to Rev.2 in Table 3.2.1-1.
		26-32	Natural vibration mode shapes in benchmark analysis are replaced in Figure 3.2.1-3 through 3.2.1-15
		36	Addition of description about the revise of cross flow loads considering with cross flow distribution.
		44	Replace the cross flow load forcing function time histories in Figure 3.2.2-8
		46	Discussion about the benchmark analysis response with the revised cross flow loads.
		47	1. Discussion about the validity of the downcomer forcing function was revised with Rev.2 analysis results. 2. Include the discussion about the validity of the modified cross

			flow forcing function.
2	August 2011	48	1. Table 3.2.3-1 was revised to include case A4 single beam model analysis with the upper plenum cross flow loads. 2. Table 3.2.3-3 was revised to reflect revised reference(7) and the analysis results with the upper plenum cross flow loads.
		51	Table 3.3.3-1 was revised based on Rev.2 analysis results.
		56,58-66	Natural vibration mode shapes in US-APWR analysis were replaced. Figure 3.3.1-6,3.3.1-9,3.3.1-10 and 3.3.1-12 through 3.3.1-19
		70	Cross flow loads in Figure 3.3.2-2 were replaced with the revise of cross flow loads considering with cross flow distribution.
		76	Refer to Appendix H related to RAI No.498-3782 Question 03.09.02-68.
		80	Table 3.3.2-7 was revised to include the RCP pulsation load amplitudes related to the blade passing frequency.
		88	1. Appendix-J was referred as the previous response to RAI 498-3782 Question 03.09.02-75 and RAI 614-4853 Question 03.09.02-90 the high cycle fatigue on Revision 1 analysis. 2. Discussion about the high cycle fatigue evaluation results was reflected with Rev.2 analysis results.
		90	Table 3.3.3-1 was revised to include case B7 single beam model analysis with the upper plenum cross flow loads.
		91-92	1. Table 3.3.3-2 , Table 3.3.3-3 and Table 3.3.3-5 were revised to reflect the US-APWR RMS responses of Revision 2 analysis. 2. Table 3.3.3-4 was revised to reflect the high cycle fatigue evaluation results based on Revision 2 analysis.
		93	Table 3.3.4-1 was revised to reflect the preoperational test sensor responses based on Revision 2 analysis.
		96	1. Table 3.4.1-1 was revised to reflect the fluid elastic instability evaluation based on the natural frequencies by Revision 2 analysis. 2. Table 3.3.4-2 was revised to reflect the vortex shedding Lock in evaluation based on the natural frequencies by Revision 2 analysis.
		97-98	Descriptions of acceptance criteria for stress due to FIV and RCP loads were modified.
		122	Summary of the non dimensional parameters in the Table A-2 was revised to reflect the design progress.
		125-129	Explanations about the turbulent force mapping in the downcomer were included in Appendix-B.

2	August 2011	138-146	Comparison of Reactor internals design between J-APWR and US-APWR were summarized in Appendix-F to include the previous response to RAI No.498-3782 Question 03.09.02-65 and Question 03.09.02-84.
		147-150	Discussion about the uncertainty of the structural model was described in Appendix-G to include the previous response to RAI No.498-3782 Question 03.09.02-66.
		151-152	Discussion about the uncertainty of the structural model was described in Appendix-H to include the previous response to RAI No.498-3782 Question 03.09.02-68.
		153-154	A sample of cross flow loads distribution on the upper plenum structures was shown in Appendix I.
		155-159	Discussion about the minimum margin of safety to the high cycle fatigue of the upper plenum structures was described in Appendix-J to include the previous response to RAI No.498-3782 Question 03.09.02-65 and Question 03.09.02-84.
		160-163	Assessment of the outlet nozzle leakage flow impact on the core barrel vibration was described in Appendix-K to include the response to RAI No.646-5065 Question 03.09.02-92.

Mitsubishi Heavy Industries, Ltd.
16-5, Konan 2-chome, Minato-ku
Tokyo 108-8215 Japan

Abstract

A comprehensive vibration assessment program for the US-APWR reactor internals is established in accordance with the United States Nuclear Regulatory Commission Regulatory Guide 1.20 Revision 3.

The US-APWR reactor internals represent a first-of-a-kind design in its size, arrangement and operating conditions, although its components are based on a well-proven 4-loop plant design with long operational experience. Therefore the first operational US-APWR reactor internals are classified as a Prototype in accordance with Regulatory Guide 1.20. After the first US-APWR is qualified as a Valid Prototype, subsequent plants will be classified as Non-Prototype Category I.

Based on its “Prototype” classification, a comprehensive vibration assessment program is established as summarized below:

- Alternating the stress levels of the reactor internals due to the flow induced vibrations are acceptably low in comparison with the limit for high cycle fatigue that is specified in the ASME Code.
- The difference in the reactor internals vibration characteristics, such as the natural frequency of the core barrel, is very small with or without the core. The vibration responses without the core are the same or slightly larger than those with the core. These are because of the flow rate increase with the elimination of the fuel assemblies and the subsequent pressure loss. Thus, in the preoperational test of the prototype plant, the results of vibration measurements after the core loading are bounded by the measurements before the core loading and only measurements before the core loading will be necessary.
- Measurements will be performed during the preoperational test to confirm the vibration characteristics and the structural integrity of the Prototype US-APWR reactor internals.
- The reactor internals of all US-APWR plants will be inspected before and after the hot functional test. The reactor internals will not be considered adequate and pass the comprehensive vibration assessment program unless no indication of harmful sign, abnormally large vibration amplitudes or excessive wear is detected.

A comprehensive vibration assessment program for the steam generator internals, the steam lines and the feed water lines are not included in this report.

Table of Contents

List of Tables

List of Figures

List of Appendixes

List of Acronyms

APWR	Advanced Pressurized Water Reactor
BMI	Bottom Mounted Instrumentation
CB	Core Barrel
CHT	Cold Hydraulic Test
FEM	Finite Element Method
FIV	Flow Induced Vibration
FSI	Fluid Structural Interaction
GT	Guide Tube
HFT	Hot Functional Test
ICIS	In-core Instrumentation System
IHP	Integrated Head Package
IST	Initial Start-up Test
LCSP	Lower Core Support Plate
LDP	Lower Diffuser Plate
LTP	Lower Tie Plate
MHI	Mitsubishi Heavy Industries
NR	Neutron Reflector
NRC	United States Nuclear Regulatory Commission
PSD	Power Spectral Density
RCCA	Rod Cluster Control Assembly
RCP	Reactor Coolant Pump
Re	Reynolds Number
RMS,rms	Root Mean Square
RV	Reactor Vessel
SMT	Scale Model Test
TSC	Top Slotted Column
UCP	Upper Core Plate
UDP	Upper Diffuser Plate
USC	Upper Support Column
UTP	Upper Tie Plate

1.0 INTRODUCTION

1.1 Background and Objective

A comprehensive vibration assessment program for the US-APWR reactor internals was established in accordance with the United States Nuclear Regulatory Commission Regulatory Guide 1.20 Revision 3 (Reference (1)).

The US-APWR reactor internals represent a first-of-a-kind design in its size, arrangement and operating conditions, although its components are based on a well-proven 4-loop plant design with many years of operational experience. Therefore the first operational US-APWR reactor internals are classified as a Prototype in accordance with the United States Nuclear Regulatory Guide 1.20 Revision 3 (Reference (1)). After the first US-APWR is qualified as a Valid Prototype, subsequent plants will be classified as the Non-Prototype Category I.

Based on its “Prototype” classification, a comprehensive vibration assessment program, consisting of four sub-programs, "Analysis, Measurement, Inspection and Evaluation”, was set up for the US-APWR. This document summaries these programs.

A comprehensive vibration assessment program for the steam generator internals, the steam lines and the feed water lines is not included in this report.

1.2 Description of Revision 1

The following modifications are included in Revision 1 of this report:

(1) To reflect the responses to the following RAIs on the DCD and Revision 0 of this Vibration Assessment Program Report.

  (a) RAI206-1576 (DCD 3.9.2.4)
  (b) RAI207-1577 (DCD 3.9.2.5)
  (c) RAI208-1574 (DCD 3.9.2.6)
  (d) RAI272-1585 (DCD 3.9.2.3)

(2) To reflect the latest analysis results including the following modifications after the completion of the Revision 0 analysis report

(a) Revision of the downcomer turbulent forcing functions based on the US-APWR test results

In Revision 0, measured data in the J-APWR scale model test was used for the forcing functions due to the downcomer flow turbulence. After the completion of Revision 0 of this report at the end of 2007, new data pertinent to the US-APWR configuration was obtained in the US-APWR Reactor Vessel Lower Plenum 1/7 Scale Model Flow Test (This test report has been submitted to NRC in

June of 2008 as MUAP-07022-P). MHI re-performed the analysis for the vibration assessment of the US-APWR with this new forcing function. The analysis result is reported in this Revision 1.

(b) Refinement of the vibration analysis caused by the RCP induced pressure pulsations

Two kinds of refinements were applied to the analysis of the vibration responses due to the RCP-induced pressure pulsations.

The first refinement was the re-evaluation of the RCP pulsation amplitude. In the Revision 0 analysis, the over all amplitude of the pressure fluctuation measured in the scale model test of the RCP for the APWR was applied. "Over all" means that the effect of local flow turbulence was included. In the Revision 1 analysis, the mean amplitude of the RCP pulsation was determined by additional study including spectral analysis of the generic RCP data. This was still conservative because the over all pressure pulsation generated by the APWR RCP is lower than that generated by the generic RCPs. As a result, the RCP pulsation amplitude was reduced to 1/5 of that in the Revision 0 analysis.

The second refinement was the justification in the time steps used in the time history analysis. The time increment was refined by an additional sensitivity study to simulate the maximum response. In the case of a perfect match of the structural modal frequency with the RCP induced pressure pulsation frequency (at the shaft rotation, blade passing frequency, BPF and higher harmonics of them), the vibration amplitude increased by a factor of 5 from that without this refinement.

As a combined result of the above two refinements, the vibration responses due to the RCP pulsation are about the same as those in Revision 0 of this report. Therefore, incorporation of the above two modifications has no impact on the conclusions in the assessment of the structural integrity and in the vibration measurement plan in Revision 0.

1.3 Description of Revision 2

The following changes are included in Revision 2 of this Report.

(1) Include Additional information in RAI responses on Revision 1 Report.

(a) RAI No.498-3782 Question 03.09.02-65 and Question 03.09.02-84
Comparison of Reactor internals design between J-APWR and US-APWR were summarized in appendix-F.

(b) RAI No.498-3782 Question 03.09.02-66:
Discussion about the uncertainty of the structural model was described in Appendix-G.

(c) RAI No.498-3782 Question 03.09.02-68:
Discussion about the uncertainty of the RCP pulsation loads were described in Appendix-H.

(d) RAI No.498-3782 Question 03.09.02-75 and RAI No. 614-4853, Question 03.09.02-90
The discussion about the minimum margin of safety to the high cycle fatigue of the upper plenum structures was included in 3.3.3.2(2) b and Appendix-J.

(e) RAI No.646-5065 Question 03.09.02-92:
Assessment of the outlet nozzle leakage flow impact on the core barrel vibration was described in Appendix-K

(2) Reflect the latest analysis results including the following modifications after the Revision 1 analysis report.

(a) The cross flow induced vibration loads on the upper plenum structures are modified by considering with the cross flow velocity distribution in the elevations for the practical analysis conditions. For this modification of the forcing function, the validation process with the benchmark analysis of the J-APWR 1/5 Scale Model Test was repeated. In this process, revise of the measurement response in Reference (7) was reflected.

(b) In the process of the US-APWR prototype analysis, refinements of the FE model were reflected. In this refinement, the correction of the damping by eliminating of dashpot elements APWR system model analysis.

As the results, the margin of safety of high cycle fatigue was improved for upper plenum structures.

2.0 CLASSIFICATION OF REACTOR INTERNALS

2.1. Design Differences and Effects on Flow Induced Vibrations

The general design concept of the APWR is based on the current 4-loop, 193-fuel assembly plants, which have many years of operating experience both in the United States and in Japan. However, the core of the APWR was designed to an accommodate 257 fuel assemblies. The US-APWR, with its 14-foot core, is a variant of the 12-foot core of the J-APWR developed for the Japanese utilities. As discussed in Appendix-A and Appendix-F, the vibration characteristics of the US-APWR is similar to those of the J-APWR, the flow induced vibration of which has been verified in a scale model test. At this point there is no operational experience in any of the J-APWR plants. Therefore, the design differences and its effect on the flow induced vibration are discussed with reference to the current 4-loop plants, for the purpose of assessing the flow induced vibration characteristics of the US-APWR reactor internals, in the following Subsection.

2.1.1. General Arrangement

The design concept of the US-APWR reactor internals is a normal evolution from the current 4-loop plant. Comparisons of the reactor vessel and internals between the US-APWR and the current 4-loop plant are shown in Figure 2.1-1. The general assembly of the US-APWR reactor internals is shown in Figure 2.1-2. The US-APWR reactor internal components are evolved from the well-proven 4-loop plant design currently operating in the United States and Japan. The differences are as follows;

- Design: The neutron reflector instead of the baffles to form the core cavity
- Size: increases in the diameters of the reactor vessel, the core barrel and the secondary core support assembly.
- Arrangement: The RCCA guide tubes and the upper support columns in the upper plenum
- Operating conditions: increase in the flow rate

The flow induced vibration characteristics of the US-APWR reactor internals are discussed and compared with the current 4-loop plant in as follows.

2.1.2. Flow Conditions

Flow paths in the US-APWR reactor as shown in Figure 2.1-3 are similar to those in the current 4-loop plant. Both the total flow rates and the areas of flow paths in the vessel downcomer and the lower plenum of the US-APWR reactor are increased by about 30% from those in the current 4-loop plant. In the upper plenum, the diameter of the upper core support is increased by about 20% from that of the current 4-loop plant but the height of the upper plenum is maintained. Therefore, the cross-flow area is increased by about 20% from that of the current 4-loop plant. Because the flow rate is increased by about 30%, the rated cross-flow velocity is about 10% higher than that in

the current 4-loop plant. Comparisons between typical flow velocities during normal operation with the current 4-loop plant are shown in Table 2.1-1.

2.1.3. Lower Reactor Internals

The Lower Reactor Internals Assembly is shown in Figure 2.1-4.

(1) Core Barrel / Lower Core Support Plate

The diameter of the core barrel of the US-APWR is about 20% larger than that of the current 4-loop design in order to accommodate an increase in the numbers of fuel assemblies from 193 to 257 to obtain a larger thermal output. The neutron reflector is a new component consisting of the solid metal blocks instead of the baffle structures in the current 4-loop plant.

The core barrel stiffness is designed taking into consideration the included mass of the neutron reflector and the fuel assemblies to maintain the vibration characteristics of the current 4-loop plant. The bending stiffness of the core barrel is approximately twice that of the current 4-loop design and the vibratory response is estimated to be lower than that of the current 4-loop plant. The diameters of the core barrel and the lower core support plate are increased from those in the current 4-loop plants. This will affect the excitation force and the vibration characteristics of the lower internals assembly.

(2) Neutron Reflector / Tie Rod

Instead of the baffle structures, a new component, the neutron reflector consisting of the perforated metal blocks, forms the core cavity.

(3) Lower Plenum Structures

The diffuser plate assemblies are placed in the lower plenum of the US-APWR. These assemblies are consisted of two ring plates and the support columns connecting to the lower core support plate. These constructions are similar to the tie plates and the bottom mounted instrumentation column used in the current 4-loop plant.

From the view point of the flow induced vibrations, the main source of excitation is the cross-flow on the support columns. The cross-flow velocities in the lower plenum are the same as those in the current 4-loop plant. Because the shape of the reactor vessel lower plenum is semi-spherical, the support column is longer and the natural frequency of the assemblies is slightly lower but the diameter of the support column is much larger. As a result, the reduced velocity (U/fn D, where U is the flow velocity, fn is the fundamental frequency, and D is the diameter of the column), a key dimensionless parameter for the flow induced vibration assessment, is reduced by 30% from that of the current 4-loop plant. Thus sufficient margin of safety in the cross-flow induced vibration such as the fluid elastic instability is maintained.

2.1.4. Upper Reactor Internals

The Upper Internals assembly is shown in Figure 2.1-5.

The US-APWR upper internals design is based on the “Inverted top hat type upper internals” used in the current 4-loop plant. The diameter of the upper core support is enlarged by about 20% from that of the current 4-loop design as in the core barrel. The axial length remains the same as that in the current 4-loop plant.

The main source of the flow induced vibration excitation is the cross-flow on the column structures such as the lower RCCA guide tube and the upper support column.

The diameter of the upper core support is increased by about 20% from that in the current 4-loop plant but the height of upper plenum is maintained, resulting in an increase of the cross-flow area near the outlet by about 20% from that in the current 4-loop plant. Because the flow rate is increased by about 30%, the rated cross-flow velocity in the upper plenum is about 10% higher than that in the current 4-loop plant,

(1) Upper Support Column (Standard Type)

The fundamental modal frequency of the upper support column is the same as that in the current 4-loop plant because the basic dimensions are not changed.

(2) Top Slotted Column

The top slotted column is another type of the upper support column located the core periphery, with the lager diameter and higher natural frequency than the standard type. With a stiffer body and smaller reduced velocity (U/fn D), the top slot column has improved the margin against cross-flow induced vibration compared with the standard type upper support column.

(3) Upper Core Support / Upper Core Plate

The diameters of the upper core support and the upper core plate are increased from those of the current 4-loop plant. This will affect the vibration characteristics of the upper internals assembly.

(4) RCCA Guide Tube

The RCCA guide tube design in the US-APWR has been changed from that of the current plants in the following aspects:

- Adoption of a square pipe for the lower guide tube enclosure,
- Extension of the upper guide tube height to fit the extended RCCA travel length for the 14ft core.

But the stiffness, width and length of the lower guide tube which is subject to the cross-flow in the upper plenum, are the same as those in the current 4-loop plant. Therefore any change in the fundamental modal frequency is negligible.

Table 2.1-1 Comparison of Typical Flow Velocities between the US-APWR and the Current 4-loop Plant

	Typical Flow Velocities (ft/s)		Ratio
	US-APWR	Current 4-loop	
Vessel Inlet Nozzle			
Down Comer			
Lower Plenum(1)			
Core			
Upper Plenum(2)			
Vessel Outlet Nozzle			

(1) Assumed same in the down comer
(2) Maximum velocities of the RCCA guide tube location considering blockage factor
(3) Values in ( ) are velocities at the neutron panel areas.

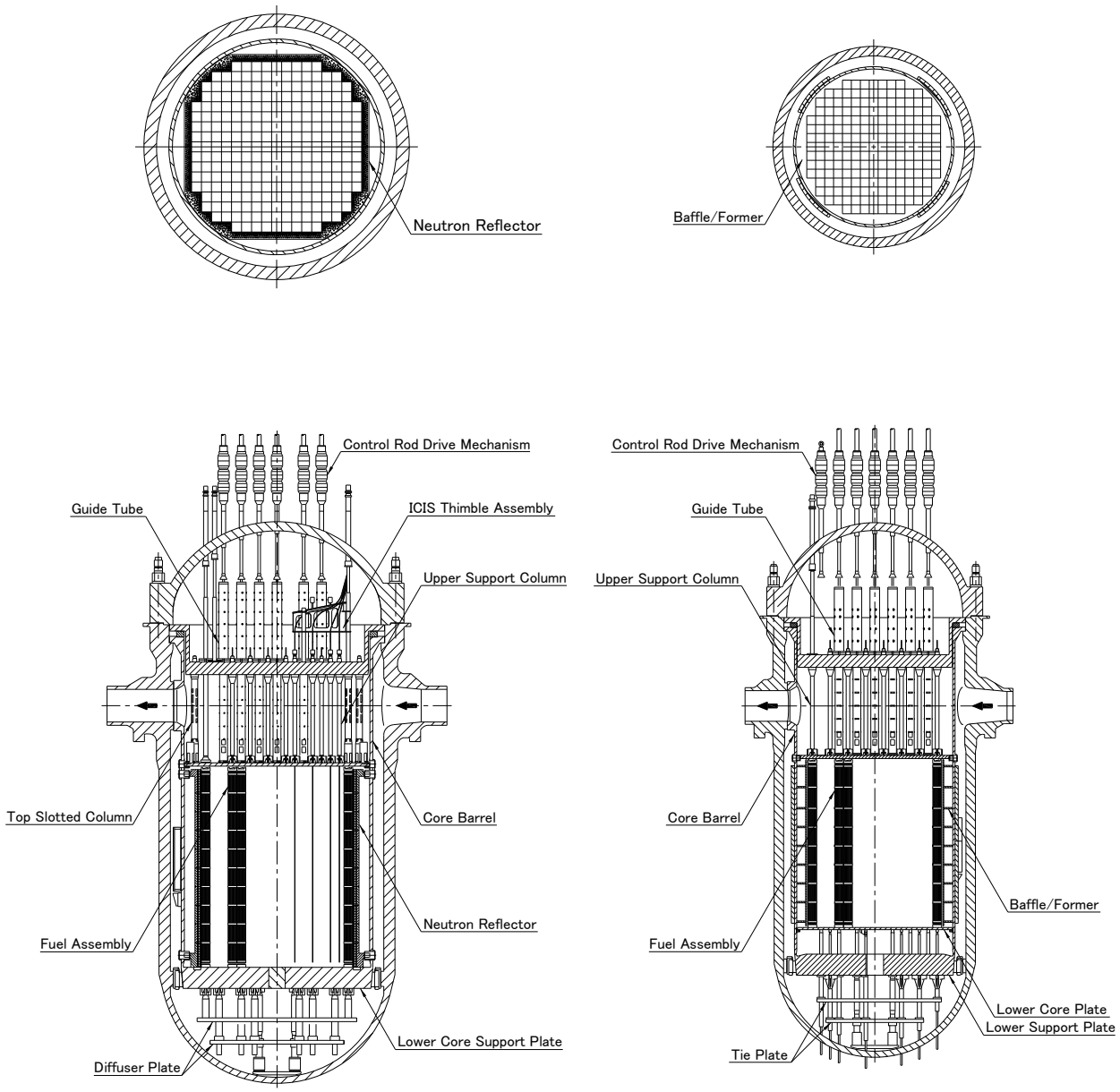

Figure 2.1-1 Comparison between the US-APWR and the Current 4-loop Reactor

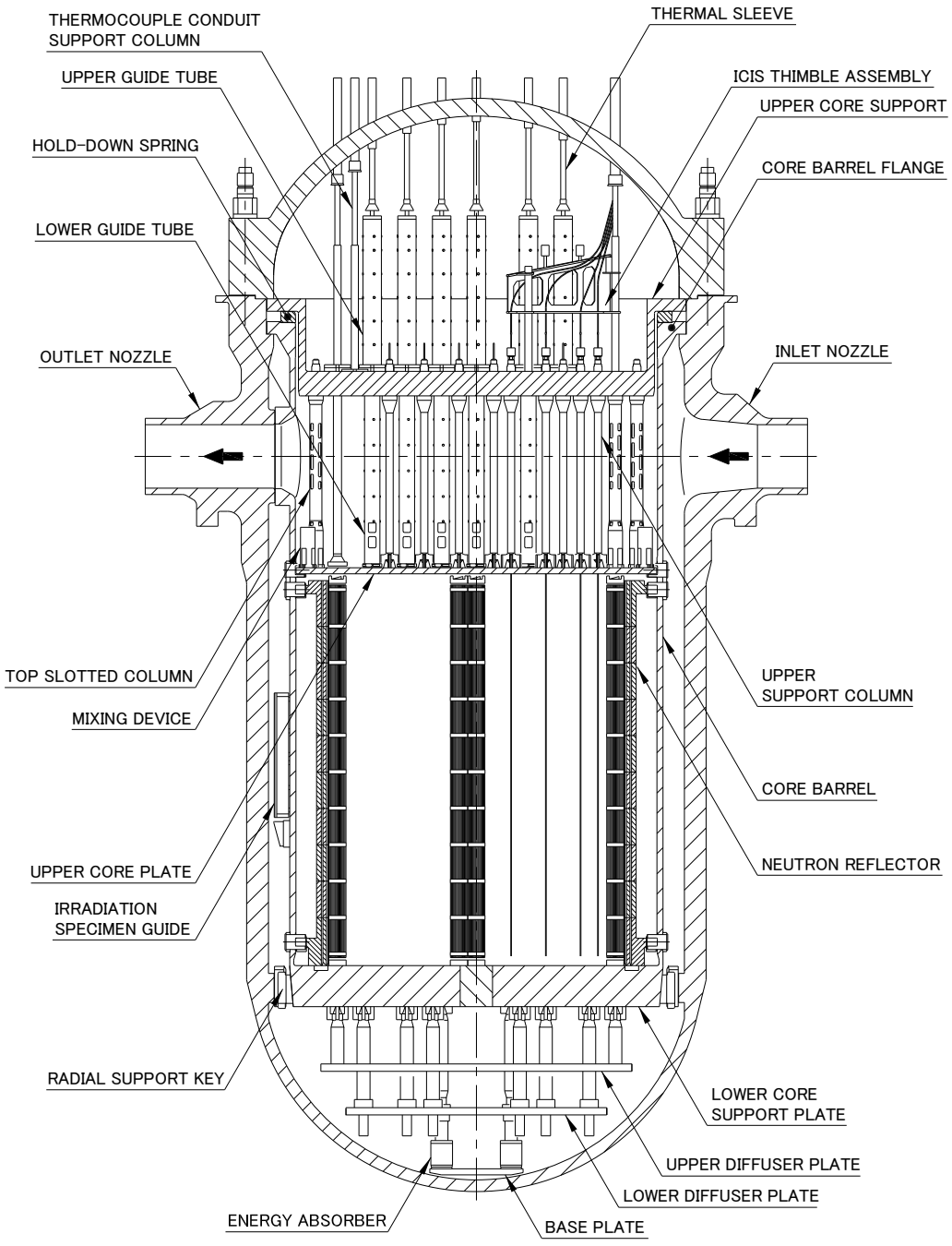

Figure 2.1-2 Reactor Internals General Arrangement

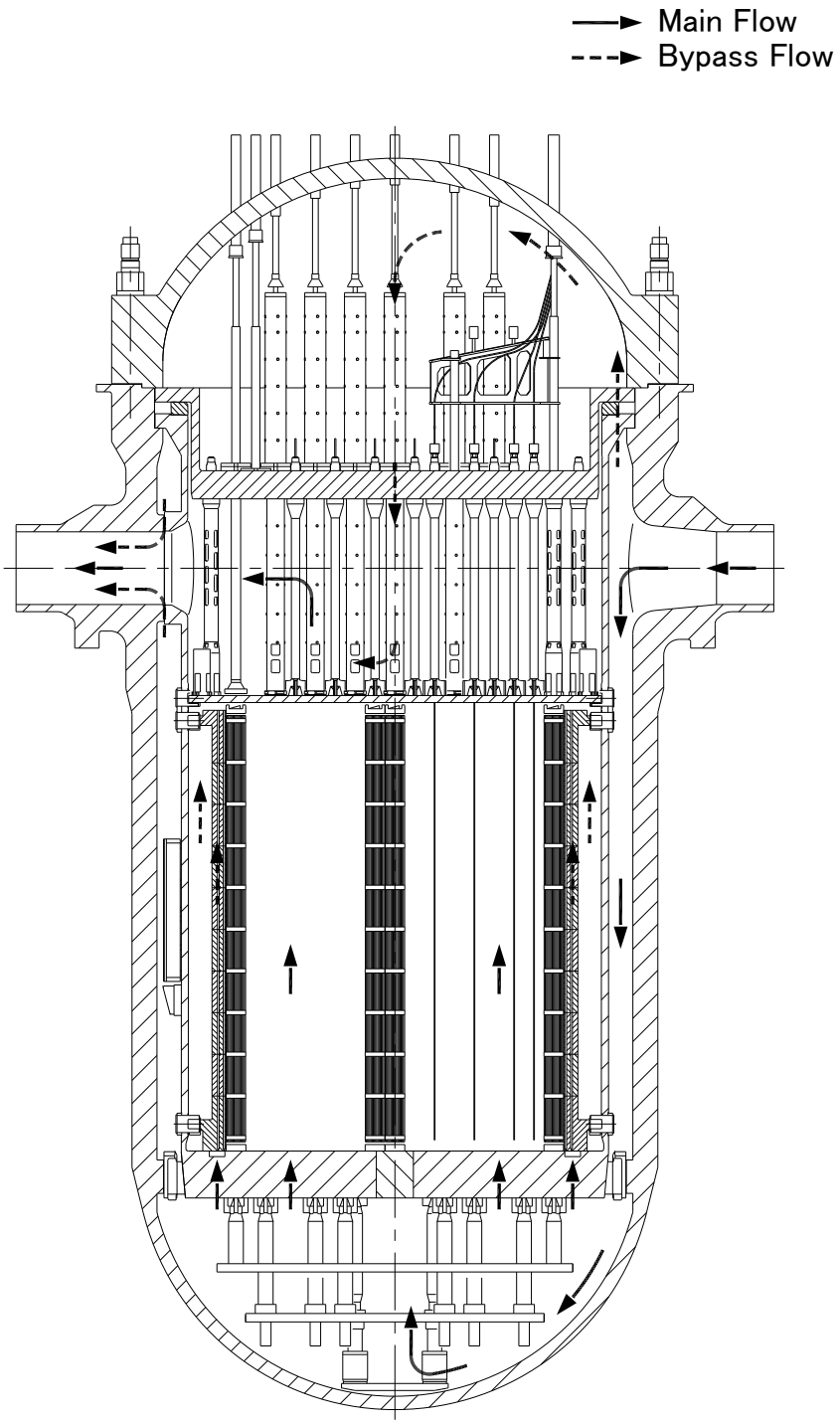

Figure 2.1-3 Reactor Internals RCS Flow and Bypass Flow Paths

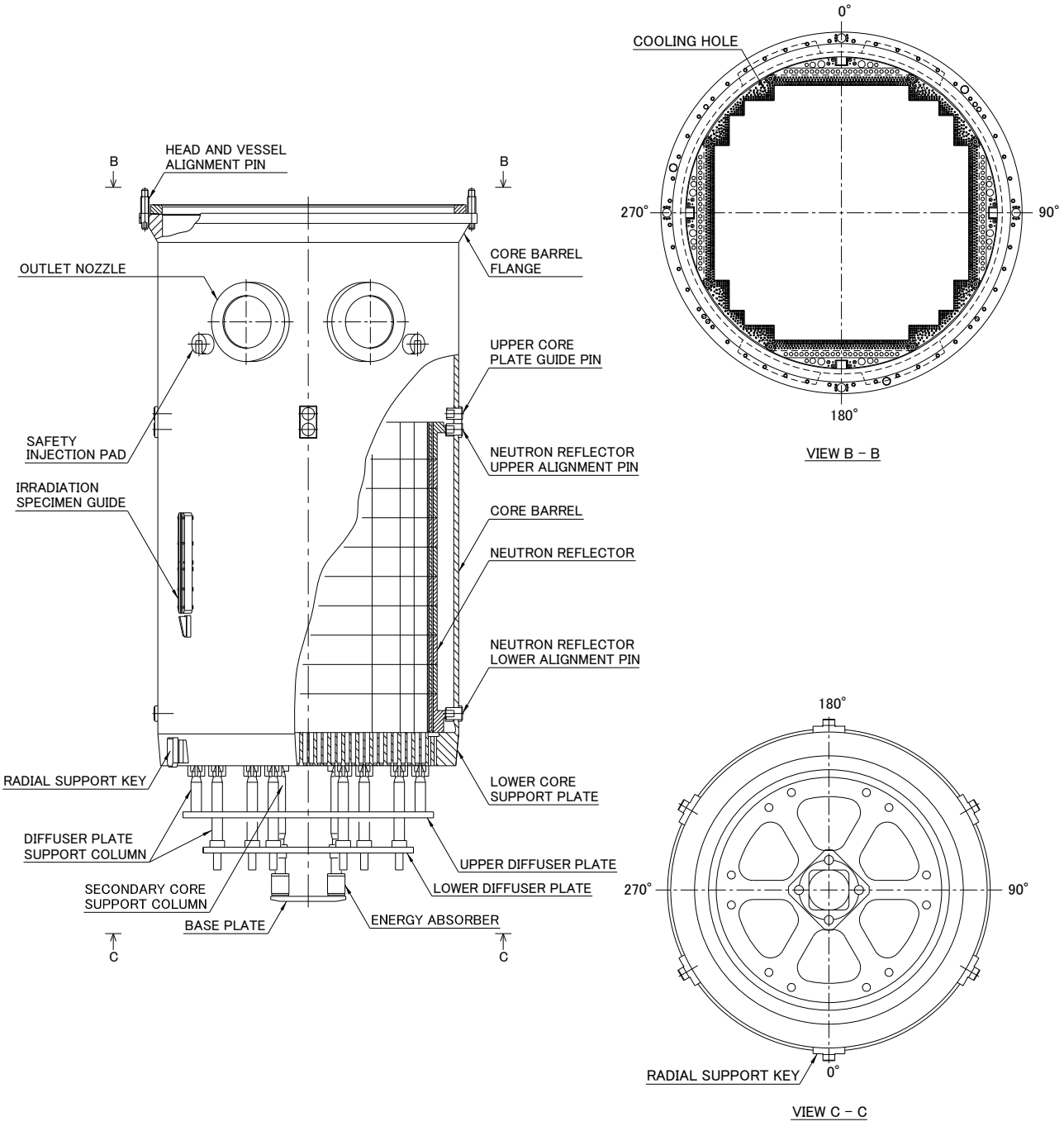

Figure 2.1-4 Lower Reactor Internals Assembly

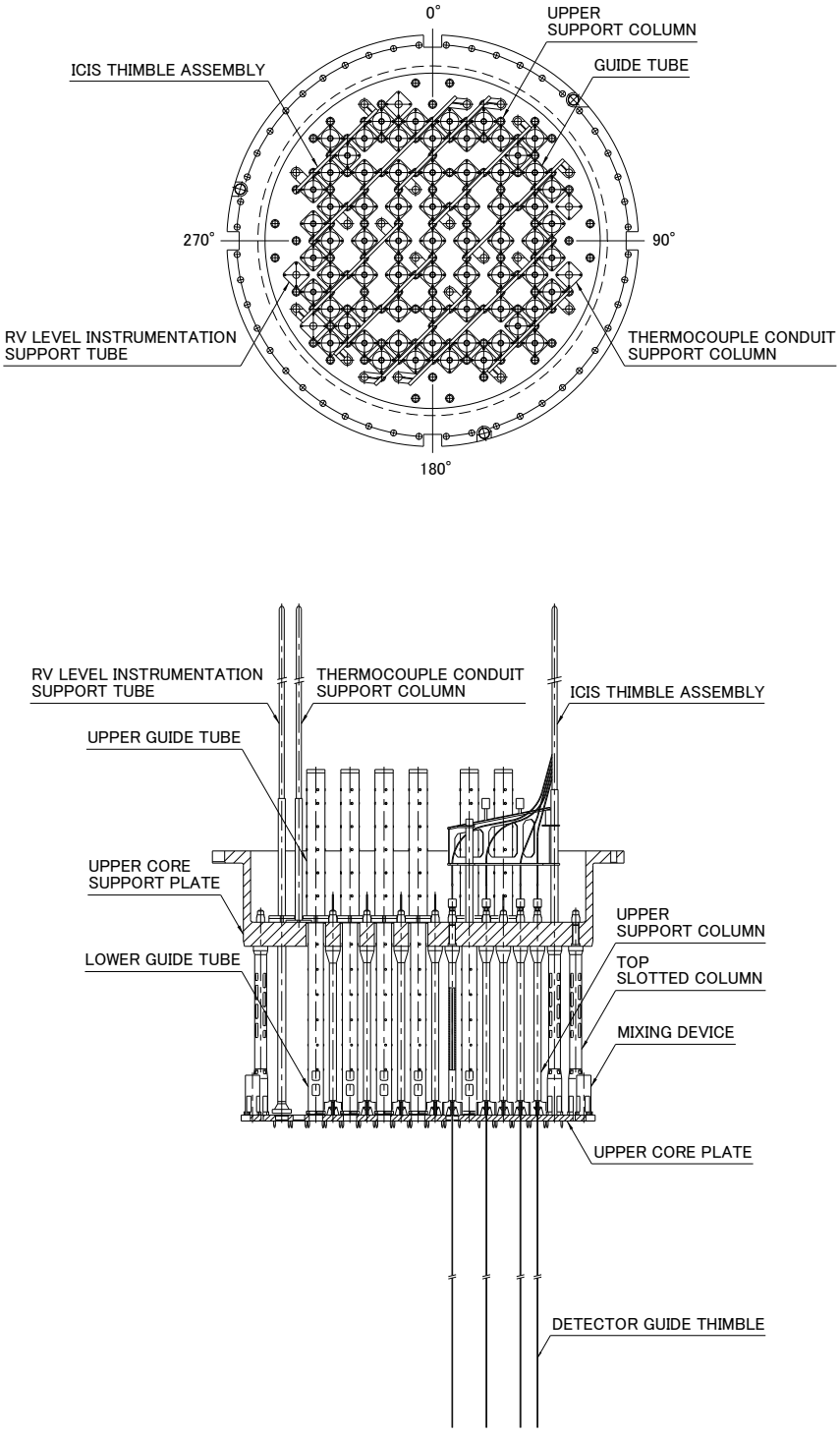

Figure 2.1-5 Upper Reactor Internals Assembly

2.2. Classification of Reactor Internals in Accordance with the Comprehensive Vibration Assessment Program

2.2.1. The first plant

The US-APWR reactor internals represent a unique, first-of-a-kind design because of its design, size, arrangements and operating conditions. Therefore, the first US-APWR will be classified as a Prototype in accordance with Regulatory Guide 1.20 Rev.3 (Reference (1)).

2.2.2. Subsequent plants

Upon qualification of the first US-APWR as a valid prototype, subsequent plants will be classified as Non-Prototype Category I.

3.0 VIBRATION AND STRESS ANALYSIS PROGRAM

In this section, the prediction analysis of the flow induced vibration response and stress of the US-APWR reactor internals are reported. At first, the procedure of the analysis is described in Subsection 3.1. Verification of the analysis method through a benchmark analysis the scale model used in the flow test is described in Subsection 3.2. The analysis results and evaluations for the US-APWR reactor internals and the predicted vibration responses under the hot functional test condition are also included are discussed in Subsection 3.3. The design margin for the adverse flow effects are discussed in Subsection 3.4 and the acceptance criteria for comparison between the analysis results and test data are given in Subsection 3.5.

3.1. Analysis Method

3.1.1. Analysis Procedure

Figure 3.1.1-1 shows the flowchart for the flow induced vibration analysis of the US-APWR reactor internals. The analysis consisted of the following two tasks. Table 3.1.1-1 shows three kinds of FE models used for the FIV response analysis in the following two tasks.

Task 1: Verification of the vibration analysis methodology

The verification of the vibration analysis methodology was demonstrated using the results of the J-APWR reactor internals 1/5 scale model flow test (J-APWR 1/5 SMT) as described in Reference (7).

The J-APWR 1/5 SMT was conducted using a 1/5 scale model that simulated the reactor vessel and the reactor internals of the 12 ft-core APWR (J-APWR). In this test, the vibration characteristics of each component, the pressure fluctuations due to the flow turbulence, and the vibration responses were measured (Reference (7)). The test was performed under the ambient temperature and pressure.
Comparisons of the dimensionless parameters between the J-APWR SMT and the US-APWR plant are discussed in Appendix-A. The J-APWR and the US-APWR of MHI APWR series have the same basic structure such as the reactor vessel, the core barrel, the neutron reflector and the upper reactor internals and similar flow rates. On the other hand, they differ from each other in the following aspects:

- Increasing fuel effective length from 12ft (J-APWR) to 14ft in the US-APWR.
- Change in the upper plenum structure array by inserting an ICIS detector from the top of the reactor vessel.
- Simplification of the structure in the lower plenum by eliminating the Bottom Mounted Instrumentation (BMI).

Therefore, the benchmark analysis of the J-APWR SMT is appropriate for the verification of the analysis methodology due to their similar flow vibration characteristics.

An alternative way of validating the analytical method is to use an operating plant as a benchmark and compare the calculated vibration responses with the field test data. MHI however, does not believe this is a better way of validation due to the following reasons.

- The vibration characteristics of the US-APWR reactor internals are close to those of the J-APWR rather than to the current 4-ioop plant, as discussed in Appendix - A.
- This method cannot be applied to fist-of-a-kind design with the significantly different dimensions or configurations, such as the neutron reflector or the core barrel.

All properties in the benchmark analysis model (the J-APWR SMT model) were adjusted to 1/5 scale. The structural model of the reactor internals was developed based on the full scale J-APWR drawings and scaled down following the scaling laws for each parameter. The stiffness of the test vessel support in the J-APWR SMT analytical model, which was not intended to simulate the vessel support stiffness in the J-APWR plant, was determined based on the measured natural frequency in the tapping test.

Two finite element (FE) models, a 3D solid system model and a 3D beam system model- were made. The modal analyses were carried out to check the validity of the structural model by comparing the computed natural frequencies with the measured frequencies in the J-APWR SMT.

The forcing functions were generated and input into the FE models, and the vibration response analyses were conducted. The computed responses of the reactor internals for the J-APWR SMT were compared with the measured values to verify the analysis methodology and the forcing function derivation. If the difference between a calculated response and measured one is not acceptable, the forcing function relate to the response should be corrected.

Task 2: US-APWR Response Analysis

The FE models of the US-APWR prototype reactor internals were constructed in the same manner as the model for the J-APWR 1/5 scale model. All properties in the US-APWR prototype analysis model were developed to a full scale, based on the US-APWR drawings. The stiffness of the reactor vessel support and primary coolant loops in the US-APWR analytical model was simulated to the actual plant. In addition, two kinds of the 3D beam elements were used to simulate the Control Rod Drive Mechanism (hereafter CRDM) and Integrated Head Package (IHP). The latter supports the structure of the CRDM. These were added at top of the reactor vessel model.
The forcing functions for the US-APWR were modified taking into consideration the differences between the J-APWR and the US-APWR in the dimensions, flow rate, fluid temperature and mass density, elasticity of the material and so on. The details of the conversion for the flow induced vibration forcing functions from the J-APWR 1/5 SMT to the US-APWR prototype conditions are described in Appendix-B and C. In addition, the forcing function due to the RCP induced pressure pulsation in the US-APWR was included in the analysis.
The analysis results were used to predict the responses, such as displacements, strains and accelerations, at the transducer locations and to confirm the structural integrity against high cycle fatigue in each component.

3.1.2. Structural Modeling

As described in Subsection 3.1.1, after verifying the methodology with the benchmark analysis of the J-APWR 1/5 SMT (Task-1), this same methodology of the structure modeling was applied to the full-scale US-APWR (Task-2). The same calculation procedure and the finite element codes used in Task 1 were also used in Task 2. Here, outlines for the modeling of the J-APWR SMT and the US-APWR are described. In the benchmark analysis of the J-APWR model, the model geometry data and physical properties were based on the dimensions and materials of the 1/5 SMT and under ambient conditions. On the other hand, the materials, coolant properties and flow rates corresponding to the general drawings of the reactor components and temperature under the actual operating conditions were inputted in the full-scale US-APWR model.

(1) FEM Code and Analysis Scheme

ANSYS computer code version 11.0 was used in the constructing all structure models for this analysis. The finite elements types such as solid, shell and beam elements used in this analysis, including the fluid element, have been verified by the benchmark analyses of simple problems and comparing the results with the theoretical values, and in the benchmark analysis of the J-APWR 1/5 SMT.

The direct time integration method was used in all vibration response analysis because of the non-linearity of the fluid element.

(2) FE Model

Three FE models were used as summarized in Table 3.1.1-1. Two kinds of system models, the 3D solid system model and the 3D beam system model were used in both the benchmark analysis of the J-APWR SMT and in the prediction analysis of the US-APWR. The third FE model was the single beam model which the simulated individual components in the upper plenum of the US-APWR

a. 3D solid system model

The reactor vessel, the core barrel and the neutron reflector form a triple co-axial system with fluid coupling between them. To compute the beam and shell mode responses of this system, the core barrel and the neutron reflector were modeled with the solid elements. The 3D-Fluid elements were used to simulate the fluid structural interaction (FSI) between the reactor vessel and the core barrel, and between the core barrel and the neutron reflector. And the reactor vessel wall was simulated with the shell elements.

The beam mode natural frequencies of the core barrel and the neutron reflector, obtained from the 3D solid element model, were used to determine the added mass matrices in the 3D beam and shell element models discussed below.

b. 3D beam system model

The 3D beam element system model consisting of the reactor vessel and the entire reactor internals was used to evaluate the fundamental beam mode responses to the flow loads and the RCP pulsation loads. The shell element was used only for the diffuser plates with this model. This model had beam elements for the CRDM and the IHP to simulate the proper vibration characteristics of the reactor vessel. The nodal point degrees of freedom and the damping ratios of the reactor internals and the surrounding structures were selected such that the most dominant frequencies were represented in the flow induced vibration and seismic-LOCA response. This formed the basis for establishing any directional decoupling and the system structural partitioning in the model.

To simulate the fluid structure interaction, the hydrodynamic mass matrices at the following three locations were included.

(a) Between the RV and the core barrel (CB) in two horizontal directions

(b) Between the CB and the neutron reflector (NR) in two horizontal directions

(c) Between the upper core support (UCS) and the RV head in the vertical direction

The mass properties in the horizontal directions, (a) and (b) above, were determined to simulate the beam mode natural frequencies obtained in the 3D solid element model. The mass property in the vertical direction (c) was derived from a hand calculation. The 3D beam and shell element model were also applied to LOCA and seismic analyses with the different boundary conditions which were justified for the larger responses.

c. Single beam element models

The single beam models for the upper plenum structures such as the GT, USC and TSC were used to the response analysis due to the cross flow load or the RCP pulsation. In case for the RCP pulsation loads, a higher mode natural frequency correspond to the RCP pulsation related to the blade passing frequency (NZ) or its second harmonics (2NZ) was simulated. If an estimated natural frequency of the vibration mode was within 10% of the NZ or 2NZ of the RCP, the natural frequency was adjusted to coincide with the NZ or 2NZ. This was to ensure conservative results in the analysis.

(3) Force loading on the model

The combination of the analysis model types and the forcing functions are summarized in Table 3.1.1-1. Each of the forcing function was generated as a time history of a distributed load. For example, the downcomer forcing functions for the 3D solid system model were determined as the force per unit area and applied to all of the elements surface of the core barrel and the inner surface of the reactor vessel. Vertical loads on the core support plates were applied in the same manner.

The forcing functions on the beam elements, such as the cross flow loads in the upper plenum were determined as the force per unit length and applied as the distributed element loads. The downcomer forcing functions on the core barrel and on the reactor vessel in the 3D beam and shell element model were applied in the same manner.

Table 3.1.1-1 FE Models Used for FIV Response Analysis

	RV/CB/NR Solid Model	Beam System Model	Single Beam Model (GT / USC / TSC)
Applied Elements	Solid + Fluid Element	Beam + Shell	Single Beam
Output	1. CB / NR beam and shell mode natural frequency with FSI 2. CB / NR beam / shell mode response	1. Beam mode and vertical mode frequency with FSI 2. RV and reactor internals beam response due to flow turbulence and RCP pulsation	1. Higher beam modal frequencies 2. Response to cross flow and RCP pulsation harmonics
Target Frequency Range			
Forcing Functions			
Flow Induced (Downcomer) (Lower Plenum) (Upper Plenum) (Vertical)			
RCP Pulsation (Downcomer) (Upper Plenum) (Vertical)			

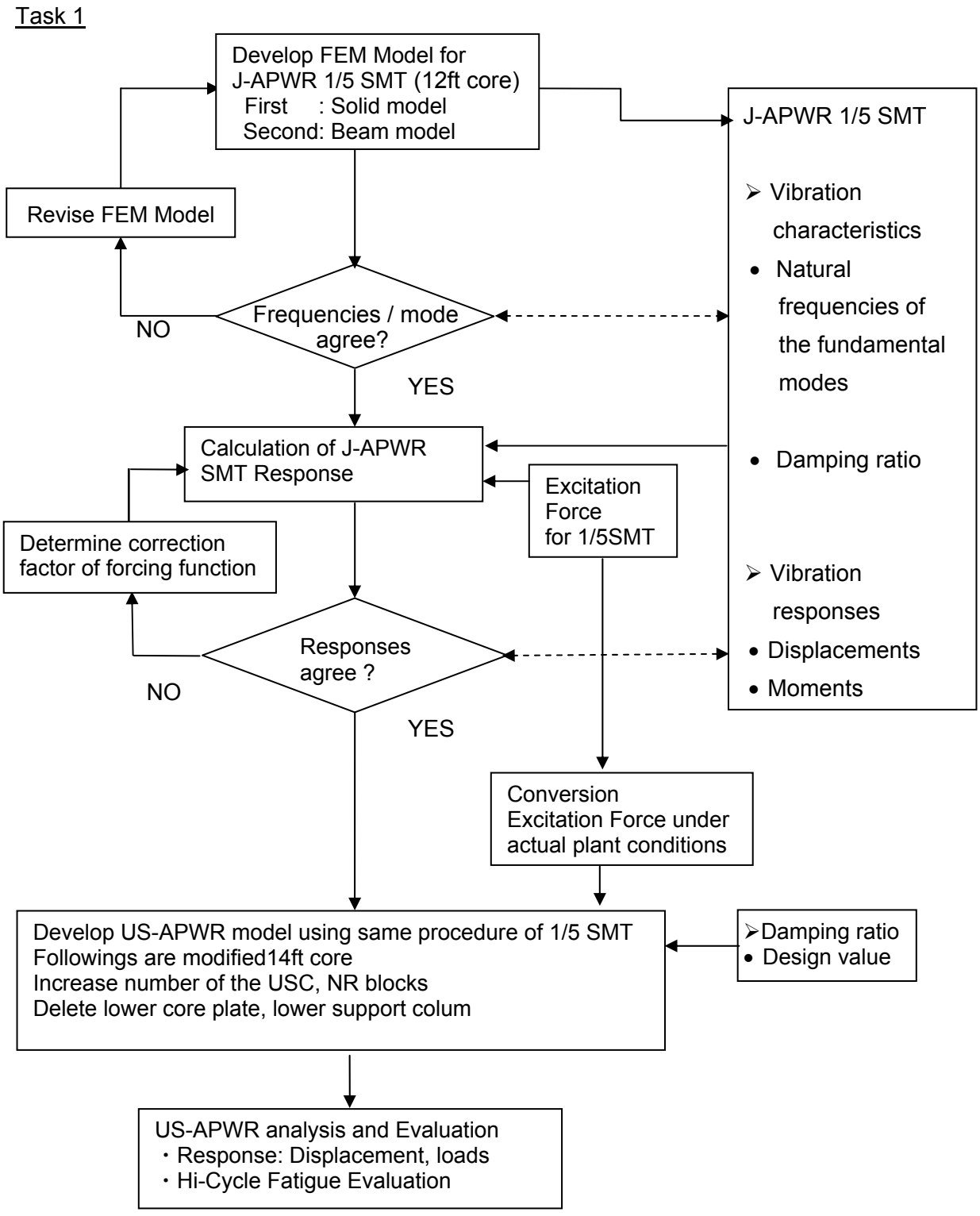

Figure 3.1.1-1 US-APWR Reactor Internals FIV Response Analysis Procedure

3.2. Verification of the vibration analysis methodology

Following the Task 1 procedure as described in 3.1.1, the vibration analysis methodology was verified by carrying out an analysis using the J-APWR 1/5 scale model as a benchmark and then comparing the computed results with the corresponding measured values in the J-APWR 1/5 SMT, as identified in Chapter 8 of Reference (7).

3.2.1. Validation of Structural Models

The J-APWR SMT was conducted using a 1/5 scale model that simulated the reactor vessel and the reactor internals of the 12 ft-core APWR (J-APWR). The test was performed under ambient temperature and pressure. In this test, the vibration characteristics of each component, the pressure fluctuations due to the flow turbulence, and the vibration responses were measured.

(1) Benchmark model analysis

As described in Subsection 3.1.2 (2), two different system models, the 3D solid system model (Figure 3.2.1-1) and the 3D beam system (Figure 3.2.1-2) were used to simulate the scale model test.
All properties of the benchmark analysis model in the J-APWR SMT were adjusted to a 1/5 scale. The structural model of the reactor internals was developed based on the full scale J-APWR drawings and scaled down following the scaling laws for each parameter. The stiffness of the test vessel support, which did not simulate the vessel support stiffness of the actual plant, was determined based on the measured natural frequency in sine wave vibration test. A modal analysis was carried out to check the validity of the structural model by comparing the computed natural frequencies with measured ones.

(2) Natural Frequencies of J-APWR 1/5 SMT

a. Results

The natural frequencies of the J-APWR 1/5 SMT are shown with the J-APWR SMT results in Table 3.2.1-1. Typical mode shape of the neutron reflector and core barrel in the lower reactor internals, and the lower and upper diffuser plate support column in the lower plenum are shown in Figures 3.2.1-3 through 3.2.1-12.

b. Uncertainties and bias errors of FE Model and analysis

A typical value of the uncertainties and bias errors of the structural natural frequencies was [ ] %, which was obtained from averaging the errors in a total of 12 pairs of the natural frequencies as shown in Table 3.2.1-1.

The effect of the [ ] % error in the structural natural frequencies on the vibration response was estimated by considering the mode shapes and the frequency response functions.
It lead to [ ] % error in the random vibration response, with a conservative assumption that the [ ] % error in the natural frequency was totally caused by the uncertainty in the stiffness of structures. However the error in the mass of the model had little effect in the vibration response.

c. Validity of Structural Models

The validity of the FE structural models were evaluated from the correlation of measured results and the frequency analysis results based on the 1/5-scale model. Category 2 acceptance criteria described in Subsection 3.5 were applied as follows.

- Natural frequency for the fundamental beam mode and the lowest shell mode: with in 10%.

The results in Table 3.2.1-1 show the beam mode and the shell mode natural frequencies of the core barrel and the neutron reflector with the 3D solid system model were within the 10% criterion. The beam modes of these structures in the 3D beam system model with the added mass matrices also satisfied this criterion.

And the beam mode frequencies of the structures in the lower plenum or the upper plenum for the 3D beam system model were also within the 10% criterion except the [ ] % for the top slotted column and [ ] % for the RCCA guide tube. As for the RCCA guide tube, the analysis result is rather reliable than the measured one because of the uncertainties to simulate the support condition with the alignment pins in a scale model. For the lower tie plate assemblies, the analysis model was refined to simulate all columns with the beam elements and the tie plate with the shell element for the US-APWR, as discussed in Subsection 3.3.1.

Therefore, the FE modeling methodology confirmed that the physical properties and fluid elements of the structure are appropriately modeled, and can be used for the calculation of vibration response of the reactor internals.

(3) Bias errors and uncertainties

Additional information in the response to RAI 498-3782 Question 03.09.02-66 is attached as Appendix G about the validation of the analysis model including the discussion of the bias error and uncertainties.

Table 3.2.1-1 Comparison of Frequencies with Test Results (J-APWR 1/5 SMT)

	Vibration Mode		Fundamental Modal Frequency (Hz)	
			Analysis	Measured
Core Barrel	Beam			
	Shell	n=2		
		n=3		
		n=4		
Neutron Reflector	Beam			
	Shell	n=2		
		n=2,diagonal		
		n=3		
		n=4		
Lower Tie Plate Assembly	Transverse			
Upper Tie Plate Assembly	Transverse			
RCCA Guide Tube (Lower Guide Tube)	Beam			
Upper Support Column	Beam			
Top Slotted Column	Beam			

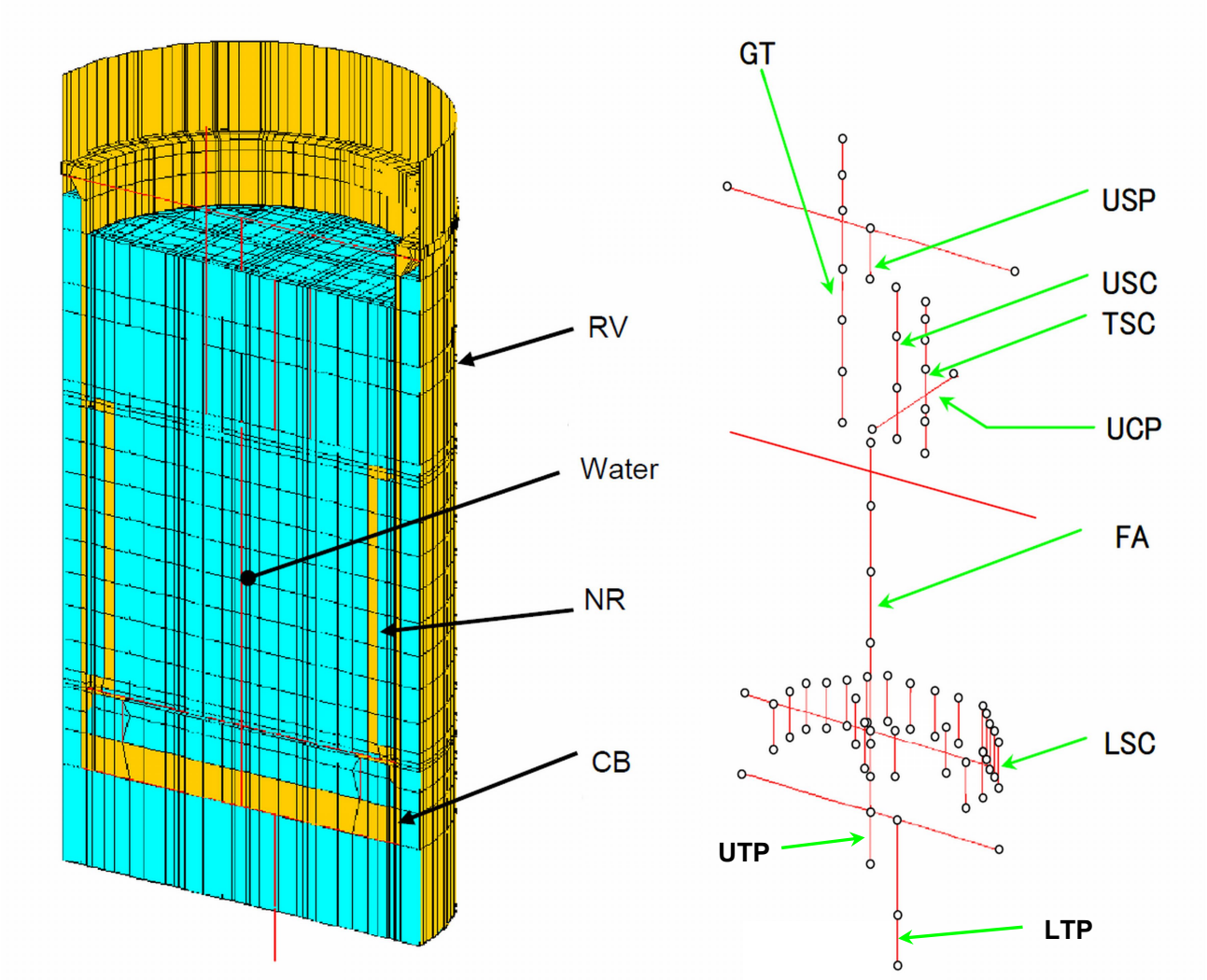

Figure 3.2.1-1 Solid System Model for J-APWR SMT Benchmark Analysis (1/2)

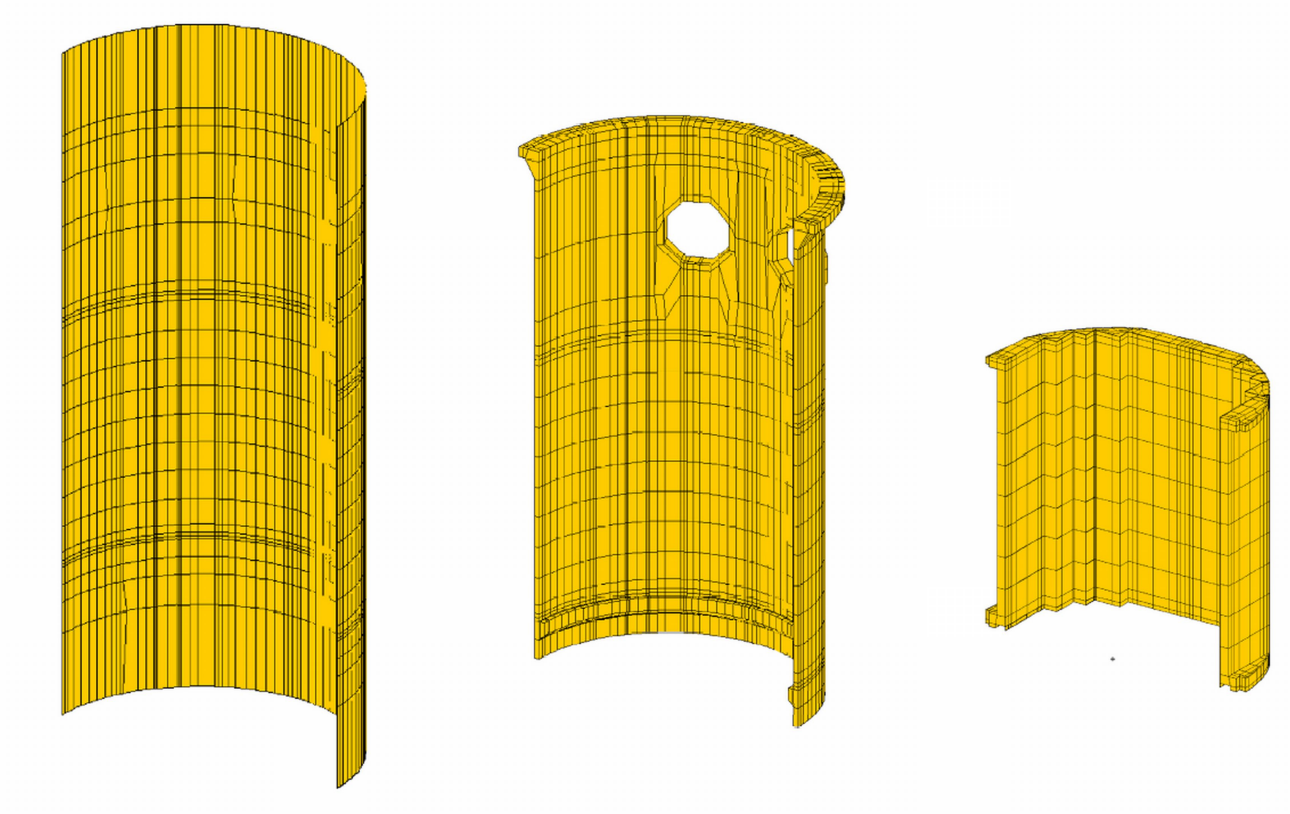

Reactor Vessel **Core Barrel** **Neutron Reflector**

Figure 3.2.1-1 Solid System Model for J-APWR SMT Benchmark Analysis (2/2)

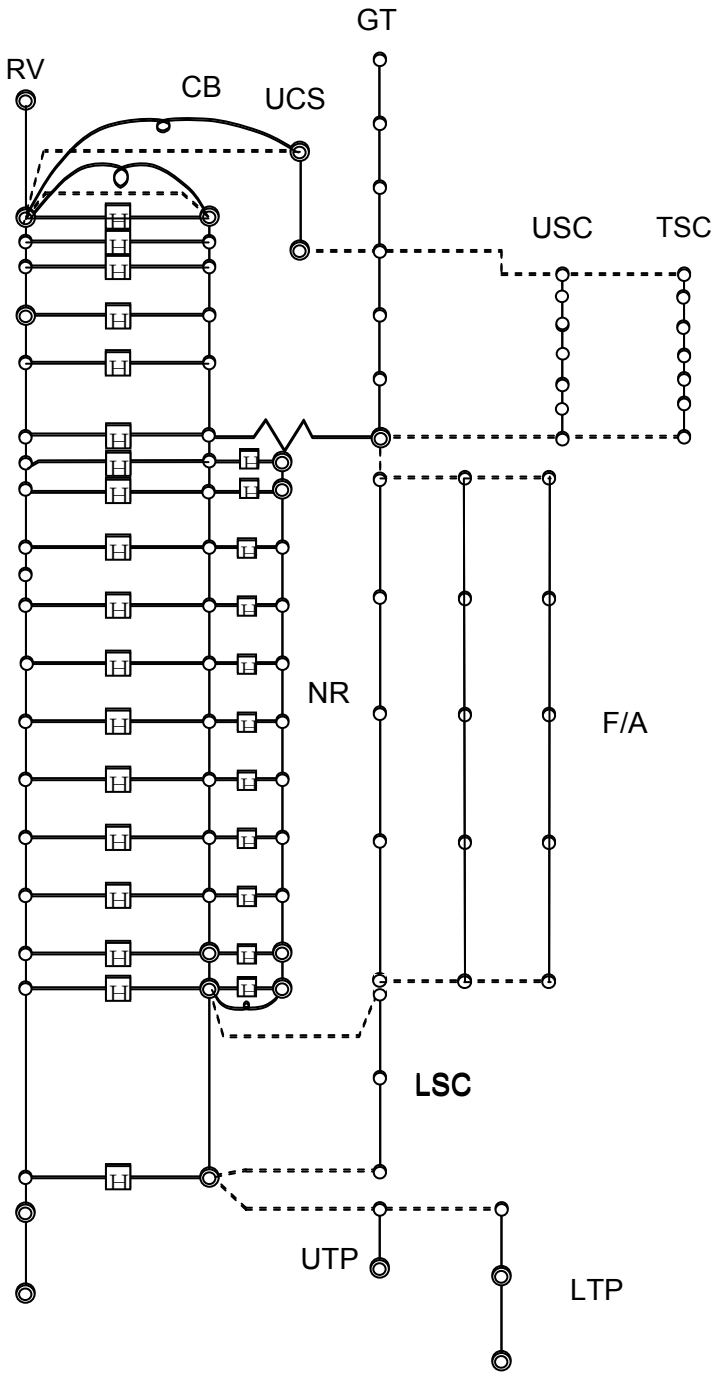

Figure 3.2.1-2 Beam System Model for J-APWR 1/5 Scale Model Analysis

Figure 3.2.1-3 Core Barrel Beam Mode
(J-APWR SMT benchmark analysis, scaled to actual dimensions)

Figure 3.2.1-4 Neutron Reflector Beam Mode
(J-APWR SMT benchmark analysis, scaled to actual dimensions)

Figure 3.2.1-5 Core Barrel Shell Model(n=2)
(J-APWR SMT benchmark analysis, scaled to actual dimensions)

Figure 3.2.1-6 Neutron Reflector Shell Mode (n=2)
(J-APWR SMT benchmark analysis, scaled to actual dimensions)

Figure 3.2.1-7 Neutron Reflector Shell Modes
(n=2, diagonal)(J-APWR SMT benchmark analysis, scaled to actual dimensions)

Figure 3.2.1-8 Neutron Reflector / Core Barrel Shell Mode (n=3)
(J-APWR SMT benchmark analysis, scaled to actual dimensions)

Figure 3.2.1-9 Core Barrel Shell Mode (n=4)
(J-APWR SMT benchmark analysis, scaled to actual dimensions)

Figure 3.2.1-10 Neutron Reflector Shell Mode (n=4)
(J-APWR SMT benchmark analysis, scaled to actual dimensions)

Figure 3.2.1-11 Core Barrel (J-APWR SMT benchmark analysis, scaled to actual dimensions)

Figure 3.2.1-12 Lower/upper the plate
(J-APWR SMT benchmark analysis, scaled to actual dimensions)

Figure 3.2.1-13 RCCA Guide Tube
(J-APWR SMT benchmark analysis, scaled to actual dimensions)

Figure 3.2.1-14 Upper Support Column
(J-APWR SMT benchmark analysis, scaled to actual dimensions)

Figure 3.2.1-15 Top Slotted Column
(J-APWR SMT benchmark analysis, scaled to actual dimensions)

3.2.2. Forcing Functions for J-APWR 1/5 SMT model

In this section, two different flow induced forcing functions, which were input into the J-APWR 1/5 scale model benchmark analysis are described. The first one is from the axial flow turbulence in the downcomer. This is the main source of the vibrations of the reactor vessel, the core barrel, the neutron reflector is excited because it is coupled with the core barrel both in beam mode and shell modes. The 2nd one is the cross flow turbulence and vortex shedding loads on the structures in the lower plenum and the upper plenum.

3.2.2.1. Axial Flow Turbulence in the Downcomer

(1) Formula of the forcing function

The turbulent pressure fluctuation has been identified as the main forcing function on the reactor internals during normal operation. The methodology of the turbulence force generation was proposed by Au-Yang (Reference (4)) was followed. The Joint acceptance is a function to determine the relationship between the turbulent pressure forcing function and the displacement response. As a result, the joint acceptance integral involves both the coherence function of the pressure field and the structural mode shapes. The coherence function of the pressure field includes a convection velocity term with the flow velocities in x and y directions. When the flow is in one direction (eg, x-direction), the convection term disappears in the cross-stream direction (in this case the y-direction).

MHI simplified the Joint acceptance integral as follows:
a. Assumed the constant mode shape functions inside the acceptance integral.
b. Assumed the downcomer flow is purely axial so that the convection term in the pressure coherence function in the circumferential direction could be eliminated.

Because the joint acceptance involves integration over the entire mode shape, Assumption 1 has only a secondary effect on the joint acceptance. An example of this is shown in Figure 8.5 in Reference (4). Assumption 2 is generally valid over most of the downcomer flow surface. Since neither assumption involved the modal frequencies, the modal transfer functions were not affected. Therefore, the above two assumptions had no significant impact on the validity of the original method.

The formulas of the forcing functions are described in equations 3.2-1 through 3.2-7.

$$P_{RMS} = \frac{1}{2} C_P \rho U^2 \quad \cdots\cdots 3.2\text{-}1$$

$$PSDP(f) = (P_{RMS})^2 \cdot \frac{PSD0(f)}{\int PSD0(f)df} \quad \cdots\cdots 3.2\text{-}2$$

$$PSDF(f) = PSDP(f) \cdot J_X J_Y \cdot (L_X)^2 (L_Y)^2 \quad \cdots\cdots 3.2\text{-}3$$

$$J_x = \left(1/L_X^{\,2}\right)\cdot \iint \Gamma(f, x_1, x_2)\,dx_1 dx_2 \quad \cdots\cdots 3.2\text{-}4$$

$$J_y = \left(1/L_Y^{\,2}\right)\cdot \iint \Gamma(f, y_1, y_2)\,dy_1 dy_2 \quad \cdots\cdots 3.2\text{-}5$$

$$\Gamma(f, x_1, x_2) = \exp\left(-\mathrm{ABS}(x_1 - x_2)/\lambda_x\right)\cos\left(2\pi f(x_1 - x_2)/U\right) \quad \cdots\cdots 3.2\text{-}6$$

$$\Gamma(f, y_1, y_2) = \exp\left(-\mathrm{ABS}(y_1 - y_2)/\lambda_y\right) \quad \cdots\cdots 3.2\text{-}7$$

where

P_{RMS}	: rms amplitude of pressure fluctuation
PSDP (f)	: power spectral density of pressure fluctuation
PSD0 (f)	: reference PSD shape
PSDF (f)	: power spectral density of force

and

J_x	: joint acceptance in axial direction
J_y	: joint acceptance in lateral direction
L_x	: length of force calculation area in axial direction
L_y	: length of force calculation area in lateral direction
Γ (f, x_1, x_2)	: coherence between 2 points x_1, x_2 in axial direction
Γ (f, y_1, y_2)	: coherence between 2 points y_1, y_2 in lateral direction
λ_x	: correlation length in axial direction
λ_y	: correlation length in lateral direction
U	: axial flow velocity (in/s)
F	: frequency (Hz)
ρ	: fluid mass density (lb/in3)
C_P	: rms pressure coefficient

(2) Measured pressure fluctuation

Normalized pressure PSD was obtained from the measured pressure fluctuation in a scale model test. In the Revision 0 analysis, results from the 1/5 scale model test of the J-APWR were used. After the completion of the Revision 0 analysis, data based on the US-APWR configurations became available from the US-APWR 1/7 scale model lower plenum test. After the detailed analysis of this new set of data, including a sensitivity analysis, this new data from the US-APWR lower plenum model test were selected for the Revision 1 analysis. More details on the effect of replacing the downcomer pressure PSD data with this new data set are described in Appendix- C.

The measurement locations of the pressure fluctuation are summarized in Table 3.2.2-1.The rms pressure fluctuation amplitudes are summarized in Table 3.2.2-2. Figure 3.2.2-1 shows the fluctuating pressure measurement locations in the 1/7 scale test model. Figure 3.2.2-2 shows the measured pressure fluctuation in the 1/7 scale model test, and Figure 3.2.2-3 shows the downcomer pressure PSD. They show the typical characteristics of the turbulence spectra, which decline exponentially with the increase of frequency. The spectrum at the upper part and 90 degree from the reference point was remarkably larger because this point was located close to the inlet nozzle of the reactor vessel. This high forcing function was caused by the jet impingement.

The local normalized dynamic pressure PSD as functions of the reduced frequency are shown in Figure 3.2.2-3 in semi-log scales and in Figure 3.2.2-4 in log-log scales. At the upper 90 - degree location, the reactor vessel inlet nozzle velocity was used for the normalization. At the other 3 locations, the average downcomer velocity was used for the normalization. The typical turbulence spectral trend is observed from the log-log plot. These logarithmic plots show that the amplitude declines did not reach the noise floor level, thus confirming that high S/N ratio was maintained in the measurement. The slope of the decline in the log-log scale plots shows the ratio of around 5 to 3 which is consistent with the 5/3rd power law of turbulence energy. This suggests that the data were physically reasonable.

(3) Correlation length

In general, the correlation length is larger in the lower frequency region. For the US-APWR analyses the following equations are defined based on the flow test data in Reference (6). The relationship between the correlation length, normalized by the downcomer width and the reduced frequency is shown in Figure 3.2.2-5.

$$\lambda_x / d = 0.6(fd/U)^{-1} \quad \cdots\cdots 3.2\text{-}8$$

$$\lambda_y / d = 0.24(fd/U)^{-1} \quad \cdots\cdots 3.2\text{-}9$$

or

$$\lambda_x = 0.6\,U/f \quad \cdots\cdots 3.2\text{-}8'$$

$$\lambda_y = 0.24\,U/f \quad \cdots\cdots 3.2\text{-}9'$$

where,

λ_x : correlation length in axial direction
λ_y : correlation length in lateral direction

U : axial flow velocity (m/s)
f : frequency (Hz)
d : downcomer width (m)

(4) Sample of generated forcing function

Samples of generated time histories of the downcomer turbulent forcing function at for the typical locations are shown in Figure 3.2.2-6

3.2.2.2. Cross-Flow Turbulence and Vortex Shedding

(1) Evaluation of the cross flow velocity

The cross flow velocities distribution around the structures in the lower and upper plenum of the reactor vessel were evaluated in the following manner.

a. Upper plenum

(a) The cross flow velocities in the upper plenum were calculated based on the potential flow theory without structures in the plenum.

(b) The cross flow velocity distribution between the structures were determined based on the equation of continuity and the pitch-to-diameter ratio of the structures

(c) Analysis in Revision 0 and Revision 1, the cross flow forcing functions are defined based on the uniform flow in elevation with the maximum velocity as a conservative assumption. As the results, the upper plenum structures of the US-APWR had the minimum margin of safety as discussed later in Subsection 3.3.3.2. In Revision 2 analysis, the cross flow forcing functions are modified by dividing into several segments in elevation to account the cross flow velocity distribution along the structures for the more precise analysis. As for the sample, the RCCA G/T forcing functions with elevations are shown in Appendix-I. (Note that the uniform distribution with the maximum flow velocity is still applied for the assessment of the adverse flow effects discussed in Subsection 3.4)

b. Lower plenum

(a) The cross flow velocity in the lower plenum was assumed to be equal to the downcomer average velocity.

(b) The cross flow velocity distribution between the diffuser plate support columns was determined based on the equation of continuity and the pitch-to-diameter ratio of the support columns.

(c) When the cross flow is not uniform along the axis, the maximum cross flow was used in the vortex shedding and the fluid elastic instability evaluations.

(2) Formula of the forcing function

The equations for the cross-flow induced loads are based on ASME Sec. III APPENDIX N (Reference (2)), “N-1300 FLOW-INDUCED VIBRATIONS OF TUBES AND TUBE BANKS” and Chapter 9 in Reference (5). These equations are applied to the column structures in the lower plenum and the upper plenum as follows.

$$PSDP(f) = \left(1/2\,\rho U^2\right)^2 \cdot (D/U) \cdot PSD0 \quad \cdots\cdots 3.2\text{-}10$$

$$PSD0 = 0.01 \text{ for } f\,D/U < 0.1 \quad \cdots\cdots 3.2\text{-}11\text{-}a$$

$$= 0.2 \quad \text{for } 0.1 \le f\,D/U \le 0.4 \quad \cdots\cdots 3.2\text{-}11\text{-}b$$

$$= 5.3E\text{-}4\ (f\,D/U)^{(-7/2)} \quad \text{for } 0.4 < f\,D/U \quad \cdots\cdots 3.2\text{-}11\text{-}c$$

$$PSDF(f) = PSDP(f) \cdot J \cdot (D)^2 (L)^2 \quad \cdots\cdots 3.2\text{-}12$$

$$J = \left(1/L_X{}^2\right) \cdot \iint \Gamma(f, x_1, x_2)\,dx_1 dx_2 \quad \cdots\cdots 3.2\text{-}13$$

$$\Gamma(f, x_1, x_2) = \exp\left(-ABS(x_1 - x_2)/\lambda\right) \quad \cdots\cdots 3.2\text{-}14$$

$$\lambda = 0.2P(1+P/2D) \quad \cdots\cdots 3.2\text{-}15$$

where,

PSDP (f) : power spectral density of pressure fluctuation
PSD0 (f) : normalized pressure PSD in Figure 3.2.2-7
PSDF (f) : power spectral density of force

J : joint acceptance
L : length of force calculation area in axial direction (in)
$\Gamma(f, x_1, x_2)$: coherence between two points oriented at x1 and x2 in axial coordinate
λ : correlation length (in)
U : flow velocity (in/s)
P : column pitch (in)
D : column diameter (in)
F : frequency (Hz)
ρ : fluid mass density (lb/in^3)

(3) Sample of the forcing function

Samples of the generated time histories of the cross-flow turbulence induced loads for the typical locations are shown in Figure 3.2.2-8.

Table 3.2.2-1 List of the Pressure Measurements in the US-APWR 1/7 Scale Model Vessel Lower Plenum Test

Measurement Item	Measuring Parts	Circumferential Location	Transducer ID	Number of Transducers
Pressure Fluctuation	Core barrel wall face to the downcomer			
Pressure Fluctuation	Vessel lower head			
Static Pressure	Along the main flow path			

Table 3.2.2-2 RMS Pressure Fluctuation of the Downcomer (Measured in the US-APWR 1/7 Scale Lower Plenum Flow Test)

Measured Locations			RMS Pressure Fluctuation (1-100Hz in actual plant scale) (psi)	Remarks
Elevation	Direction	Transducer ID		
upper	90º	PD2	1.88	nearest to the inlet nozzle
	0º	PD1	0.70	
lower	90º	PD4	0.58	
	0º	PD3	0.49	

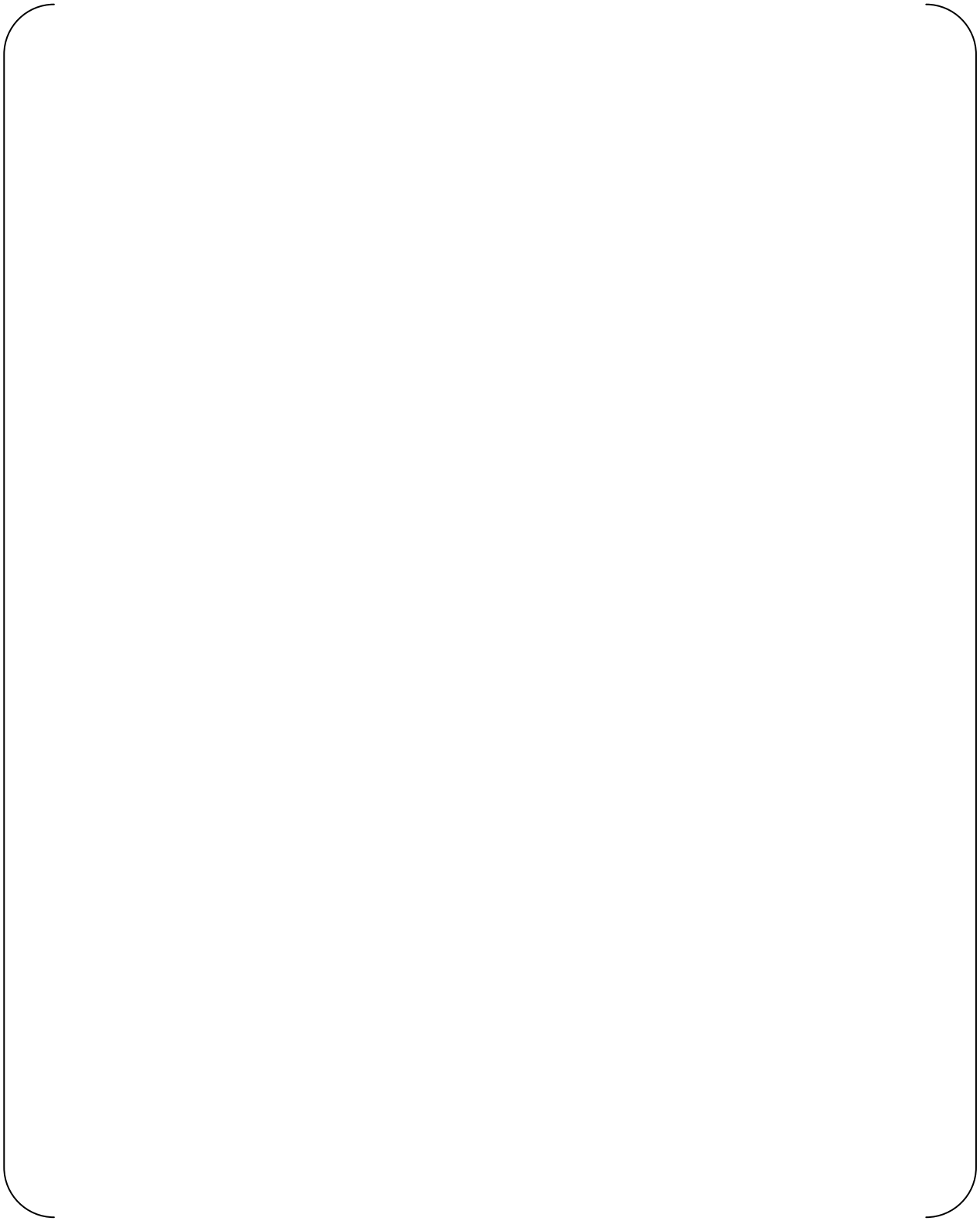

Figure 3.2.2-1 Pressure Measurement Locations in the US-APWR 1/7 Scale Vessel Lower Plenum Test

Figure 3.2.2-2 Measured Downcomer Pressure PSD vs. Frequency

Figure 3.2.2-3 Normalized Pressure PSD vs. Reduced Frequency (Semi-log Scales)

Figure 3.2.2-4 Normalized Pressure PSD vs. Reduced Frequency (Log-log Scales)

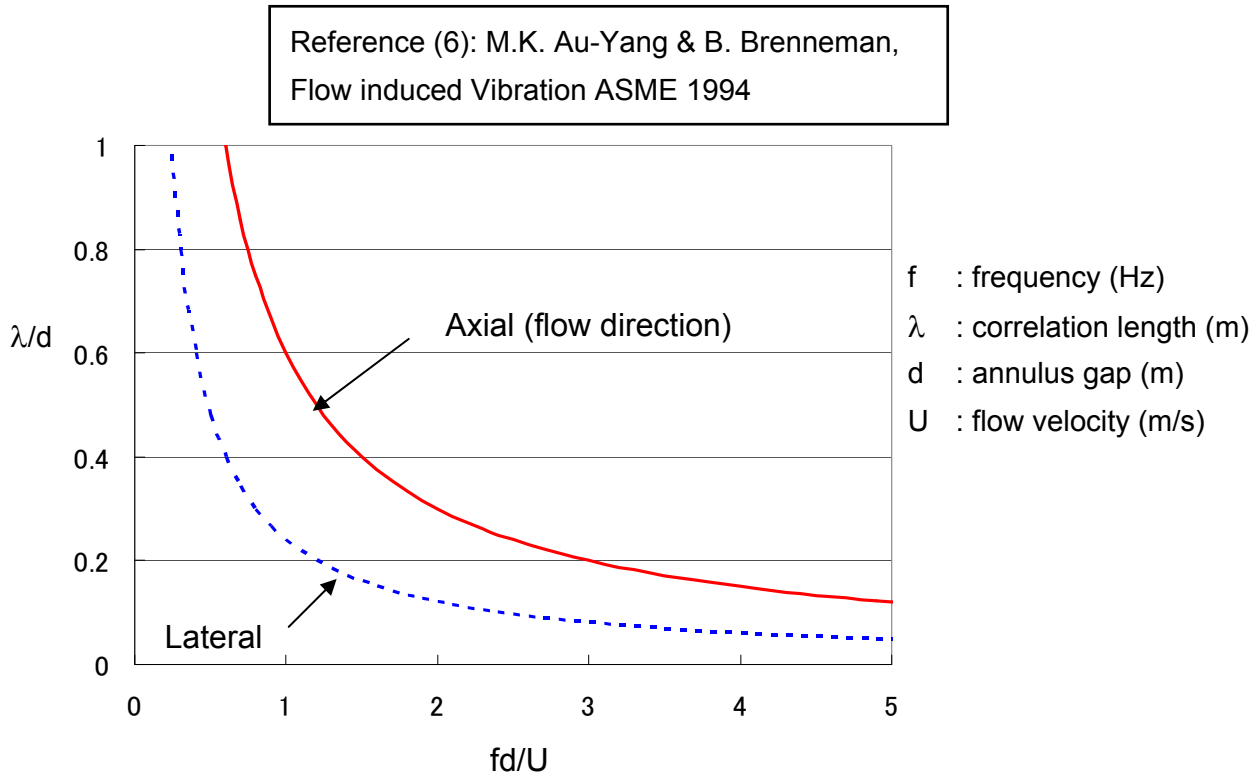

Figure 3.2.2-5 Correlation Length for the Downcomer

Figure 3.2.2-6 Downcomer Turbulent Forcing Functions
(Input of J-APWR SMT Benchmark Analysis)

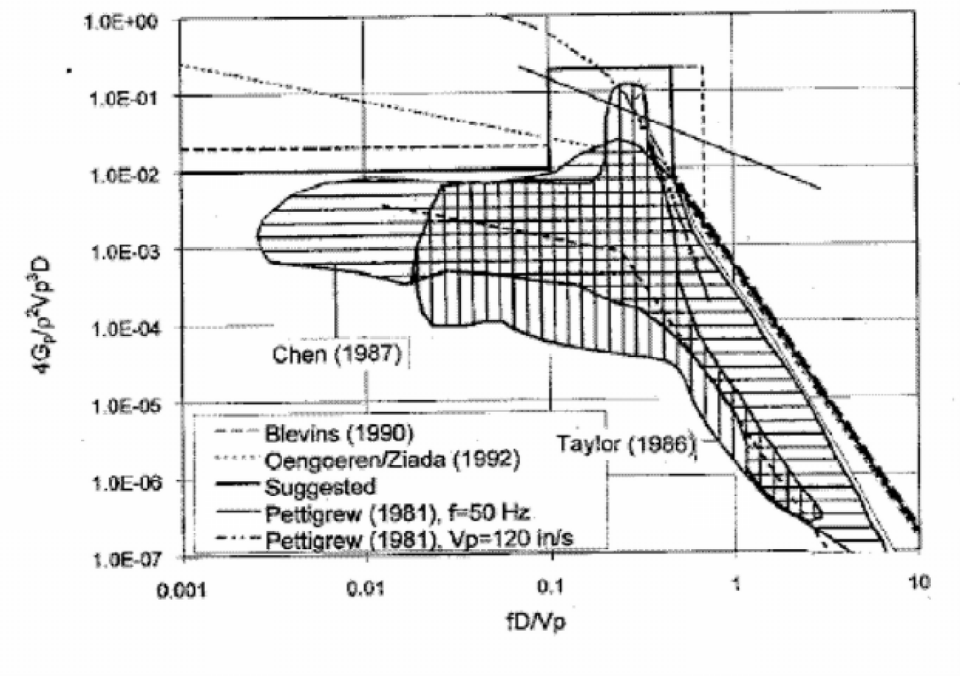

Figure 3.2.2-7 Normalized PSD for Cross Flow Turbulence from Reference (5)

Upper Tie Plate Column RCCA Guide Tube

Upper Support Column Top Slotted Column

Figure 3.2.2-8 Cross Flow Vibration Load on Columns (Input for J-APWR SMT Benchmark Analysis)

3.2.3. Response Results of the J-APWR Benchmark Analysis

(1) Analysis conditions

The response analyses were performed under the J-APWR SMT conditions as described in Table 3.2.3-1. For the support conditions at the key supports, such as the bottom of the core barrel and top of the neutron reflector, are assumed to be free to simulate the maximum displacement. In the scale model test, these the key supports were not supported such as “open gap condition”. The time histories of the forcing functions were generated and applied on the model elements as described in Subsection 3.1.2 (3).

(2) Criteria for the comparison with measured response

The validity of the flow induced forcing functions was verified by comparison with the measured responses. The following two criteria were applied for the validity check of the benchmark analysis which is based on the category 2 acceptance criteria as described in Subsection 3.5.

a. The natural frequency for the fundamental beam mode and the lowest shell mode: with in 10%

b. The ratio of the analysis response (displacement or moment) to measured one should be in the factor of 3.0 as the acceptance criteria with the random response discussed in Subsection 3.5.

(3) Vibration Response

Response results of the J-APWR benchmark analysis are summarized as below.

The results are shown in Table 3.2.3-2, Table 3.2.3-3, Figure 3.2.3-1 and Figure 3.2.3-2. The response of the core barrel and the neutron reflector due to the downcomer turbulences were adjudged acceptable based on the following rationale:

a The Core barrel / Reactor vessel relative displacement

(a) The ratio of the rms relative displacement from the analysis results to the measured one is [ ] which satisfies the acceptance criterion factor of 3.0.

(b) In Figure 3.2.3-1, the dominant frequency of the displacement response for the core barrel is observed around [ ] Hz both in the analysis and measured data. The difference was in the 10% as the acceptance criterion for the natural frequency.

(c) The peak of the response in the spectrum for the relative displacement between the bottom of the core barrel and the reactor vessel was around [ ] Hz in the measurement was identified to be related to the test vessel mode.

b The core barrel and neutron reflector relative displacement

(a) The ratio of the computed rms relative displacement between the core barrel and the neutron reflector to the measured value was [ ] which satisfies the acceptance criterion factor of 3 as the random vibration response.

(b) In Figure 3.2.3-2, the dominant peak in the frequency of the neutron reflector in the response spectrum is observed to be around [ ] Hz both in the analysis and measured data. The difference was within the 10% as the acceptance criteria for the natural frequency.

(c) The peak of the response in the spectrum for the core barrel and neutron reflector relative displacement was around [ ] Hz in the measurement and was identified to be related to the test vessel mode.

From above discussions the analysis method is adequate for FIV response analysis.

c Response due to the cross flow

The validity of cross flow forcing functions was confirmed by comparison of the dynamic moment for the columns in the lower and upper plenum as shown in Table 3.2.3-3. The ratios for the upper plenum structures (RCCA GT, USC and TSC) are in the range of [ ] to [ ]. Considering of the fact that the base of the cross flow forcing functions are not a custom measured data in the same configuration (like downcomer forcing functions) but a general design data, the geometric mean [ ] seems to be reasonable and acceptable. It is supposed that the considering of the cross flow velocity distribution based on the potential flow theory makes some advantage on this result.

For the two part of assemblies in lower plenum, range of the analysis/measured ratio is [ ] to [ ]. For the geometric mean [ ] satisfy the acceptance criteria factor of 3.0.
Although the upper value [ ] for the support column of lower tie plate assemblies might be too conservative, no modification of the forcing function was conducted from following reasons.
(a). Present cross flow velocity in the lower plenum was assumed same to the axial flow velocity in the downcomer because of the complicated flow fields in the lower plenum, Thus determine of more reasonable cross flow velocity and modification of cross flow loads based on that is not practical.
(b) Potential conservativeness of the cross flow load on the lower plenum structures can be taken into consideration in the assessment of stress evaluation for the US-APWR with un-modified loading. (Assessment of high cycle fatigue evaluation for the US-APWR reactor is discussed in Subsection 3.3.3.2)

3.2.4. Validity of the Analysis Methodology

Incorporating with the discussions in Subsections 3.2.1 and 3.2.3, the validity of the modeling methodology and formulation of the forcing functions is summarized as follows:

(1) Validity of the Analysis Model

a. The computed results using this model in which the components in the J-APWR 1/5 SMT were modeled with solid and fluid elements agreed well with the in-water measured results.

b. The computed natural frequencies of the fundamental mode of the J-APWR 1/5 SMT model agreed with the test results to within ±10% except for the RCCA guide tube and top slotted column. As for the guide tube, the analysis result is rather reliable than the measured one because of the uncertainty of the pin support benchmark in the scale model. For the top slotted column the analysis model refinement was reflected to the US-APWR modeling.

(2) Validity of forcing functions

a. The formulation of the turbulent forcing functions in the downcomer was adequate because the rms vibration amplitude of the core barrel and the neutron reflector are in a factor of [ ] to [ ] of the corresponding measured values and met the acceptance criterion factor of 3.0 for the random response.

b. The formulation of the cross flow loads in the upper plenum was adequate, because the rms response of the bending moment on the upper plenum and lower plenum structures were in the ratio of [ ] to [ ] and satisfied the acceptance criterion factor of 3.0 for the random response. The ratio of [ ] to [ ] for the support column of the lower plenum structure assemblies was exceeded the acceptance criterion. Although the upper value [ ] for the support column of the lower tie plate assemblies might be too conservative, no modification of the forcing function was conducted. The potential conservativeness of cross flow loads on the lower plenum structures can be taken into account in the assessment of the stress analysis for the corresponding structures (the lower diffuser plate assembly) of US-APWR with un-modified loads.

Table 3.2.3-1 J-APWR SMT Benchmark Analysis Conditions

Case ID	Configuration	Model Type	Forcing Functions[1)]	Ratio to the Critical Damping
A1	1/5 scale test model	Solid	DC	[ ]%
A2	Ditto	Beam System	Ditto	Ditto
A3	Ditto	Beam System	DC+LP+UP	Ditto
A4	Ditto	Single Beam	UP	Ditto

Note 1) DC : Downcomer Turbulence
LP : Lower Plenum Cross Flow
UP : Upper Plenum Cross Flow
V : Vertical Load
RCP : RCP Pulsation

Table 3.2.3-2 Correlation of Test Results of CB / NR RMS Response with Results from the J-APWR SMT Benchmark Analysis

Components	Rms Response (mil rms)		Analysis /Measured
	Measured*	Analysis*	
CB bottom –RV relative displacement			
NR top –CB relative displacement			

*Both results are converted to actual plant scale.

Table 3.2.3-3 Correlation of Test Results in Cross Flow Induced Vibration, with Computed Results from the J-APWR SMT Benchmark Analysis

Components	Rms Response (column moment in Lb-in rms)		Analysis /Measured
	Measured* (Reference (7))	Analysis*	
Lower Tie Plate BMI Column			
Upper Tie Plate BMI Column			
RCCA Guide Tube			
Upper Support Column			
Top Slotted Column			

*Both results have been converted to actual plant condition.

Figure 3.2.3-1 CB Bottom / RV Relative Displacement Linear Spectral (Test Scale)
(J-APWR SMT Measured and Analysis Results)

Figure 3.2.3-2 NR Top / CB Relative Displacement Linear Spectral (Test Scale)
(J-APWR SMT measured and analysis results)

3.3. US-APWR Response Analysis

In this section, the prediction analysis of the US-APWR reactor internals vibration response as the Task-2 is described in Subsection 3.1. The analysis methods which were verified through the benchmark analysis in Subsection 3.2 were applied. Additional information on the analysis models and the conversion of the forcing functions from the J-APWR SMT benchmark model to the US-APWR normal operating condition are described in Subsection 3.3.1 and Subsection 3.3.2. The results of vibration response under the US-APWR normal operating conditions and the assessments for the high cycle fatigue are discussed in Subsection 3.3.3. In Subsection 3.3.4, vibration response under the HFT conditions are described. Based the comparison with the vibration responses under the normal operating condition, the needs of the vibration measurements after the core loading are discussed.

3.3.1. Structural Model

(1) Model definition for the US-APWR

Two structural system models, a 3D solid system model consisting of the reactor vessel, the core barrel and the neutron reflector, and a 3D beam system model were constructed similar to those in the benchmark analysis as described in Subsection 3.1.2. In the analytical model for the full-scale prototype model, the 3D solid and 3D beam system model were made based on the following actual structural properties and operating conditions and with the same modeling methodology as in the J-APWR analysis. This methodology has been verified in the previous section. The following are high lights in the US-APWR analytical model.

a. Full-scale dimensions
b. RV support stiffness of the US-APWR
c. Addition of the CRDM and IHP models
d. Average temperature at the inlet and outlet of the reactor vessel for the physical properties of the structure
e. Analytical conditions without the fuel assemblies to allow the prediction analysis under the HFT conditions

After the above changes and the addition, the 3D solid and 3D beam system model was made. The single beam element model for RCP pulses was made for the pole-structure placed on the upper plenum. The 3D solid system model, the 3D beam system model, and the single beam model are shown in Figures 3.3.1-1 through 3.3.1-3.

(2) Vibration characteristics of the US-APWR reactor internals

The fundamental modal frequencies of the US-APWR reactor internals obtained by the FE modal analysis using the solid system model both with and without the core to simulate the operating condition and hot functional test condition are shown in Table 3.3.1-1 and Figures 3.3.1-4 through 3.3.1-19. The results confirmed that the loading of the fuel assemblies has little effect on the reactor internals vibration characteristics.

Table 3.3.1-1 Natural Frequencies of US-APWR Reactor Internals (US-APWR Analysis Results)

	Vibration Mode		Natural Frequency (Hz)		Ratio
			With Core	Without Core	
Core Barrel	Beam				
	Shell	n=2			
		n=3			
		n=4			
Neutron Reflector	Beam				
	Shell	n=2			
		n=2, diagonal			
		n=3			
		n=4			
Lower Diffuser Plate Assembly	Transverse / Rotational				
Upper Diffuser Plate Assembly	Transverse				
RCCA Guide Tube (Upper / Lower)	Beam				
Upper Support Column	Beam				
Top Slotted Column	Beam				

*These values are obtained by 3D beam system model

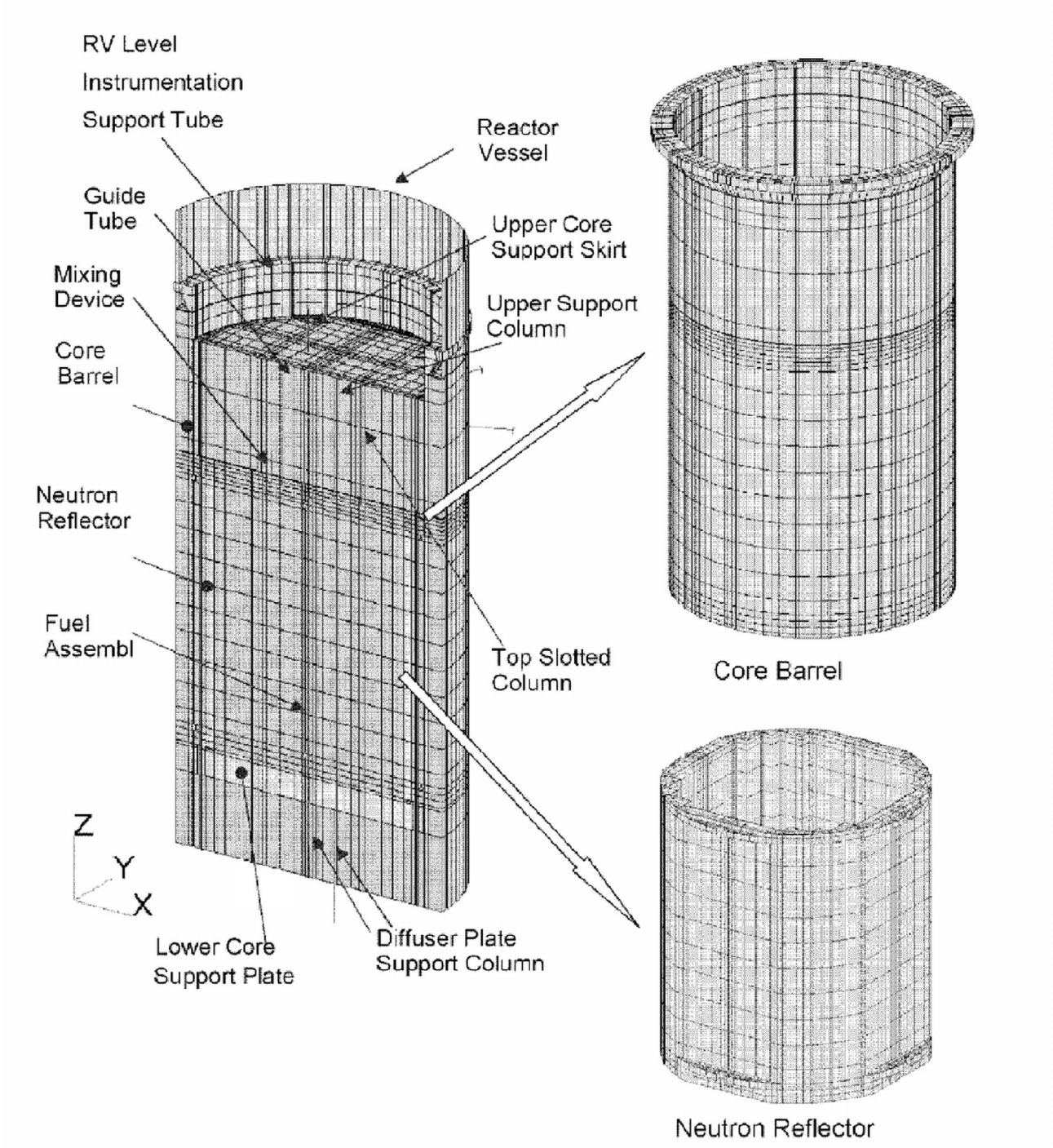

Figure 3.3.1-1 Solid Model for Core Barrel / Neutron Reflector(US-APWR Analysis Model)

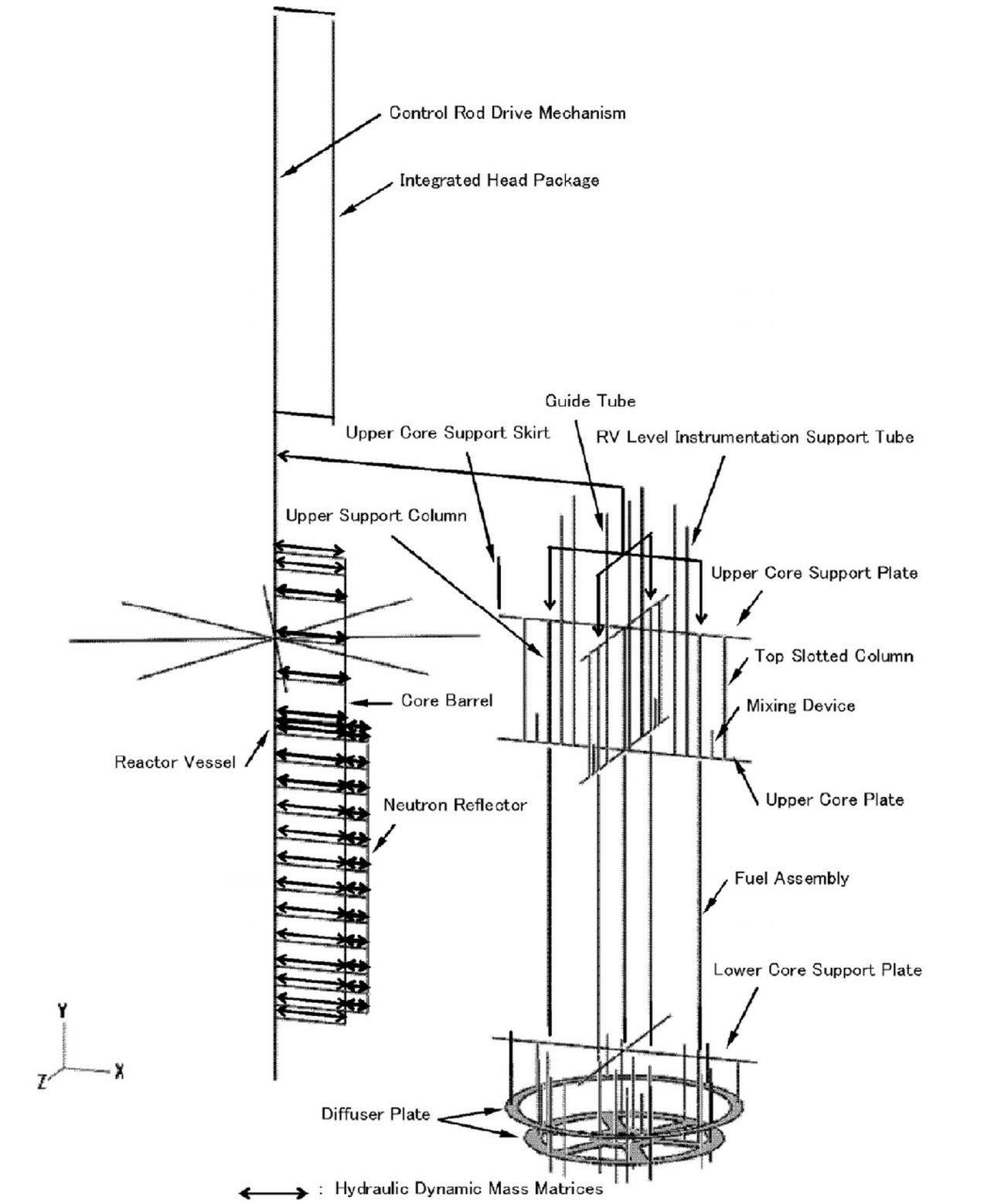

Figure 3.3.1-2 Beam Elements System Model for Reactor Vessel / Internals (US-APWR Analysis Model)

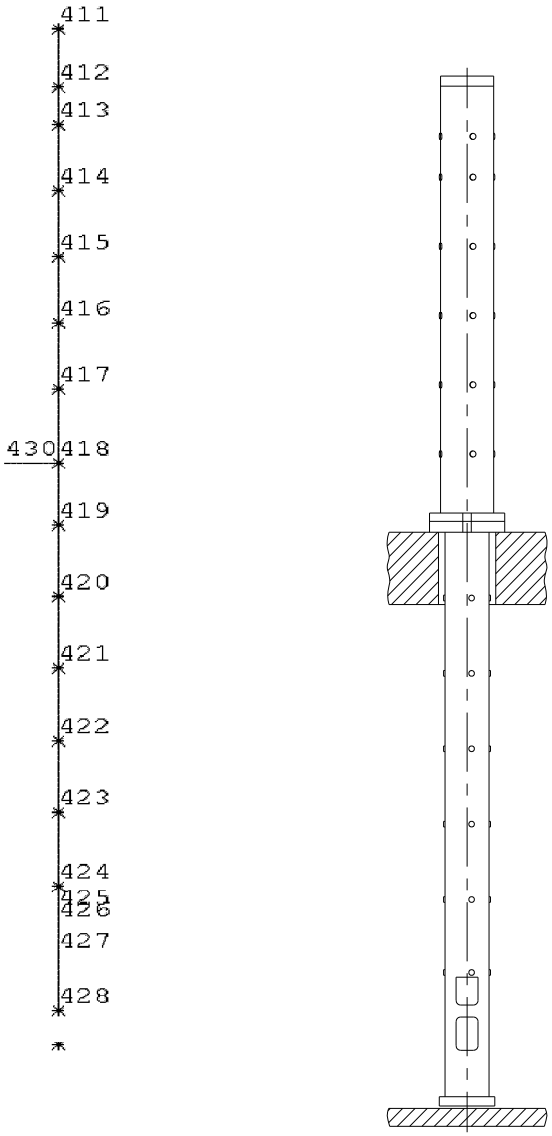

Figure 3.3.1-3 Single Beam Element Model for the Components in the Upper Plenum (US-APWR RCCA Guide Tube Analysis Model)

with core ([ ] Hz) without core ([ ] Hz)

Figure 3.3.1-4 Core Barrel Beam Mode (US-APWR Analysis Results)

with core ([ ] Hz) without core ([ ] Hz)

Figure 3.3.1-5 Neutron Reflector Beam Mode (US-APWR Analysis Results)

with core ([ ] Hz) without core ([ ] Hz)

Figure 3.3.1-6 Core Barrel Shell Mode (n=2) (US-APWR Analysis Results)

with core ([ ] Hz) without core ([ ] Hz)

Figure 3.3.1-7 Neutron Reflector Shell Mode (n=2) (US-APWR Analysis Results)

with core ([ ] Hz) without core ([ ] Hz)

Figure 3.3.1-8 Neutron Reflector Shell Mode (n=2, diagonal) (US-APWR Analysis Results)

with core ([ ] Hz) without core ([ ] Hz)

Figure 3.3.1-9 Neutron Reflector / Core Barrel Shell Mode (n=3)(US-APWR Analysis Results)

with core ([ ] Hz) without core ([ ] Hz)

Figure 3.3.1-10 Core Barrel Shell Mode (n=4) (US-APWR Analysis Results)

with core ([ ] Hz) without core ([ ] Hz)

Figure 3.3.1-11 Neutron Reflector Shell Mode (n=4) (US-APWR Analysis Results)

Figure 3.3.1-12 Core Barrel Beam Mode by 3D Beam System Model (US-APWR Analysis Results)

Figure 3.3.1-13 Lower Diffuser Plate Assembly Transverse Mode (US-APWR Analysis Results)

Figure 3.3.1-14 Lower Diffuser Plate Assembly Rotational Mode(US-APWR Analysis Results)

Figure 3.3.1-15 Upper Diffuser Plate Assembly Transverse Mode (US-APWR Analysis Results)

Figure 3.3.1-16 Upper RCCA Guide Tube Beam Mode(US-APWR Analysis Results)

Figure 3.3.1-17 Lower RCCA Guide Tube Beam Mode(US-APWR Analysis Results)

Figure 3.3.1-18 Upper Support Column Beam Mode(US-APWR Analysis Results)

Figure 3.3.1-19 Top Slotted Column Beam Mode(US-APWR Analysis Results)

3.3.2. Forcing Functions for the US-APWR

The US-APWR and J-APWR SMT have similar geometries for the downcomer turbulent flow and the cross flow in the upper plenum. Therefore, the time history data of these forcing functions, which had been verified in the benchmark analysis of the J-APWR 1/5 SMT, were used after scaling up to the conditions for the full-scale US-APWR. The detailed conversion methodology is discussed in Appendix-B. Because the dimension and location of the columns in the US-APWR are different from those in the J-APWR, the cross flow loads on the structures in the lower plenum were derived specifically for the US-APWR using the same method used in establishing the loads for the J-APWR. In addition, the vertical vibration of the perforated plates and loads induced by the RCP pulsations were derived. These loads are described below.

3.3.2.1. Flow Induced Vibration Loads

(1) Downcomer turbulence

The time histories of the downcomer flow turbulence for the US-APWR were converted from those of the J-APWR SMT benchmark analysis as described in Subsection 3.2.2.1, considering with the scaling law and the following differences of conditions on the coolant density and flow rates. The details are shown in Appendix-B.

a. Reference temperature of coolant density

With the core : Temperature at the inlet of the reactor vessel during normal operation was used
Without the core : Temperature at the inlet of the reactor vessel at hot standby was used

b. Coolant flow rates

With the core : Mechanical Design Flow
Without the core : Mechanical Design Flow x [ ]

Some samples of the downcomer flow turbulence loads for the US-APWR analysis are shown in Figure 3.3.2-1.

(2) Cross flow loads

The time histories of the cross flow induced loads on the upper plenum structures of the US-APWR were converted from those of the J-APWR SMT benchmark analysis as described in Subsection 3.2.2.2, considering with the scaling law and the following differences of conditions on the coolant density and flow rates. The details are shown in Appendix-B.

a. Reference temperature of coolant density

With the core : For the lower plenum, temperature at the inlet of the nuclear reactor vessel during normal operations was used.
For the upper plenum, temperature at the inlet of the nuclear reactor vessel during normal operations was used.

Without the core : Temperature at the inlet of the reactor vessel at hot standby was used

b. Coolant flow rates

With the core : Mechanical Design Flow
Without the core : Mechanical Design Flow x [ ]

For the lower plenum structures, because of the difference of the support column diameter, the PSD of the cross flow loads are not in proportion with the J-APWR. Therefore, cross flow loads for the US-APWR were originally made with the US-APWR configurations using the same method as preparing the load of the J-APWR.

Some samples of the cross flow vibration loads for US-APWR analysis are shown in Figure 3.3.2-2.

(3) Vertical vibration load

The vertical vibration loads were estimated from the integral of random pressure fluctuation through the flow holes in the lower core support plate and the upper core plate, respectively. The same PSD function in the downcomer (Figure 3.2.2-4) was assumed, but the downcomer width was replaced with the diameter of flow hole. The justification for this premise is based on the assumption that the pressure fluctuation close to the RPV inlet nozzle is caused by the jet flow turbulence exiting from the inlet nozzle and, therefore is assumed to be similar to the jet flow turbulence through the lower core support plate and the upper core plate flow holes. The adequacy to use the downcomer pressure data as the vertical loads on the perforated plate is discussed in Appendix-E.

An example of the measured pressure PSD of the vertical loads on the lower core support plate and the upper core plate are shown in Figure 3.3.2-3, and the samples of generated time histories of vertical vibration loads are shown in Figure 3.3.2-4.

The joint acceptance and the correlation length were not known. The total force on the plate was calculated as the SRSS due to the flow through all the holes in the plate. This is because the Jet flow turbulence in each flow hole is statistically independent of the others.

Figure 3.3.2-1 Downcomer Turbulent Forcing Functions (US-APWR)
(Input for US-APWR Analysis)

Diffuser Plate Support Column RCCA Guide Tube

Upper Support Column Top Slotted Column

Figure 3.3.2-2 Cross Flow Vibration Load on Columns (US-APWR Analysis)
(Input for US-APWR Analysis)

Figure 3.3.2-3 PSD of Vertical Vibration Force on the Lower Core Support Plate and Upper Core Plate (Input for US-APWR Analysis)

Figure 3.3.2-4 Vertical Vibration Force Time Histories on Lower Core Plate and Upper Core Plate (Input for US-APWR Analysis)

3.3.2.2. Pump Pulsation Load

(1) RCP characteristics

The specifications related to the RCP pulsation characteristics, such as the rotational speed and the number of impellers for US-APWR are same as those of the generic RCP as shown in Table 3.3.2-1. Therefore the frequencies of the RCP pulsation for US-APWR do not changed from those generated by the generic RCP. The difference in the hydraulic head was accounted for in determining the absolute amplitude of the RCP pulsation.

(2) Estimation of the US-APWR RCP pulsation

Pressures fluctuations were measured at the outlets of both generic and the APWR-specific RCPs, as discussed in Appendix. D.

In the Revision 0 analysis, the amplitude of the RCP pulsation was determined based on the pressure fluctuation at the outlet in the APWR test. Note that this measured pressure fluctuation included not only the RCP induced acoustic pulsation but also the fluctuating pressure due to local turbulence.

In the Revision 1 and Revision 2 analysis, the ratios of the acoustic pulsations at the shaft rotation and at each blade passing frequency were determined based on the spectral analysis of acoustic pulsations generated by the generic RCPs.

The RCP pulsation amplitudes at the shaft rotation and the first two blade passing frequencies were determined as shown in Table 3.3.2-2.

(3) Acoustic analysis

a. Analysis code

The acoustic resonance modes in the reactor vessel and their gains of the amplification with the RCP pulsations were determined by the acoustic analysis with the FE analysis code ‘SYSNOISE ‘.

b. Code verification

The SYSNOISE code was verified with two kinds of the bench mark calculations as follows.

The downcomer and the upper plenum were selected for the verification of the SYSNOISE acoustic analysis because there are high possibilities of the acoustic resonance induced by the RCP.

The downcomer was analyzed as an annulus while the upper plenum was analyzed as a cylinder to compare with the theoretical results.

The results of the verification analysis are summarized in Table3.3.2-3. The computed acoustical modal frequencies were within 1.0 %, of the corresponding theoretical values and met the acceptance criterion.

c. Acoustic analysis model of the US-APWR.

The outlines of the US-APWR acoustic model is shown in Table 3.3.2-4, Figure 3.3.2-5 and Figure 3.3.2-6. The analytical model for the SYSNOISE code was composed of the RCP, RV, inlet plenum of the steam generators and the main coolant piping.

In the reactor vessel, the downcomer and the upper plenum have high possibilities of the acoustic resonance induced by the RCP. The lower plenum and the reactor core connecting the above region were added. The head plenum was excluded from the model because it is an acoustically-isolated closed space. In addition, a sensitivity analysis was conducted for the effect of the reactor internals in the lower plenum and the upper plenum. The internals of the lower plenum was omitted because the presence of the internal components there has insignificant effect on its acoustic characteristics. On the other hand, in the upper plenum, the presence of internal components alters its acoustic characteristics. Therefore they were included in the model to keep the uncertainty and bias errors of the calculated resonance frequencies to within [ ] %, even with uncertainties in the sound speed

d. Acoustic damping (Sound attenuation)

Sound attenuation included in the SYSNOISE model is discussed in the analysis of the acoustic loading in the reactor internals of the US-APWR.

Table 3.3.2-5 shows the mechanisms causing sound attenuation in the reactor vessel. Test data for the validation of sound attenuation are limited. Therefore, for obvious reasons, only attenuation through the perforated plates (spray nozzles, lower core support plate, and upper core plate) was conservatively included in the model. The derivation of acoustic attenuation through perforated plates is described in Reference (9). The acoustic resistance was obtained with an equivalent the diameter of hole, plate thickness, opening ratios in the spray nozzle, lower core support plate, and upper core plate respectively. At this time, steady flow along the perforated plates was ignored for a conservative evaluation. Table 3.3.2-6 shows values for the acoustic resistance in each perforated plate derived as shown above.

(4) RCP pulsation forcing functions related to structures

The forcing functions due to the RCP pulsation for the reactor internals were defined considering with the possibility of the resonant vibration of the structural components.

a. Core barrel and neutron reflector

In the RCP pulsations, the shaft rotational speed [ ] Hz is nearest to the fundamental beam or shell modes of the core barrel or the neutron reflector as discussed in Subsection 3.3.
In addition, from the acoustic analysis by SYSNOISE code, an acoustic resonance mode with the RCP blade passing frequency [ ] Hz is identified in the downcomer. Although this frequency is much higher than the fundamental mode beam or shell mode frequencies of the core barrel or the neutron reflectors, some vibration response with higher shell mode may be induced.
Therefore, the RCP pulsation forcing functions on the core barrel and the neutron reflector are the sum of the sine waves of [ ] Hz and [ ] Hz as equation 3.3-1. The amplitudes and phase angles related to the locations are determined from the SYSNOISE acoustic analysis.

$$F(x, y, z, t) = A \sum \{P(f,x, y, z) \sin(2\pi ft + \phi(x, y, z))\} \quad \cdots\cdots\cdots\cdots\cdots\cdots \quad 3.3\text{-}1$$

Where,

F : force on the core barrel or the neutron reflector (lb)
P : amplitude of standing wave pressure fluctuation (psi) with the function of the frequency f and location x, y, z.
A : area where the force is defined (in^2)
t : time (s)
ϕ : phase angle (rad)
f : RCP shaft rotational speed (Hz)

The maximum pressure amplitudes on the core barrel and the neutron reflector are shown in Table 3.3.2-7. The RCP forcing function time history waves on the core barrel and the neutron reflector are shown in Figure 3.3.2-8 and Figure 3.3.2-9.

b. Upper plenum structures

The modal frequencies of components in the upper plenum-the RCCA guide tubes, the upper support columns, and the top slotted columns were much higher than the RCP shaft rotational speed [ ] Hz, but the beam modal frequencies were close to the higher harmonics of the RCP blade passing frequency. Thus, exact resonance with the RCP pulsation harmonics was assumed to be conservative. The forcing functions on these structures were defined in the form of equation 3.3-2.

$$F(z, f) = D(D \text{ grad } P(z)) \sin(2\pi ft + \phi(z)) L \cdots\cdots\cdots\cdots\cdots\cdots \quad 3.3\text{-}2$$

Where,

D : diameter of the structures (in)
ϕ : phase angle (rad)
z : elevation (in)
grad P : pressure gradient in the force acting direction (psi/in)
f : RCP pulsation frequency (Hz)
L : length of force calculation area in axial direction (in)

The RCP pulsation loads on the upper plenum structures are summarized in Table 3.3.2-8. The RCP pulsation time history wave on the RCCA Guide Tube is shown in Figure 3.3.2-10.

c. Vertical force on support plates

The dynamic vibration force on the lower core support plate and the upper core support plate were determined from the pressure difference across each plate for [ ] Hz which was closest to the vertical natural frequencies of these components. The pressure difference on each plate is shown in Table 3.3.2-9.

d. Bias error and uncertainties

The response to RAI 498-3782 Question 03.09.02-68 is attached as Appendix H about the bias error and uncertainty on the RCP pulsation forcing functions.

Table 3.3.2-1 Comparison of RCP Specification of US-APWR / Current 4-loop

	US-APWR	Current 4-loop
RCP Model	Type MA25S	Type 93A-1
Shaft Power	8200 HP	6000 HP
Head	306.9 ft	276.9 ft
Flow Rate(TDF)	(	)
Shaft Rotational Speed	(	)
Number of Impeller Blades	7	7

Table 3.3.2-2 US-APWR RCP Pulsation Amplitude for the Vibration Analysis

	Shaft Rotational Speed (N)	Blade Passing Frequency (NZ)	2nd Harmonic of Blade Passing (2NZ)
Frequency(Hz)	(		)
Amplitude(psi)	(		)

Table 3.3.2-3 SYSNOISE Code Verification Analysis

		Boundary Condition	Application for PWR Reactor	Resonance mode frequency error with theoretical value	Judgment
1	Annulus	Top closed Bottom open	Down Comer	( )	Acceptable
2	Cylinder	Top closed Bottom open	Upper Plenum	( )	Acceptable

Table 3.3.2-4 SYSNOISE US-APWR Acoustic Model

Components	Use of Simplified method	Remarks
RCP	Simulated as a point source of pressure wave	Figure 3.3.2-6
Inlet Pipe	(Not Simplified)	
Vessel Down Comer	(Not Simplified)	
Lower Plenum	(Not Simplified)	
Lower Support Plate	Damping matrix for Pressure loss model	Figure 3.3.2-5
Core (Fuel Assembly)	Not Simulated	
Neutron Reflector	Not simulated. (Considered as core boundary walls)	
Upper Core Plate	Damping matrix for Pressure loss model	Figure 3.3.2-5
Upper Plenum	Number reduction of column structures (GT / USC / TSC)	
Outlet Pipe	(Not Simplified)	
Steam Generator	Simulated to the inlet of SG Plenum	

Table 3.3.2-5 Mechanism by Sound Attenuation in Reactor(Input for US-APWR Analysis)

Sound attenuation mechanism	Description	Analysis in DCD
Perforated plate	Attenuation of acoustic energy is caused by resistance during passing through holes of perforated plates.	Considered ;spray nozzle, lower core support plate, and upper core plate
Viscosity of fluid itself	Acoustic energy is converted to thermal energy during shear deformation due to viscosity of fluid itself.	Not considered
Friction between fluid and wall	Acoustic energy is converted to thermal energy when fluid moves contacting the wall.	Not considered
Coupling of eddy	Acoustic energy is converted to eddy energy by eddy in fluid with steady flow.	Not considered
Attenuation due to vibration of internals	Converted to kinetic energy of internals	Not considered

Table 3.3.2-6 Value of Sound Attenuation with SYSNOISE Input(Input for US-APWR Analysis)

Location	Value of acoustic resistance Re[ ]	Remarks
Spray nozzle		Acoustic impedance has an effect on frequency response.
Lower core support plate		
Upper core plate		

Table 3.3.2-7 RCP Pulsation Loads on Core Barrel and Neutron Reflector (Input for US-APWR Analysis)

Components	Frequency (Hz)	Pressure Amplitude (psi)
Core Barrel (down comer)		
Neutron Reflector (core)		

Table 3.3.2-8 RCP Pulsation Loads on the Upper Plenum Structures (Input for US-APWR Analysis)

Components	Beam Mode Nodal Number	Pressure Gradient (psi/in)		
RCCA Guide Tube				
Upper Support Column				
Top Slotted Column				

Table 3.3.2-9 RCP Pulsation Loads on Core Support Plates(Input for US-APWR Analysis)

Components	Frequency (Hz)	Pressure Difference (psi)
Lower Core Support Plate		
Upper Core Support Plate		

Figure 3.3.2-5 SYSNOISE Acoustic Analysis Model (Modeling of Components)

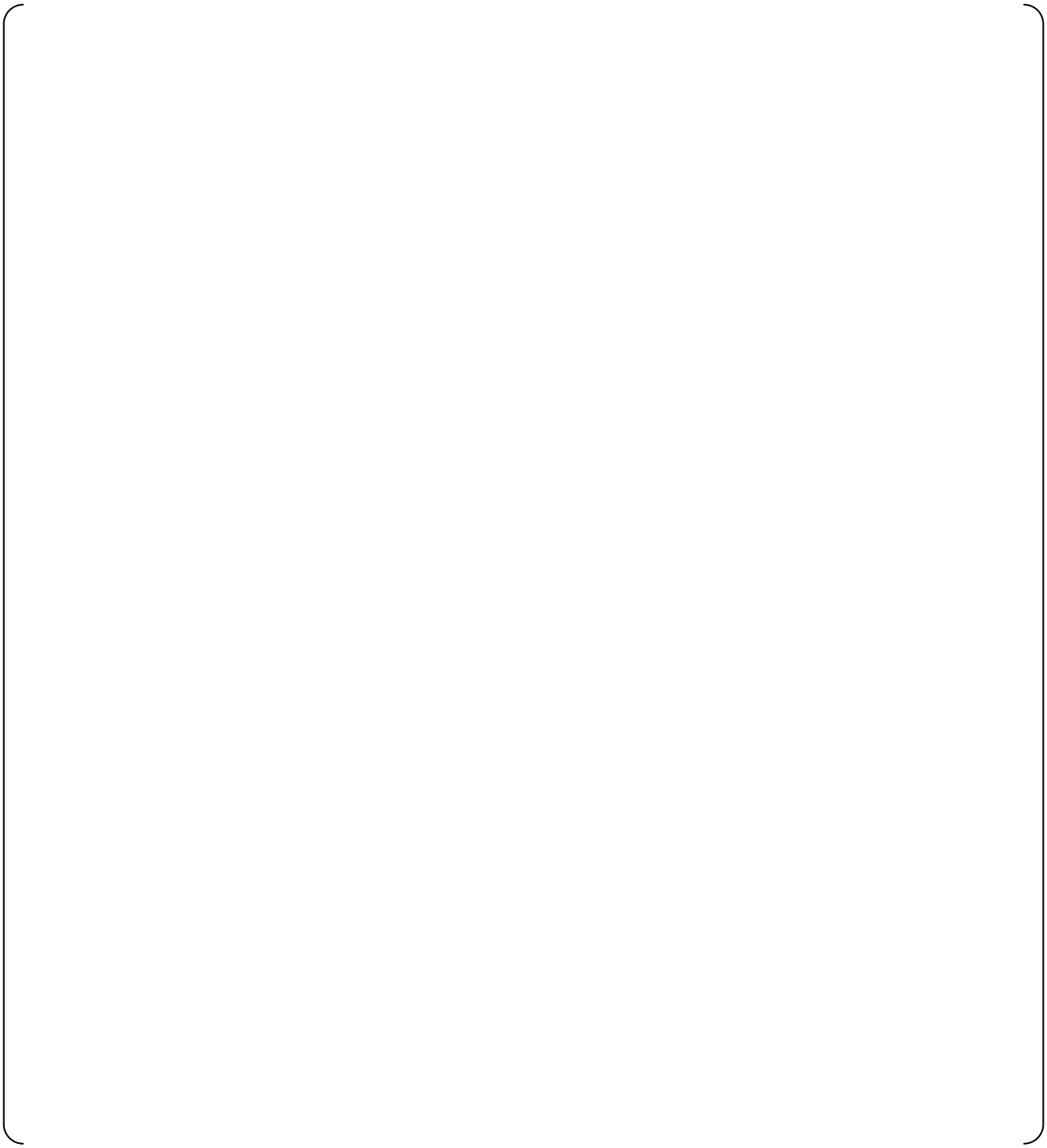

Figure 3.3.2-6 SYSNOISE Acoustic Analysis Model (Boundary Condition)

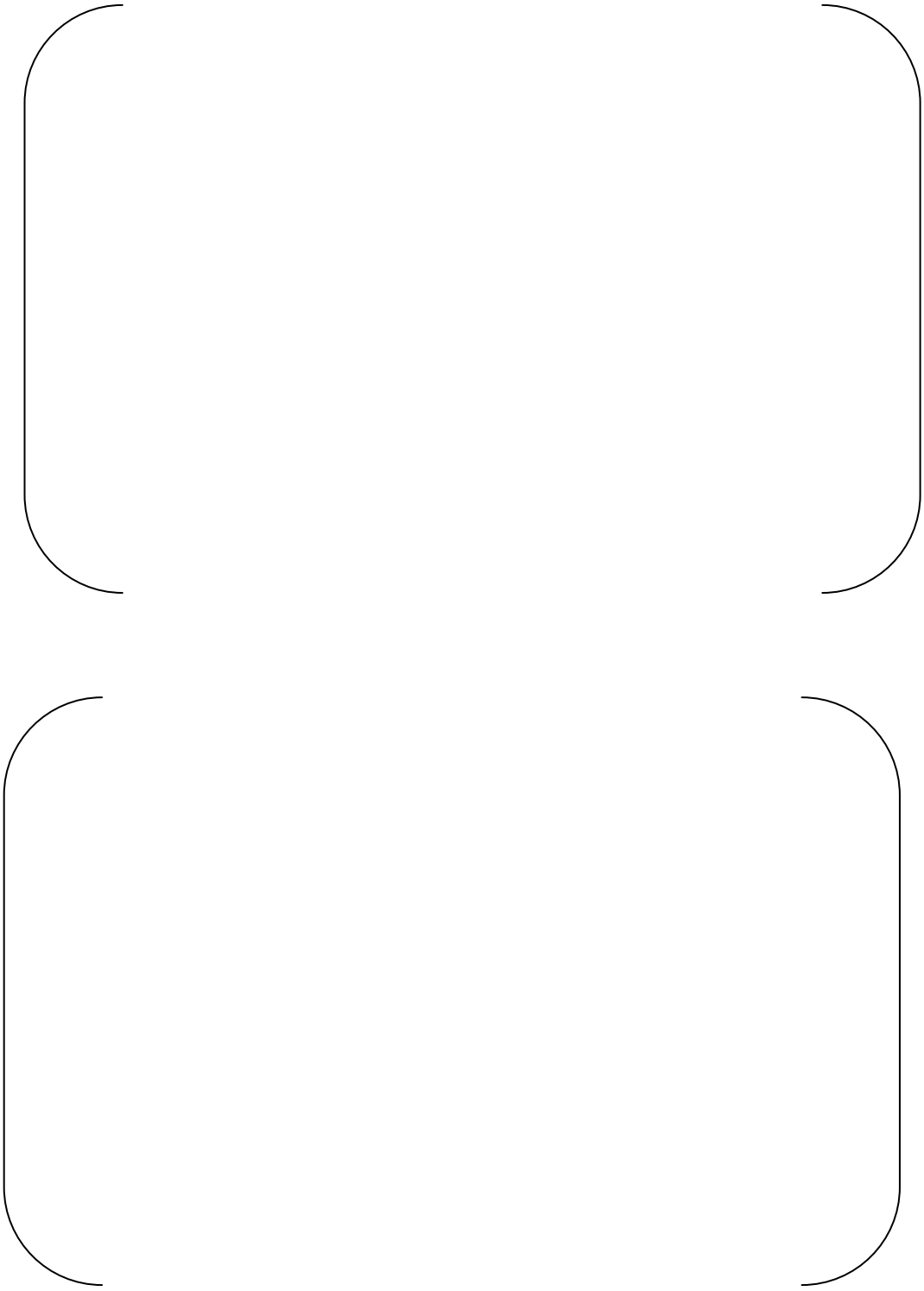

Figure 3.3.2-7 Samples of the SYSNOISE Acoustic Analysis Result

Figure 3.3.2-8 RCP Pulsation Wave on the Core Barrel (N+NZ)

Figure 3.3.2-9 RCP Pulsation Wave on Inside of the Neutron Reflector (N+NZ)

Figure 3.3.2-10 RCP Pulsation Wave on a RCCA Guide Tube (2NZ)

3.3.3. Results of the US-APWR Vibration Analysis

3.3.3.1. Response Analysis Conditions

The vibration response analysis conditions for the US-APWR reactor internals are summarized in Table 3.3.3-1. Cases identified as B1 to B6 are analyses for the US-APWR normal operating conditions with the fuel assemblies, and cases C1 to C6 are those for the HFT conditions.

The vibration responses of the core barrel and the neutron reflector including shell modes due to the downcomer flow turbulence are obtained from Case B1 or C1 with the 3D solid system model. There is no account of the effect of cross flow loads because the core barrel and the neutron reflector vibration response have been verified with the downcomer flow turbulence alone in the benchmark analysis case A1 in Table 3.2.3-1 of J-APWR 1/5 SMT, as discussed in Subsection 3.2.3 (3) b.

The flow induced vibration responses of the structures in the lower and the upper plenum were determined from the case B3 or C4 with the 3D beam system model with all of the flow induced loads. Case B2 or C3, the system beam model with the downcomer flow turbulence, were referred to separate the effect of the base excitation from the results of B3 or C4.

The vibration responses due to the RCP pulsations were represented by analyses case C2, C5 and C6 under without the core conditions, because the fuel assemblies act as the acoustic absorbers.

In discussed above, the all of the key supports, such as the radial keys on the bottom of the core barrel, the upper radial reflector alignment pins and the upper core plate alignment pins were assumed to be free for the larger response. The design loads for these key supports were determined the case B5 and B6 by the 3D beam system model with the spring elements to represent the key supports.

3.3.3.2. Vibration Responses under the Full Power Conditions

(1) Vibration Response

a. Responses due to the Flow Induced Vibration

The flow induced response by the analysis of the US-APWR reactor internals are shown in Table 3.3.3-2.
The relative displacement between the core barrel and the reactor vessel with the downcomer turbulence was about twice of that in the J-APWR SMT benchmark results scaled to the actual dimensions. It is supposed by the effect of the decrease of the damping ratio from [ ]% with the J-APWR SMT benchmark analysis to 1% with the US-APWR analysis.

b. Responses due to the RCP pulsation

The RCP induced vibration responses by the analysis of the US-APWR are shown in the Table 3.3.3-3. For the RCP induced vibration, the response level depends on the vibration characteristics of the each component. For the core barrel, and the structures in the upper or lower plenum, the RCP induced response (0-peak) was not larger than the flow induced responses ([ ] x rms). But for the neutron reflector, the RCP induced vibration response was equivalent with the FIV response in displacement. Note that this RCP induced response was based on the acoustic analysis with empty the core cavity without the fuel assemblies. In the US-APWR operating condition after the core loading, the RCP induced response will be reduced by the acoustic damping with the fuel assemblies between the inside walls of the neutron reflector.

(2) High Cycle Fatigue Evaluation

a. Evaluation method

The evaluation was performed considering the maximum displacement (strain) or components with the maximum values in dynamic response results with combination of the loads caused by the flow turbulence and the RCP pulsation response (horizontal and vertical), which were obtained from the above.

The high cycle fatigue was evaluated by obtaining of the stresses and caused by the largest dynamic responses and considering the stress concentration factors were applied in the calculation of the peak stresses. Since the uniform cross sections of the core barrel and column structures have lower stress, a stress concentration factor 5 was used. The cross-shaped legs in the fixed parts of the column structures, however, have the higher stress due to the larger loads. Therefore, a stress concentration factor 2 was used to calculate the peak stress according to the FE model analysis.

The alternating peak stress due to the flow turbulence and due to the RCP pulsation is determined from the FE analysis response as following equations.

$$Sa_{FIV} = [\ ]\ (\sigma\ rms_{FIV})\ K\ (E/E\ p)$$

$$Sa_{RCP} = (\sigma\ 0\text{-}P_{RCP})\ K\ (E/E\ p)$$

Where,
Sa_{FIV} : alternating peak stress due to the flow
Sa_{RCP} : alternating peak stress due to the RCP pulsation
$\sigma\ rms_{FIV}$: rms amplitude of alternating stress due to the flow
$\sigma\ 0\text{-}p_{RCP}$: zero to peak amplitude of the alternating stress due to the RCP
K : stress index for the structural discontinuous

E : Young's modulus in the room temperature
Ep : Young's modulus in the plant operating condition
〔 〕 : ratio between 0-peak and rms value for random vibration response

The combined alternating peak stress was assumed to be the simple sum of those due to the flow turbulence and the RCP induced pulsation as shown in the following equation.

$$Sa_{total} = Sa_{FIV} + Sa_{RCP}$$

b. Evaluation results

The evaluation results of the high cycle fatigue analysis are summarized in Table 3.3.3-4. The margin of safety of the upper plenum structures are improved to minimum [ ] from [ ] in Revision 1 Report because of the updating cross flow forcing functions considering with the cross flow velocity distribution in elevations. This results is reasonable based on the expected bias in the assumption of the uniform cross flow with the maximum velocity which is discussed in the response to RAI 498-3782 Question 03.09.02-75 and RAI 614-4853 Question 03.09.02-90 as shown in Appendix-J.
Over all minimum margin of safety is [ ] with the support column of the lower diffuser plate assembly. Considering with the conservative cross flow loading ([ ] times to the best estimate value as discussed in Subsection 3.2.4 (2)), the margin of safety [ ] can be acceptable in this case.

As the conclusion, the reactor internals of the US-APWR have the sufficient margin of safety against the high cycle fatigue as specified in ASME Code Section III, Subsection NG. (Reference (2))

(3) Interface load

The vibration load acting on the alignment key supports are summarized in Table 3.3.3-5.
These are applied for the stress or functional analysis combined with other design loads.

3.3.4. Structural Responses in the Preoperational Test Conditions

The analysis simulating the hot functional testing condition was performed. Because the hot functional test is conducted before the core loading, the fuel assemblies were excluded from the analysis models for the normal operating conditions. The increase of total flow rate ([ ]%) was assumed by the effect of the reduction of the flow resistance in the core was reflected to the flow induced forcing functions with the square of flow rates from those in the normal operating conditions.

The vibration responses in the hot functional test are used for following assessments.
(a) Needs of the vibration measurement after the core loading by comparison with the vibration responses under the normal operating conditions
(b) Selection of the transducer type and locations in the hot functional test as discussed in Section 4.

(1) Comparison with Normal Operation Response

The typical vibration responses in the preoperational hot functional testing condition (without the core) are compared with the initial startup testing after core loading (with core) of the US-APWR as shown in Table 3.3.3-2, Figure 3.3.4-1 and Figure 3.3.4-2.

The ratio of vibration responses in the hot functional test conditions to those after core loading are within the ratio of [ ] to [ ]. It is concluded that the vibration responses in the hot functional test conditions are the equivalent or slightly larger than those after the core loading. These are because of the flow rate increase with the elimination of fuel the assemblies and the subsequent pressure loss. As discussed with Table 3.3.1-1, the effect on the vibration characteristics of the core loading is also small.

Thus, in the preoperational test of the prototype plant, the results of the vibration measurements after the core loading are bounded by the measurements before the core loading and only measurements before the core loading will be necessary.

(2) Vibration Responses on the each Transducer Location

The transducer type and locations for the vibration measurement are discussed in Section 4 of this program. The responses on each transducer were predicted from the analysis results as follows.

a. Accelerometers: The time history of acceleration at the transducer location was obtained by the second order differential of the displacement time history from the analysis. The rms amplitude is determined from the acceleration time history.

b. Strain gages : The amplitude of the dynamic strain was determined from the dynamic bending moment from the analysis divided with the section modulus and the Young's modulus.

The predicted responses of the transducers are summarized in Table 3.3.4-1.

Table 3.3.3-1 Analysis Matrix(US-APWR Analysis Conditions)

Case ID	Configuration	Model Type	Forcing Functions[1)]	Key Support Gap[2)]	Ratio to the critical damping
B1	US-APWR with Core	Solid	DC	Open	[ ]%
B2	↓	Beam System	DC	↓	↓
B3	↓	↓	DC+LP+UP+V	↓	↓
B4	↓	↓	RCP	↓	↓
B5	↓	↓	DC+LP+UP+V	Close	↓
B6	↓	↓	RCP	Ditto	↓
B7	↓	Single Beam	UP	out of model	↓
C1	US-APWR without Core	Solid	DC	Open	↓
C2	↓	Ditto	RCP	↓	↓
C3	↓	Beam System	DC	↓	↓
C4	↓	↓	DC+LP+UP+V	↓	↓
C5	↓	↓	RCP	↓	↓
C6	↓	Single Beam	RCP	out of model	↓

Note 1) DC : Downcomer Turbulence
LP : Lower Plenum Cross Flow
UP : Upper Plenum Cross Flow
V : Vertical Load
RCP : RCP Pulsation

Note 2) Boundary conditions at the key supports in the bottom of the core barrel and the top of the neutron reflector

Table 3.3.3-2 US-APWR Reactor Internals RMS Response (FIV) (US-APWR Analysis Results)

Components	Remarks	RMS Response		
		with core	without core	Ratio
Core Barrel-RV Relative displacement	Bottom (Beam+Shell)			
Neutron Reflector-Core Barrel Relative displacement	Top (Beam)			
	Top (Shell)			
Lower Diffuser Plate Support column	Moment			
Upper Diffuser Plate Support column	Moment			
RCCA Guide Tube	Moment			
Upper Support Column	Moment			
Top Slotted Column	Moment			

Table 3.3.3-3 US-APWR Reactor Internals Response (RCP pulsation) (US-APWR Analysis Results)

Components	Remarks	0-p response
Core Barrel-RV Relative displacement	Bottom	
Neutron Reflector-Core Barrel Relative displacement	Top (Beam)	
	Top (Shell)	
Lower Diffuser Plate Support column	Moment	
Upper Diffuser Plate Support column	Moment	
RCCA Guide Tube	Moment	
Upper Support Column	Moment	
Top Slotted Column	Moment	

Table 3.3.3-4 High Cycle Fatigue Evaluation Based on Analysis Responses (US-APWR Analysis Results)

Components	Locations or parts	Alternating Stress (ksi)			Limit	Margin of Safety [1)]
		Flow	RCP	Total		
Core Barrel	Flange				13.6 ksi	
Neutron Reflector	Block Alignment Pin					
Diffuser Plate Assembly	Support Column Upper Assembly Lower Assembly					
UCS	Flange Skirt					
RCCA GT	Top of Lower GT					
USC						
TSC						

Note

1) Margin of safety = (Allowable Stress Limit) / (Alternating Stress) - 1

Table 3.3.3-5 Interface Loads(US-APWR Analysis Results)

	Load (lbf, FIV 4.5rms+RCP 0-P)
Core Barrel Radial Key	
Neutron reflector alignment Pin	
Upper core plate Alignment Pin	

Table 3.3.4-1 Estimated Transducers Responses in US-APWR Reactor Internal Vibration Measurement in Hot Functional Testing (US-APWR Analysis Results)

Subassembly	Location and Transducer Type	Sensitive Direction	Flow Excitation Response (rms)	RCP Pulsation Response (0-peak)
Core Barrel	Flange Strain Gages	axial		
	Middle: ACC	radial		
Lower Core Support Plate	1-D Accelerometers	vertical		
Neutron Reflector	1-D Accelerometers	vertical radial		
	Displacement Transducers	radial		
Upper Diffuser Plate Support Column	Strain Gages	axial		
Lower Diffuser Plate Support Column	Strain Gages	axial		
Upper Core Support	Skirt: Strain Gages	axial		
	1-D Accelerometers	vertical		
Upper Support Column	Strain Gages	axial		
Top Slotted Column	Strain Gages	axial		
Upper Guide Tube	Strain Gages	axial		
Lower Guide Tube	Strain Gages	axial		

with core without core

Figure 3.3.4-1 CB Bottom / RV Relative Displacement FFT Analysis Results (US-APWR Analysis Results)

with core without core

Figure 3.3.4-2 NR Top / CB Relative Displacement FFT Analysis Results (US-APWR Analysis Results)

3.4. Adverse Flow Effects

3.4.1. Evaluation of the Cross Flow Velocity

The cross flow velocity around the structure in the lower and upper plenum of the reactor vessel was evaluated in the manner as described in Subsection 3.2.2.2 (1). The maximum flow velocity was referred in the evaluations of the vortex shedding and fluid elastic instability.
The calculation results of the cross flow velocities are shown in Table 3.4.1-1 as “U”.

3.4.2. Margin for Vortex Shedding Lock-in and Fluid Elastic Instability

For the column structures in the reactor vessel lower plenum and the upper plenum, the margin of safety for the cross flow induced vibrations were evaluated based on the FIV guidelines in the ASME Code Section III (Reference (2), Appendix-N1300).

(1) Fluid elastic instability

The critical velocity is estimated with the Conner’s equation as below.

$$Uc / fn\ D = C\ (m\ \delta / \rho\ D^2)^{\alpha}$$

Here,

U	: axial flow velocity (in/s)
Uc	: critical flow velocity for fluid elastic instability (in/s)
D	: diameter (in)
m	: mass per unit length (lb/in)
δ	: logarithmic damping ratio
fn	: fundamental mode frequency of column（Hz）
ρ	: fluid mass density (lb/in^3)
C, α	:coefficients for critical velocity, C=2.4 and α =0.5 are applied as most conservative value which are suggested in FIG.N-1331-4 in the APPENDIX N of Reference (2).

The evaluation results are shown in Table 3.4.1-1. The US-APWR reactor internals have the sufficient margin of safety against the fluid elastic instability.

(2) Vortex shedding lock-in
The design guidelines to avoid vortex shedding lock-in in the ASME Code Section III (Reference (2), appendix N1324) were followed check the column structures in the lower plenum and those in the upper plenum based on the computed natural frequencies. The results of vortex shedding lock-in evaluation are summarized in Table 3.4.2-1. As result, the lock-in of vortex shedding is avoided for all reactor internal structures.

3.4.3. Conclusions of the Assessment for Adverse Flow Effects

It is concluded that the reactor internals of the US-APWR have sufficient margins of safety against the adverse flow effects due to the cross flow, including the lock-in of vortex shedding or fluid elastic instability.

Table 3.4.1-1 Cross Flow Parameters and Margin for Fluid Elastic Instability (US-APWR Analysis Results)

	U (in/s)	D (in)	fn (Hz)	fs (Hz)	Vr = U/fn D	$m\delta/\rho D^2$	Uc (in/s)	M.S = Uc/U-1
Lower Diffuser Plate Support Column								
Upper Diffuser Plate Support Column								
RCCA Guide Tube								
Upper Support Column								
Top Slotted Column								

M.S: Margin of Safety

Table 3.4.2-1 Evaluation for Vortex Shedding Lock-in(US-APWR Analysis Results)

ASME Design Guidelines to avoid vortex shedding lock-in	N1324.1-(a) U/fn D<1.0	N1324.1(c) U/fn D<3.3 and $2m\delta/\rho D^2$>1.2	N1324.1(d) fn<0.7fs or fn>1.3fs	Evaluation
Lower Diffuser Plate Support Column	—	X	X	Lock-in avoided
Upper Diffuser Plate Support Column	X	X	X	Lock-in avoided
RCCA Guide Tube	X	—	X	Lock-in avoided
Upper Support Column	—	X	X	Lock-in avoided
Top Slotted Column	X	—	X	Lock-in avoided

Note

X : satisfied

—: not satisfied

3.5. Acceptance Criteria

Following Regulatory Guide 1.20 and SRP 3.9.2, the data from the preoperational vibration test described in Subsection 3.9.2.4, including the accelerations, amplitudes, strains and component modal frequencies, will be compared with the corresponding predicted and allowable values. The following lists the specific items to be evaluated together with their acceptance criteria. In general, Category 1 criteria are related to the integrity of the components while Category 2 criteria are related to the adequacy of the analysis technique. Contingency plans in case these criteria are not met are given.

(1) Modal Frequencies

Category 2 Criterion: The measured frequencies for the fundamental beam mode and the lowest shell modes must not differ from the predicted values by more than 10%.

(2) Damping Ratios

Category 2 Criterion: The measured damping ratios, as determined from the half-power point method, must be within a factor of 2.0 of what are used in the prediction analysis.

(3) Forcing Function due to Flow Turbulence

Category 2 Criterion: The rms amplitude of measured broad –band random turbulence pressure fluctuation in the downcomer must be within a factor of 2.0 of the corresponding predicted values in the analysis.

(4) Forcing Function due to RCP Pulsation

Category 2 Criterion: The measured 0-p amplitude of the RCP induced acoustic loads in the downcomer and the upper plenum must be within +0 or -50% of the corresponding predicted values in the analysis.

(5) Stress due to FIV and RCP Loads

Category 1 Criterion: For deterministic stresses (such as those induced by the RCP loads), the stress levels as deduced from the measured strains (using strain gages) must not incur any fatigue usages on the components. For random stresses (such as those induced by the flow turbulence), the stress levels as deduced from [ ] times the measured rms strains must not incur any fatigue usages on the components. The combined stresses of the above two, as determined by the absolute sum, must not incur any fatigue usages on the components.

Category 2 Criterion: For deterministic stresses, the stress levels as deduced from the measured strains must be within + 0 or – 50% of the corresponding computed values in the prediction analysis. For random stresses, the rms stresses as deduced from the measured rms strains must

be within a factor of 3.0 of the corresponding computed values, with the correction of damping ratios between measured and analysis condition.

(6) Similarity of the Dynamic System Model between FIV and Seismic/LOCA

Category 2 Criterion: The dynamic models in the FIV and in the seismic/LOCA analyses are generally similar except in the assumed boundary conditions. Because of the much larger displacements experienced in seismic and LOCA events compared with those experienced in the flow induced vibrations, the assumed boundary conditions in the former type of analysis may be different from those in the FIV analyses in order to better simulate the larger displacements anticipated.

(7) Adverse Flow Effects

Category 1 Criterion: No fluid-elastic instability or lock-in vortex induced vibration is experienced in the preoperational test.

(8) Contingency Plans in Case the Acceptance Criteria are not met

Category 1 Criteria
In case any category 1 criterion is not met, the overall impact on the design of the reactor internals will be evaluated. The reactor will not put into operation until it is sure that the design can accommodate the larger than expected vibration responses.

Category 2 Criteria
In case any category 2 criterion is not met, the difference will be resolved by the post-preoperational test analysis.

4.0 VIBRATION AND STRESS MEASUREMENT PROGRAM

In accordance with the United States Nuclear Regulatory Commission Regulatory Guide 1.20 Revision 3, a vibration measurement program is developed for the first US-APWR unit. US-APWR has reactor internals based on well-proven 4-loop plant but the reactor core is enlarged and the new design structures such as the neutron reflector are adopted. As written in section 1, the reactor internals is classified to “Prototype” for the first US-APWR, the preoperational measurement program is planned.
The purpose of the measurement program is to verify the structural integrity of the reactor internals, determine the margin of safety associated with the steady-state and anticipated transient conditions for the normal operation, and confirm the results of the vibration analysis.
Instrumentation consisting of the strain gages, accelerometers, pressure transducers and displacement transducers are mounted on the selected assemblies and their specified locations. The lead wires of the transducers inside the reactor vessel will be guided to outside the vessel through the ICIS and / or thermocouples penetrations in the vessel head. The ICIS thimbles and thermocouples will not be installed prior to the core loading.
The measurements will be conducted without a core during cold hydraulic test (CHT) and the hot functional test (HFT), and with core but pre-critical phase in initial start-up test (IST). However, the measurement in with the core conditions can be eliminated if it can be shown that the conditions in without the core result severe response relative to without the core conditions. In each stage, testing will be done at all steady state and pump startup / shutdown conditions corresponding to the normal and part loop operation.
All of the transducers, lead wires and attachments inside the reactor vessel will be removed after the all measurements will be done.

4.1. The Data Acquisition and Reduction System

4.1.1. Transducer Types and Specifications

The environment of preoperational test including a cold hydraulic test and hot functional test is in water and covered by the conditions of the pressure at about 3100 psi and temperature of [ ] °F. All of the transducers installed inside the reactor vessel should endure these conditions. The insulation tests will be conducted for all of the transducers at a test pressure and temperature in water to confirm their integrity. Helium leak test will be also conducted.

(1) Strain Gage

The frequency response should be ± [ ]% in 0Hz -[ ]Hz to cover the secondary blade passing frequency of [ ] Hz, and the dynamic resolution is expected to be better than [ ] micro strain.
“[ ]” high-temperature weldable strain gages will be used. The gages will be attached to the locations described in previous section by the electrical resistance spot welds.
The dual head gages which have two sensing units are bundled to one lead wire will be used to reduce the number of wires through the penetration.

(2) Accelerometer

Two types of accelerometers will be used. One is "[ ]" that will be installed inside the flow hole of the neutron reflector. The frequency response should be better than ±[ ]% in [ ] Hz - [ ]Hz. The other type is "[ ]". The frequency response of this should be in "[ ]". The frequency response of this should be ±[ ]% in [ ]Hz-[ ]Hz to cover the secondary blade passing frequency of [ ] Hz, and the resolution is expected to be better than [ ]g.

The frequency response of this should be ±[ ]% in [ ]Hz-[ ]Hz to cover the secondary blade passing frequency of [ ] Hz, and the resolution is expected to be better than [ ]g.

(3) Displacement Transducer

The frequency response should be better than [ ]% in [ ]Hz-[ ]Hz and the dynamic resolution should be better than [ ] mils.
There are two options for the transducer. One is the cantilever type that is mounted on the top of the neutron reflector and its end is contacted to the core barrel inner surface. A pair of the strain gages is attached on the root to measure the bending strain. The relationship between the strain and the relative displacement will be obtained prior to the test. The other option is to use the non-contacting eddy current type transducer like "[ ] ". The transducer type will be determined in the detail design phase.

(4) Pressure Transducer

The frequency response should be better than [ ]% in [ ]Hz- [ ]Hz to cover the secondary blade passing frequency of [ ] Hz. "[ ]" will be selected.

4.1.2. Transducer Locations

The type, number and locations of the measurement program instrumentation are shown in Table 4.1-1 and Figures 4.1-1 through 4.1-8. The lead wires of the transducers will be guided along the reactor internals surface and go through the penetrations on the reactor vessel head.

(1) Core Barrel / Lower Core Support Plate

The core barrel and the lower core support plate are enlarged in their diameters from current. The frequency response of this should be ± [ ]% in [ ]Hz - [ ]Hz to cover the secondary blade passing frequency of [ ] Hz, and the resolution is expected to be better than [ ]g.
4-loop plants, which affect to the excitation force and the vibration characteristics of the lower internals assembly.
Three pressure transducers are installed on the outer surface of the core barrel as the inputs to evaluate the forcing function of the down comer.

To confirm the vibration response of beam mode for the lower internals, three strain gages are needed to separate the vibration response of horizontal two directions and a vertical direction; however, total four gages will be installed in considering of the redundancy. These strain gages will be installed on just below the core barrel flange outer surface. Furthermore, two additional gages will be installed on inner surface to confirm the stress caused from the local bending of the core barrel flange.
Accelerometers are needed to be installed on the outer surface of the core barrel to obtain the shell mode responses. In order to confirm the response against the 1st frequency of the pump pulsation (approx.[ ]Hz), the shell mode natural frequencies up to [ ]Hz should be identified. According to the tentative analysis results, acquisition of 4h mode is corresponding to this target, and thus four accelerometers will be installed.
An accelerometer will also be installed on the center of lower surface of the lower core support plate to acquire the vertical vibration characteristics.

The frequency response of this should be ± [ ]% in [ ]Hz - [ ]Hz to cover the secondary blade passing frequency of [ ] Hz, and the resolution is expected to be better than [ ]g.

(2) Neutron Reflector / Tie Rod

Since a neutron reflector is the new design structure, it is necessary to acquire the basic behavior data and confirm that unexpected vibration does not occur. Four accelerometers in the radial direction will be installed to consider the symmetry and redundancy, and an accelerometer in the vertical direction will be installed. The relative displacement between the neutron reflector and the core barrel is also measured. Two displacement transducers will be mounted on the top surface of the neutron reflector.
A tie rod of the neutron reflector is also the new design structure and its natural frequency is predicted to be low, it is planned to acquire the vibration response to confirm the structural integrity. Two strain gages will be installed for a tie rod.

(3) Lower Plenum Structures

In regards to the lower plenum structures, these structures consist of two sub assemblies, the upper diffuser plate assembly and the lower diffuser plate assembly. All of the diffuser plate support columns (here after support columns) are tightly connected by the diffuser plate; so the expected vibration response of each support column should be similar. In addition, the natural frequency of the assembly and the stress of the support columns can be confirmed by the strain measurement on a support column for the each assembly. Considering the original design of these structures, the strain on two support columns will be measured for each assembly to maintain sufficient redundancy. Six strain gages are installed to the upper diffuser plate support columns to evaluate the horizontal, rotation and oval motions, and five strain gages are installed to the lower diffuser plate support columns to evaluate the horizontal, vertical and rotation motions.

(4) Upper Core Support / Upper Core Plate

The upper core support and the upper core plate are enlarged in their diameters from the current 4-loop plant, which affect to the forcing function of the upper plenum. To obtain the forcing function, a pressure transducer is installed on the lower surface of the upper core support plate rim.
The design difference also affects the vibration characteristics of the upper internals assembly. To confirm the vibration response of the beam mode for the upper internals, strain gages will be installed on the top end of the upper core support skirt. Two strain gages are needed to confirm two directional behaviors. An accelerometer will also be installed on the center of the upper surface of the upper core support plate to acquire the vertical vibration characteristics.

(5) Upper Plenum Structures

A top slotted column is a first-of-a-kind design in the US-APWR. For this component, three strain gages are installed to obtain horizontal two directional responses and for the redundancy. Although the upper support column design is almost the same as that of the current 4-loop plant, it is planned to measure since the flow pattern in the upper plenum will be changed from the current 4-loop plant. Two strain gages are installed for this component.
The mixing device and the level instrumentation support tube are not instrumented because these components are located where the cross flow velocity is not so high, and have been successfully used in the conventional plants.

(6) RCCA Guide Tube

The guide tube design in the US-APWR has been changed from that of the current 4-loop plant as following points;
- Adoption of square pipe for the lower guide tube enclosure,
- Extension of the upper guide tube.

Therefore, strain gages will be installed to confirm the vibration characteristics and the response on both top end of the lower guide tube and bottom end of the upper guide tube. Three strain gages will be installed to obtain three directional responses for one specific lower guide tube. For the same guide tube, two strain gages will be installed in the upper guide tube. In addition to that, two strain gages will be installed on another lower guide tube in consideration of the redundancy since the guide tube has a safety related function and one of the most important subassembly of the reactor internals. The guide tube closest to outlet nozzle will be selected to the measurement.

(7) Head Plenum Structures

The excitation force in head plenum is predicted not to be severe because the flow velocity in this area is not so high. Therefore, the measurement for the head plenum structures such as the thermocouple conduit support columns and the ICIS thimble assemblies are unnecessary.

(8) The transducers exterior the reactor vessel

The accelerometers will be mounted on the bottom and head vessel in order to monitor the base motion.

4.1.3. Precautions to Ensure Acquisition of Quality Data

All of the transducers are tested before they are installed to the components. The autoclave test at each test temperature and pressure for 24 hours, and the sensitivity, background noise level and resistance of each transducer is confirmed after the test. The calibration test for all transducers will be also performed in this phase.
The frequency band from [ ] Hz to [ ] Hz, which covers second blade passing frequency of the RCP, should be recorded. Theoretically the upper frequency limit is a half of the sampling rate, and then the sampling rate should be over [ ] Hz. In this program, the sampling rate is set to [ ] Hz considering some margin.

4.1.4. Online Data Evaluation System

The data recording system is designed to record the time historical electrical signals from the transducers on the data storages of the personal computer as the digital data.
The transducers hard cable (mineral insulation cable) will be terminated at a junction box. The signal is connected to the data acquisition system via the soft cable. The charge signals from the accelerometers and pressure transducers will be input to the charge amplifiers, while the strain gages will be connected to the dynamic strain amplifiers to convert to the voltage signal. These voltage signals will be lead to the personal computer via the frequency filters and the analog-digital (A/D) converters.
The signal level of each transducer will be checked prior to the test to adjust the gains of the charge amplifiers for the accelerometers and pressure transducers. The dynamic strain amplifiers will be balanced and their sensitivities will be selected.
The spectrum of each signal will be monitored through the test to verify the recording process and adequacy of the level of data signals.

4.1.5. Procedure for Determining Frequency, Modal Content and Maximum Values of Responses

Reduction of the data will be done during the test to determine whether the responses are within the acceptable or not. The spectrum analyzer will be used to analyze the natural frequencies of each component, and the vibration characteristics obtained from the measurement results will be compared with the prediction analysis results described in Subsection 3.3. The maximum stress values will be also calculated to confirm the structural integrity.

4.1.6. Bias Errors and Random Uncertainties

Acceptance criteria, described in Subsection 3.5, are the maximum values. These values do not reflect the effect of bias errors and / nor uncertainties due to the errors in the measured values. The bias error and uncertainty depend on the accuracy of both the acquisition and reduction of the data. The accuracy of the data acquisition is primarily a function of the instrument error, and the accuracy of the data reduction is a function of the number of data samples, the bandwidth, etc. Thus the all bias errors and random uncertainties are defined after the specification of data acquisition systems is determined.

Table 4.1-1 Reactor Internals Transducers Arrangement

Subassembly	Transducer Type	Number	Sensitive Direction
Core Barrel			
Lower Core Support Plate			
Neutron Reflector			
Tie Rod			
Upper Diffuser Plate Support Column			
Lower Diffuser Plate Support Column			
Upper Core Support			
Upper Support Column			
Top Slotted Column			
Upper Guide Tube			
Lower Guide Tube			
Sub Total			
Total			-

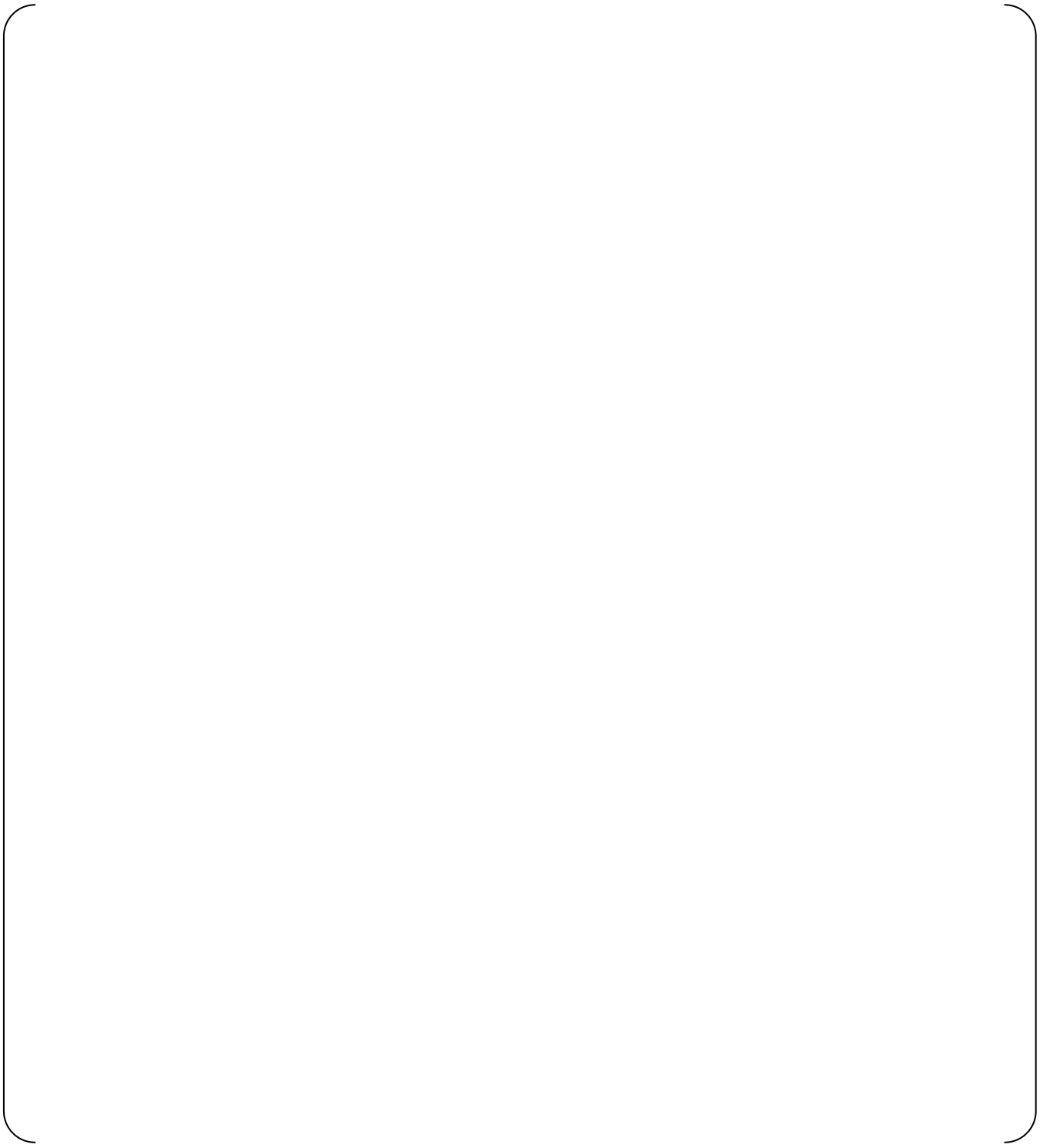

Figure 4.1-1 Schematic View of Transducers Arrangement

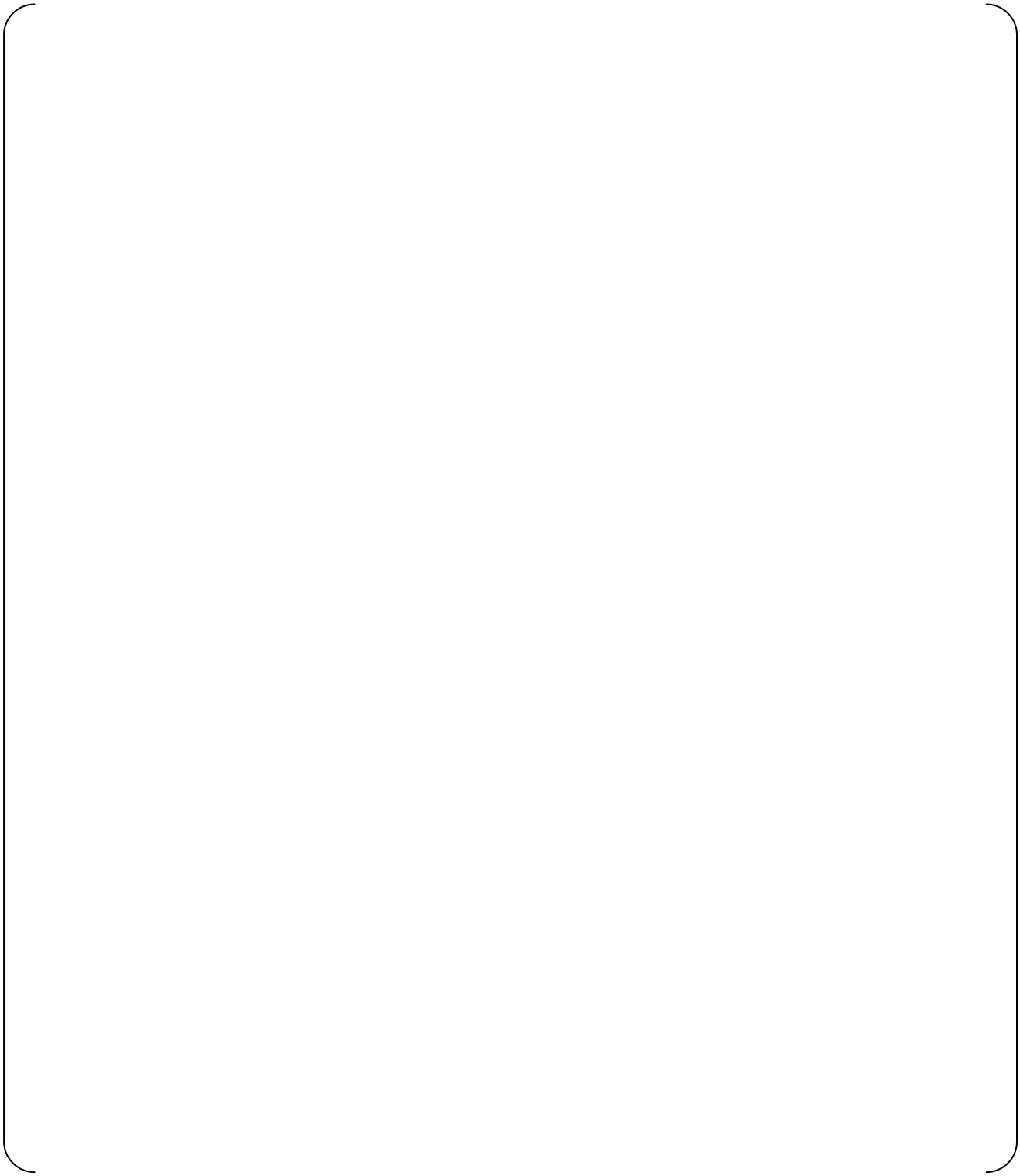

Figure 4.1-2 Core Barrel Measurement

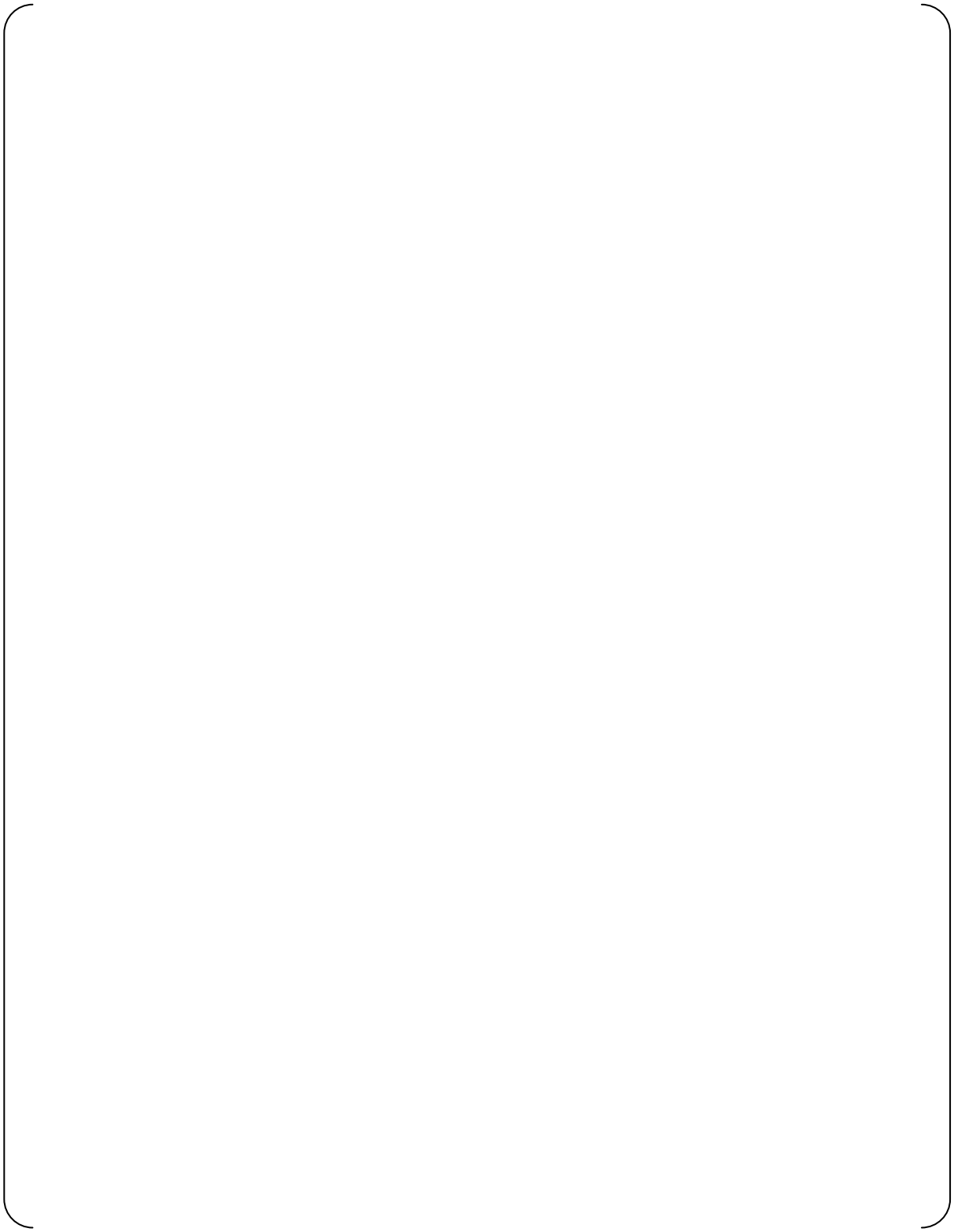

Figure 4.1-3 Neutron Reflector Measurement

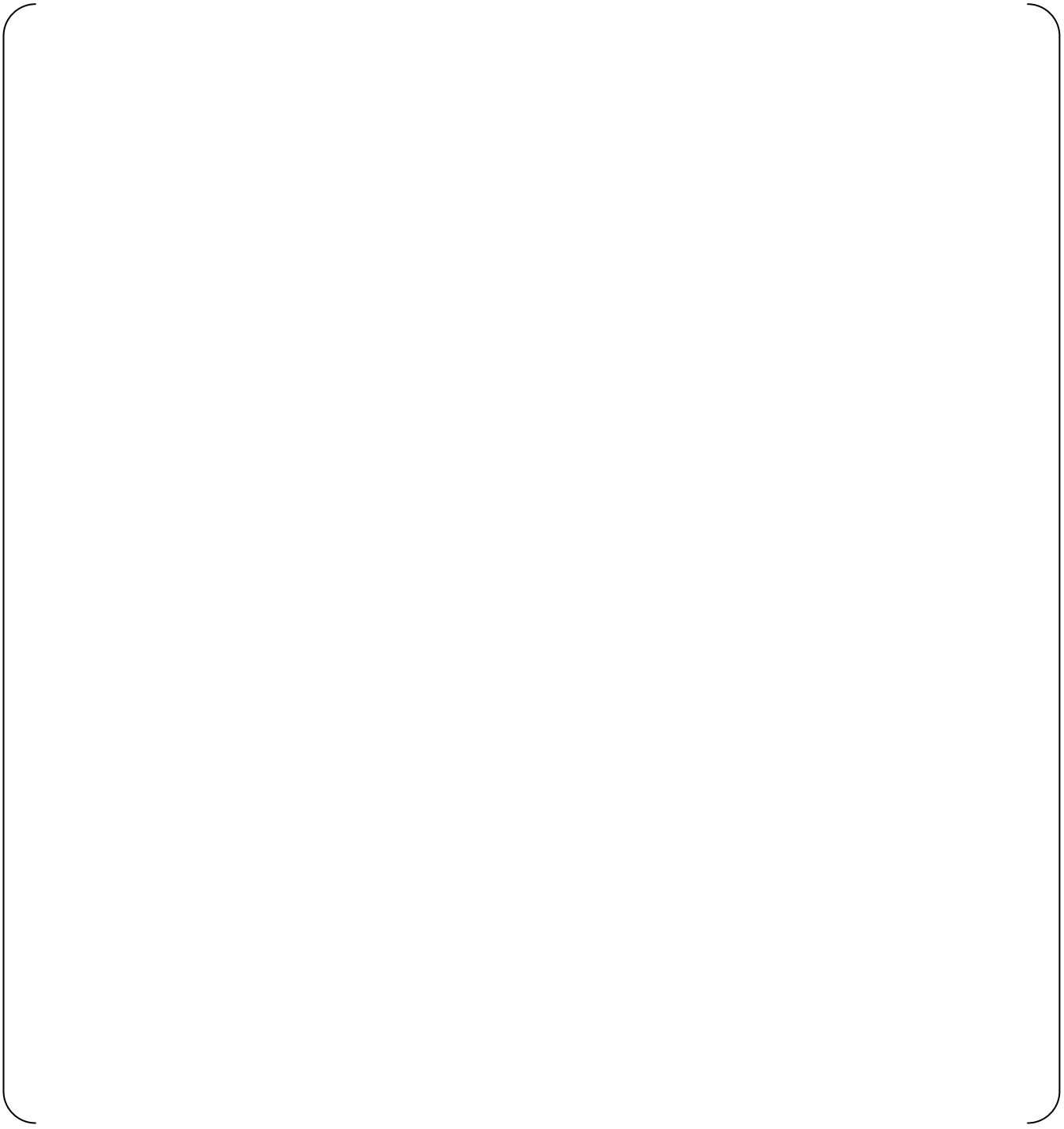

Figure 4.1-4 Tie Rod Measurement

Figure 4.1-5 Lower Plenum Structure Measurement

Figure 4.1-6 Upper Core Support Measurement

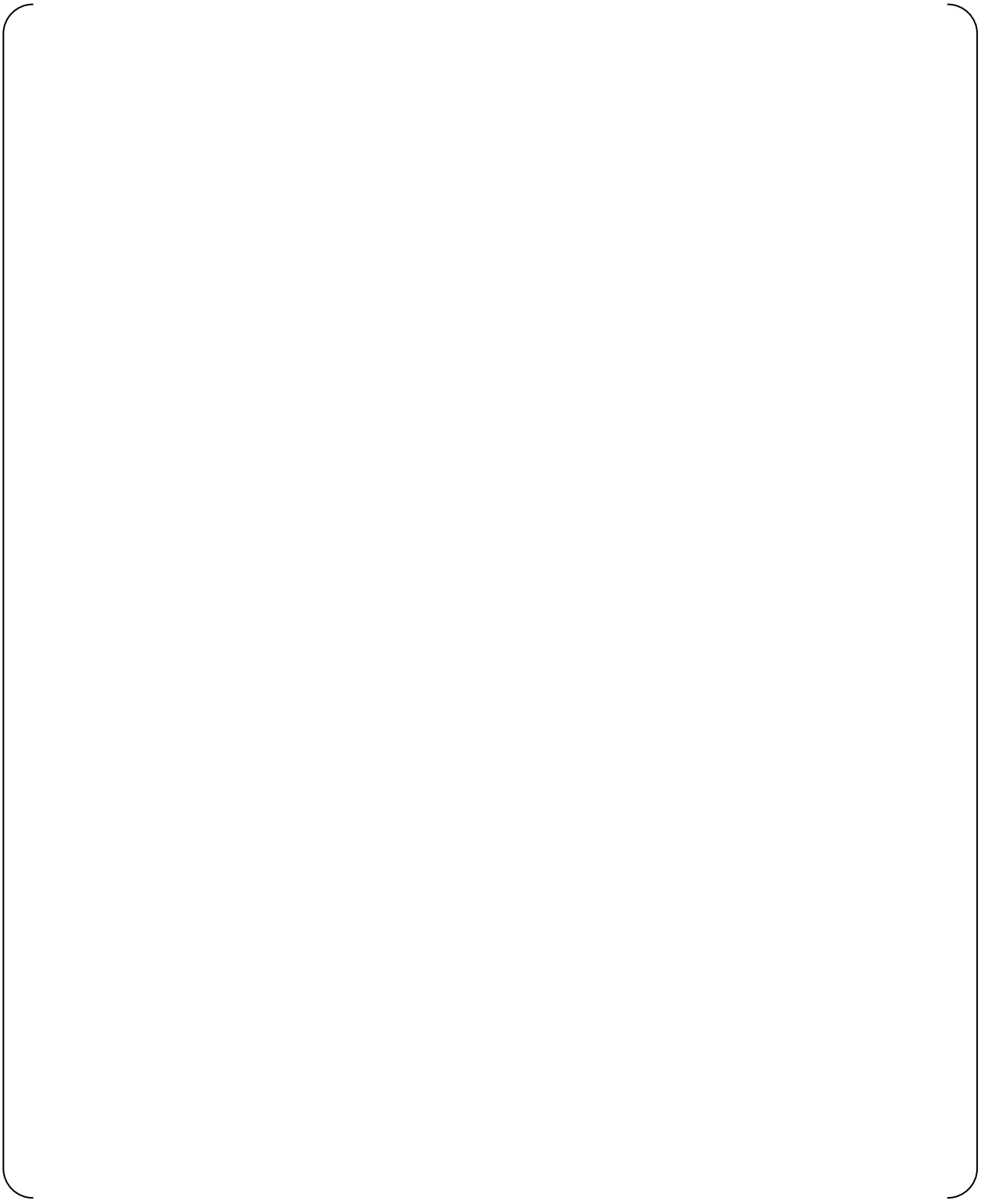

Figure 4.1-7 Upper Support Column Measurement

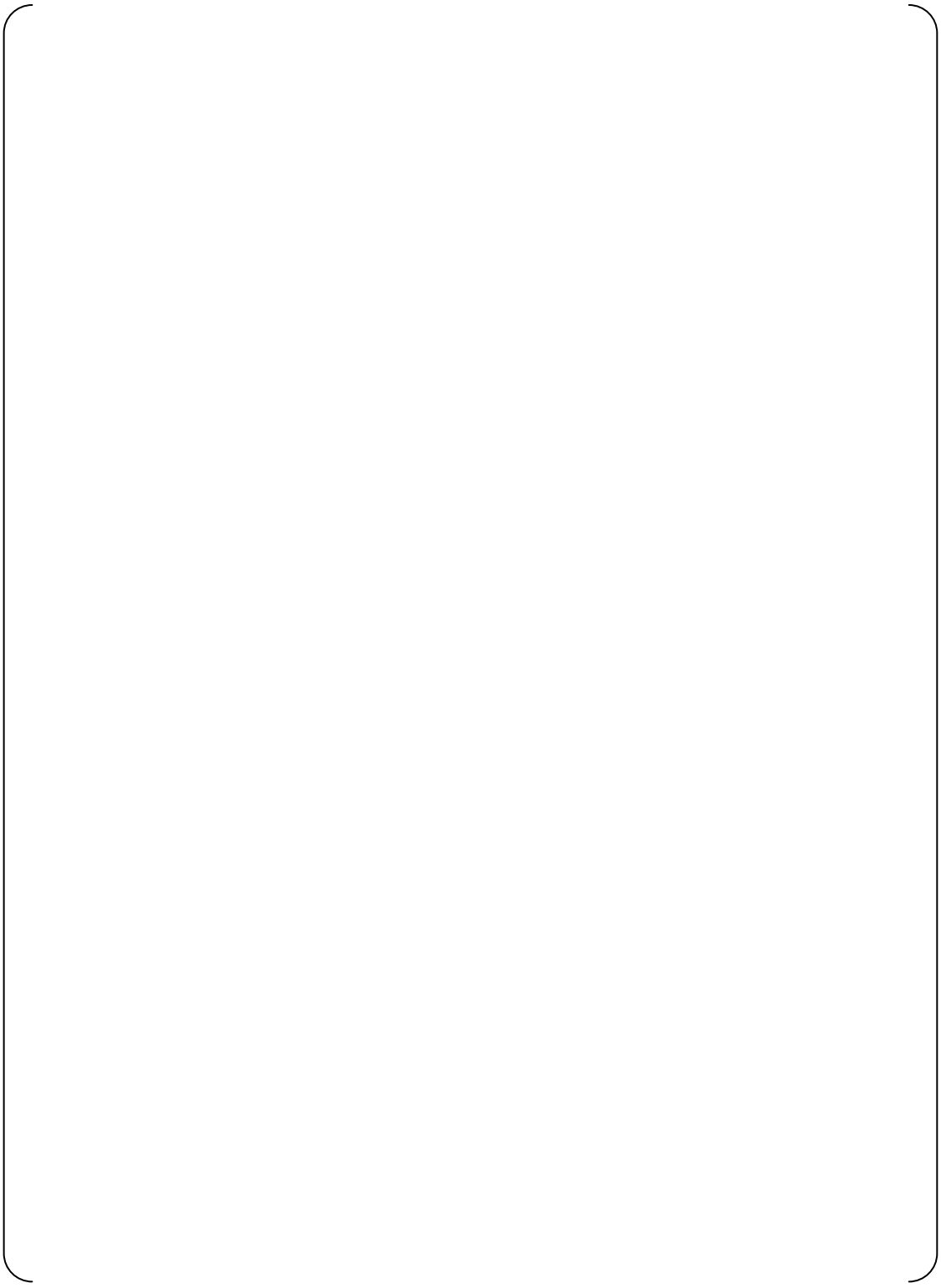

Figure 4.1-8 Guide Tube Measurement

4.2. Test Conditions

4.2.1. Operating Modes

Measurements will be conducted during the cold hydraulic test (CHT) and the hot functional test. The flow rate and the temperature is changed in these test phases, the responses will be varied depending on these conditions, i.e. as a function of the dynamic pressure. Since the fluid density is larger in the lower temperature, it is expected that the vibration response in a cold full flow condition is the maximum.
The data will be recorded at the no pump operation condition to obtain the background noise, startup and shutdown transient to record mean strains and the transient vibration behavior that, and steady-state operations condition of the possible pump combinations to obtain the vibration response of the instrumented components during various flow conditions.

4.2.2. Duration of Tests

Recording time for each steady pump operation condition will be determined to allow for the proper signal averaging in later analysis.

4.2.3. Disposition of Fuel Assemblies

Since dynamic response of each structure depends on the excitation force and the vibration characteristics of itself, in general, the excitation force which is close to a natural frequency of the structure will produce a larger response. In this section, the effects of the core on the vibration characteristics of the components and the hydraulic loading are discussed to determine the more conservative test conditions.
The presence of the core has following effects;

- -change in the flow rate due to the increase of the pressure drop in the core region,
- -changes in pump pulsation loads due to the flow resistance in the core region,
- -changes in the natural frequencies of structures due to the additional mass of the fuel assemblies and reaction force caused by the hold down springs

Analyses have been done for both without and with the core conditions considering the differences mentioned above as written in Subsection 3.3.4. The results show that the amplitudes of the vibration response due to the flow turbulence were decreased in with the core conditions at all components and locations. This is mainly because the flow rate without the core is larger relative to with the core conditions, while the natural frequencies of beam and shell modes of each component were almost unchanged as shown in Subsection 3.3.1. The pump pulsation loads with core conditions will be lower due to the acoustic damping in core region so that the vibration responses will be decreased from without the core conditions.
In conclusion, without the core conditions will result in higher response than with the core conditions, and thus the test is conducted only during HFT without the core.

5.0 INSPECTION PROGRAM

The internal components of all US-APWR plants will be inspected before and after the hot functional test. The reactor internals will not be considered adequate and pass the comprehensive vibration assessment program unless no indication of harmful sign, abnormally large vibration amplitudes or excessive wear is detected.

- Acceptance Criteria

Broken components and / or excessive wear or deformation is not observed in the post-hot functional test inspection.

6.0 EVALUATION

The results of the vibration and stress analysis, measurement, and inspection programs will be reviewed and correlated to determine the extent to which the test acceptance criteria as described in Subsection 3.5 are satisfied.

7.0 CONCLUSIONS

(1) The US-APWR reactor internals represent a unique, first of a kind design because of its design, size, arrangements and operating conditions. Therefore, the first US-APWR will be classified as a Prototype in accordance with the United States Nuclear Regulatory Guide 1.20 Rev.3 (Reference (1)).

Upon qualification of the first US-APWR as a valid prototype, subsequent plants will be classified as a Non-Prototype Category I.

(2) Alternating stress levels of the reactor internals due to the flow induced vibrations are acceptably low in comparison with the limit for the high cycle fatigue that is specified in the ASME Code.

(3) The difference in reactor internals vibration characteristics, such as the natural frequency of the core barrel, is very small with or without the core. The vibration responses without the core are the same or slightly larger than those with the core. These are because of the flow rate increase with the elimination of the fuel assemblies and the subsequent pressure loss. Thus, in the preoperational test of the prototype plant, the results of vibration measurements after the core loading are bounded by the measurements before the core loading and only measurements before the core loading will be necessary.

(4) Measurements will be performed during the preoperational test to confirm the vibration characteristics and structural integrity of the Prototype US-APWR reactor internals.

(5) The reactor internals of all US-APWR plants will be inspected before and after the hot functional test. The reactor internals will not be considered adequate and pass the comprehensive vibration assessment program unless no indication of the harmful sign, abnormally large vibration amplitudes or an excessive wear is detected.

8.0 REFERENCES

(1)Comprehensive Vibration Assessment Program for Reactor Internals during Preoperational and Initial Startup Testing. Regulatory Guide 1.20, Rev.3, U.S. Nuclear Regulatory Commission, Washington, DC, March 2007.

(2)“Nuclear Power Plant Components,” ASME Boiler and Pressure Vessel Code. Section III, Division 1, American Society of Mechanical Engineers. Includes: NCA, NB, NC, ND, NF, NG, Code Cases and Appendices including Appendix I, F, and N, 2001 edition thru 2003 Addenda.

(3)ANSYS, Finite Element Structural Analysis Program, Release 11.0, ANSYS, Inc., Canonsburg, PA, 2007.

(4)“Flow-Induced Vibration of Power and Process Plant Components: A Practical Workbook”, M.K.Au-Yang ,2001, ASME Press.

(5)Au-Yang, M.K. and Connelly, W.H.A Computerized Method for Flow-Induced Random Vibration Analysis of Nuclear Reactor Internals. Nuclear Engineering and Design 42, 1977, pp 277-263.

(6) Au-Yang, M.K, “Flow Induced Vibration Test of an Advanced Water Reactor Model Part1 Turbulence - Induced Forcing Function”, PVP Vol.273, pp43-69, Flow Induced Vibration ASME 1994.

(7)APWR Reactor Internals 1/5 Scale Model Flow Test Report. MUAP-07023 R2, Mitsubishi Heavy Industries, Ltd. August 2011.

(8)“Pressure spectra in turbulent free shear flows”, Journal of Fluid Mechanics, 1984, vol. 148, pp. 155-191.

(9)A.W.Guess 1975 Journal Sound and Vibration 40(1), pp119-137 Calculation of Perforated Plate Liner Parameters from Specified Acoustic Resistance and Reactance.

(10)“Flow-Induced Vibration of Power and Process Plant Components: A Practical Workbook”, M.K.Au-Yang ,2001, ASME Press.

Appendix-A Comparison of US-APWR with J-APWR and J-APWR SMT

(Related to RAI#206-1576 Question 03.09.02-43)

The data in the J-APWR scale model test (SMT) was used to confirm the adequacy of the MHI's flow-induced vibration analysis methodology and as a comparison reference for the response level of the reactor internals. The results of structural integrity evaluations for the reactor internals flow induced vibration in the J-APWR SMT benchmark analysis were not directly applied to the US-APWR vibration assessment, as explained below.

As shown in the analysis flow diagram, Figure 3.1-1 of MUAP-07027-P, Revision 1, the measured natural frequencies and the vibration response levels were used as reference data for the validation of the analysis methodology through the benchmark flow-induced vibration analysis of the scale model used in the J-APWR SMT. In addition, the normalized pressure power spectral densities (PSDs) measured in the downcomer of the J-APWR SMT were used in both the J-APWR SMT benchmark analysis and the US-APWR prototype flow-induced vibration analysis. This was based on the similarity of the downcomer geometrical dimensions and flow rate as discussion below.

Responses to the pertinent RAIs (3.9.2-43) are given in (a) through (f).

(1)Comparison of the reactors - the current 4-loop / the J-APWR / the US-APWR plants:
The key specifications of the reactors for the current 4-loop, the J-APWR, and the US-APWR are summarized in Table A-1.

The core lengths in the J-APWR and the US-APWR are different, but the number of fuel assemblies is the same. The dimensions of the reactor vessel and the core barrel are also the same as is the flow rate. These parameters do differ from the current 4-loop plants with the exception of the core barrel (downcomer) length.

Therefore, the flow-induced vibration response characteristics of the US-APWR reactor internals are similar to those of the J-APWR.

(2)Comparison of dimensionless parameters between the J-APWR SMT and the US-APWR plant:
The dimensionless parameters related to the flow-induced vibrations, the Reynolds number (Re), and the reduced velocity (Ur) for the J-APWR SMT, the J-APWR plant, and the US-APWR plant are shown in the Table A-2. In addition, the Strouhal numbers (St) are also summarized in the same table for structures exposed to the cross-flow in the lower and the upper plenums.

a.Reynolds number

Under operating conditions of a PWR, the coolant flow inside the reactor vessel will be in the turbulent flow regime. It is considered that the flow characteristics would remain the same in sufficiently developed turbulent flow regime. The transition from the laminar flow to the turbulent flow occurs at Reynolds number ($Re = U D / \nu$) around 10^3 in general. For this reason, we selected the scale model test condition to keep the Reynolds number greater than 10^4.

As shown in the TableA-2, the sufficiently high Reynolds number was maintained in the downcomer, the lower plenum and the upper plenum under the test conditions of the J-APWR SMT. This is also true under the plant operating conditions.

b. Reduced velocity

The reduced velocity (Ur = U / (fn D)) is generally used in the dimensional analysis of the flow-induced vibration. Ur represents the ratio of the path length per cycle (U / fn) to the model width (D). From another view point, Ur represents the ratio of the fluid force frequency (proportional to U / D, the vortex shedding frequency (fs) is a typical example) to the natural frequency of the model. As shown in Table A-2, the reduced velocities in the J-APWR SMT were close to those under the J-APWR plant operating conditions and were also similar to those of the US-APWR plant.

c.Strouhal number

The Strouhal number (St = fs D / U) is the non-dimensional parameter for the vortex shedding frequency. As is well known, St of a cylinder in the cross-flow is almost constant (around 0.2) below the critical Re number based on the cylinder diameter. As shown in Table A-2, St in the SMT, at room temperature, was also around 0.2. But under plant operating conditions, St will be around 0.3 because the Re will be in the super critical region. So the evaluation based on the analysis as shown in Table 3.2-4 of MUAP-07027-P, Revision 1, is also required for checking the vortex shedding lock-in, even though the lock-in was not observed in the SMT.

(3) Effect of fuel assemblies on the flow

The fuel assemblies have little effect on the reactor vessel flows, including the cross flows in the lower and the upper plenums, for reasons given below.

The maximum cross-flow distribution in the upper plenum depends on the outlet nozzle flow velocity and geometries of the structures near the outlet. It does not depend on the core outlet flow distribution into the upper plenum. And because of a small increase of total flow rate with a lower pressure loss in the core, the maximum cross flow velocity in the upper plenum during the hot functional test without the core will be higher than that under the normal operating condition.

The maximum cross flow distribution in the lower plenum depends on the flow velocity in the downcomer and the geometries of structures in the peripheral region of the lower plenum. It does not depend on the core inlet flow distribution in the downstream side. And because of the increase of total flow rate with the lower pressure loss in the core, the maximum cross flow velocity in the lower plenum during the hot functional test without the core will be higher than that under normal operating conditions.

Therefore, the mechanical integrity of the structures subjected to the cross-flow in the lower and the upper plenums can be conservatively verified without the fuel assemblies.

(4) The bypass flow rate from the outlet nozzle gap between the Core Barrel/the RV under plant operating conditions will not be larger than that during the preoperational test, because the gap clearance is designed to be minimum under normal operating conditions as a result of core barrel thermal expansion.

In any case, the bypass flow through the outlet nozzle gap has little effect on the core barrel vibration because both the flow rate and the surface area of the flow channel are much smaller than those of the downcomer flow.

The difference of operating point on the reactor coolant pump (RCP) Q-H curve has been considered in the estimation of the test flow rate from that under the normal operating conditions with the fuel loaded.

(5)There is little need for the fuel assembly vibration measurement in the preoperational or start – up test because of following reasons.

a.The flow induced vibration response of the fuel assembly will be confirmed in a mock-up test.

b.Vibration of the fuel assemblies in the core can be checked by the spectral analysis of the ex-core nuclear instrumentation signals in the start-up test, if needed.

Table A-1 Comparison of Reactor of Current 4-loop /J-APWR / US-APWR

	Current 4-loop	J-APWR	US-APWR
Number of RC Loops	4	4	4
Numbers of Fuel Assemblies	193	257	257
Core length (ft)	12	12	14
Downcomer length (inch)	[ ]	328	328
Vessel Inside Diameter (inch)	[ ]	202.8	202.8
Numbers of RCCA/GT	53	69 / 77 / 85	69
Loop flow rate for Mechanical Design (GPM)	[ ]	129,000	130,000
Structure around the core	Core Baffle	Neutron Reflector	Neutron Reflector

Table A-2 Comparison of Dimensionless Parameters between J-APWR SMT, J-APWR plant, and the US-APWR Plants

	J-APWR plant	J-APWR 1/5 SMT	US-APWR plant
Downcomer /Core Barrel Flow Velocity U (m/s) Annulus width h (m) Core barrel fn (Hz)			
Re = Uh/ν Vr = U/fnh			
Lower plenum / Lower Diffuser Plate Support Column Flow Velocity U (m/s) Column diameter D (m) Column fn (Hz)			
Re = UD/ν Vr = U/fnD St = fsD/U			
Upper Plenum / Top Slotted Column Flow Velocity U (m/s) Column diameter D (m) Column fn (Hz)			
Re = UD/ν Vr = U/fnD St = fsD/U			

Appendix-B Conversion Process of Forcing Functions from the Scale Model Test benchmark analysis to those for the US-APWR prototype analysis

(Related to RAI#272-1585 Question 03.09.02-03)

1. Analysis procedure, modeling and forcing functions

The analysis procedure, modeling and forcing functions for the US-APWR prototype are discussed in this Appendix.

As described in Subsection 3.1.1 of the vibration assessment program report MUAP-07027-P, Revision 1, the FIV analysis program consists of two separate tasks. One was to validate the analysis method by a benchmark analysis to simulate the J-APWR scale model test (SMT) and the other was the analysis of the US-APWR prototype. The structural model and the forcing functions were customized for each task as follows.

Task 1: J-APWR SMT benchmark analysis

This task was performed to validate the analysis method.

All properties of the reactor internal model in the scale model benchmark analysis were developed in 1/5 scale. The structural model of the reactor internals was developed based on the full scale J-APWR drawings and scaled down following the scaling laws for each parameter. However the stiffness of the test vessel support, which did not simulate that in the actual plant, was determined based on the measured natural frequency of the test model by the sine wave excitation with sweep of frequency.

The forcing functions for the scale model benchmark analysis were determined at the test flow rate at room temperature consistent with the 1/5 SMT conditions.

Task 2: Analysis for the US-APWR prototype

The analysis of the US-APWR prototype was performed with a full scale model and the forcing functions for the US-APWR operating conditions. Tables B-1 give a side-by-side comparison of the US-APWR prototype analysis and the J-APWR SMT benchmark analysis.

In the US-APWR prototype analysis, the model structural properties were developed based on the drawings of the US-APWR in the same manner which was verified by the 1/5 J-APWR SMT benchmark analysis.

The flow-induced forcing functions in the horizontal direction were scaled up from the J-APWR 1/5 SMT analysis input. The time history data of the downcomer turbulence and the cross flow loads in the upper plenum generated for the J-APWR 1/5 SMT benchmark analysis were directly converted to those for the US-APWR prototype in the following manner. Conversion factors f1, f2 and f3 were

determined as shown in Table B-2. Here, the constants of proportionality are assumed to be the same because the structural configurations and the flow conditions are the same in these regions in both plants. .

$$F_{uspro}(t) = f_1 f_2 F_{jsmt}(t/f_3)$$

Here,

Fuspro: force for analysis of the US-APWR prototype
Fjsmt : force for the benchmark analysis of the 1/5 scale model of the J-APWR
t : time
f1 : conversion factor related to the force area
f2 : conversion factor related to dynamic pressure
f3 : conversion factor related to time (or frequency)

Above simple conversion can be applied because the key dimensions are his conversion

As the base assumption of this scaling process, the consistency of the forcing function between a scale model test under the room temperature and the actual plant scale under operating conditions has been validated by Au-Yang in Reference B1. In Figure B-1 from Reference B1, the lines of empirical forcing functions determined based on the scale model test show good agreement with the plot data from the actual plant of the PWR).

For the lower plenum cross flow loads, the original forcing functions in the US-APWR prototype were re-constructed for the diffuser plate configurations, because the key dimension for the cross flow forcing functions such as the column diameter is not identical with the BMI columns in the J-APWR.

The vertical loads was also developed specifically for the US-APWR prototype.

2. Validation of the analysis method

The validation of method of the structure modeling was conducted by comparing the computed natural frequencies of the J-APWR SMT with the measured data, as discussed in Subsection 3.2.1 of the Vibration Assessment Program Report MUAP-07027-P, Revision 1.

The validation of the forcing functions was performed by comparing the computed responses of the model in the J-APWR SMT with the measured responses as discussed and verified in Subsection 3.2.3 of the Vibration Assessment Program Report MUAP-07027-P, Revision 1. From this, the empirical forcing functions based on a scale model can represent the actual plant conditions.

The power spectral density (PSD) of the downcomer pressure fluctuation measured in the US-APWR 1/7 Scale Lower Plenum Test is shown in Figure B-3. Each PSD is normalized with the downcomer width and the average axial flow velocity in the same manner with the Au-Yang data in

Figure B-1. For easy comparison, the empirical fitting lines from Figure B-1 were also indicated in Figure B-2. 4 kinds of PDSs are identified with symbol “A” to “D” with the pressure transducer locations as shown in Figure B-3. Except of the PSD “A” near the inlet nozzle, measured data in US-APWR 1/7 scale model shows not so differ from Au-Yang data although the reactor designs are not identical in each other, This agreement indicates the adequacy of the force normalization process and the reliability of measured data.

Please note that the empirical functions from Figure B-1 are based on a measured point in the middle of the downcomer. “Upper bound” does not mean the upper bound of the entire downcomer but the envelope of spectral peaks at that single measuring point. The PSD “A’ is located in the upper portion of the downcomer as shown in Figure B-3. The magnitude of the pressure fluctuation near the inlet nozzle was [ ] times larger than that at the mid-section of the downcomer. This difference is reasonable because the local flow velocity in the inlet nozzle is about twice the average velocity in the downcomer, which results in [ ] times larger in the dynamic pressure level.

3. Mapping of the downcomer forcing functions

Same force mapping as shown in Figure B-3 was applied both for J-APWR SMT benchmark and the US-APWR prototype analysis. The entire surface of the core barrel facing to the downcomer was divided into 16 segments (8 in circumferential and 2 in vertical) which correspond to the nozzle layouts. For example, forcing functions for the upper segments including the inlet nozzle were generated from the same PSD “A” .The time histories for the 4 segments from one PSD were independent of one another by use of random phase. In the same manner, total 16 time histories were defined from 4 PSDs.

Reference

(B1) **“**Pressure spectra in turbulent free shear flows”, Journal of Fluid Mechanics, 1984, vol. 148, pp. 155-191

Table B-1 Comparison of the models in the benchmark analysis of the J-APWR SMT and the US-APWR prototype vibration assessment

	J-APWR SMT model	US-APWR Proto-type model
Configurations and dimensions of analysis model	1/5 of J-APWR	1/1 of US-APWR
Properties of vessel support stiffness	Test vessel support	Plant design value
Reference temp. for metal / fluid material properties	Room temp.	Temp. in normal operation
Vessel inlet flow rate for flow velocity definition	28,200 / 25 m^3/h/loop (=test condition)	29,600 m^3/h/loop

Table B-2 Conversion of Flow- Induced Forcing Functions in the benchmark analysis of the J-APWR SMT into US-APWR prototype vibration assessment

	f1: Scale effect on force area	f2: Ratio of ρv^2	f3: Scale effect on time
Down comer Turbulence	25	[ ]	5
Cross flow loads in Lower Plenum	Defined with the US-APWR configuration		
Cross flow loads in Upper Plenum structures	25	[ ]	5

Notes

- Plots : Measured data in a PWR in plant operating conditions.
- Additional lines are mean and Upper Bound based on a scale model test date.
- All date were measured in mid elevation of the downcomer.

Figure B-1 Comparison of empirical normalized PSD equation with field measured data (Au-Yang and Jordan,1980, Figure 8-17 in Reference (B1)

Figure B-2 Down comer Pressure PSD from US-APWR1/7 Scale Lower Plenum Test (Identical with Fig. 3.2.3.4 of MUAP-07027P-R2)

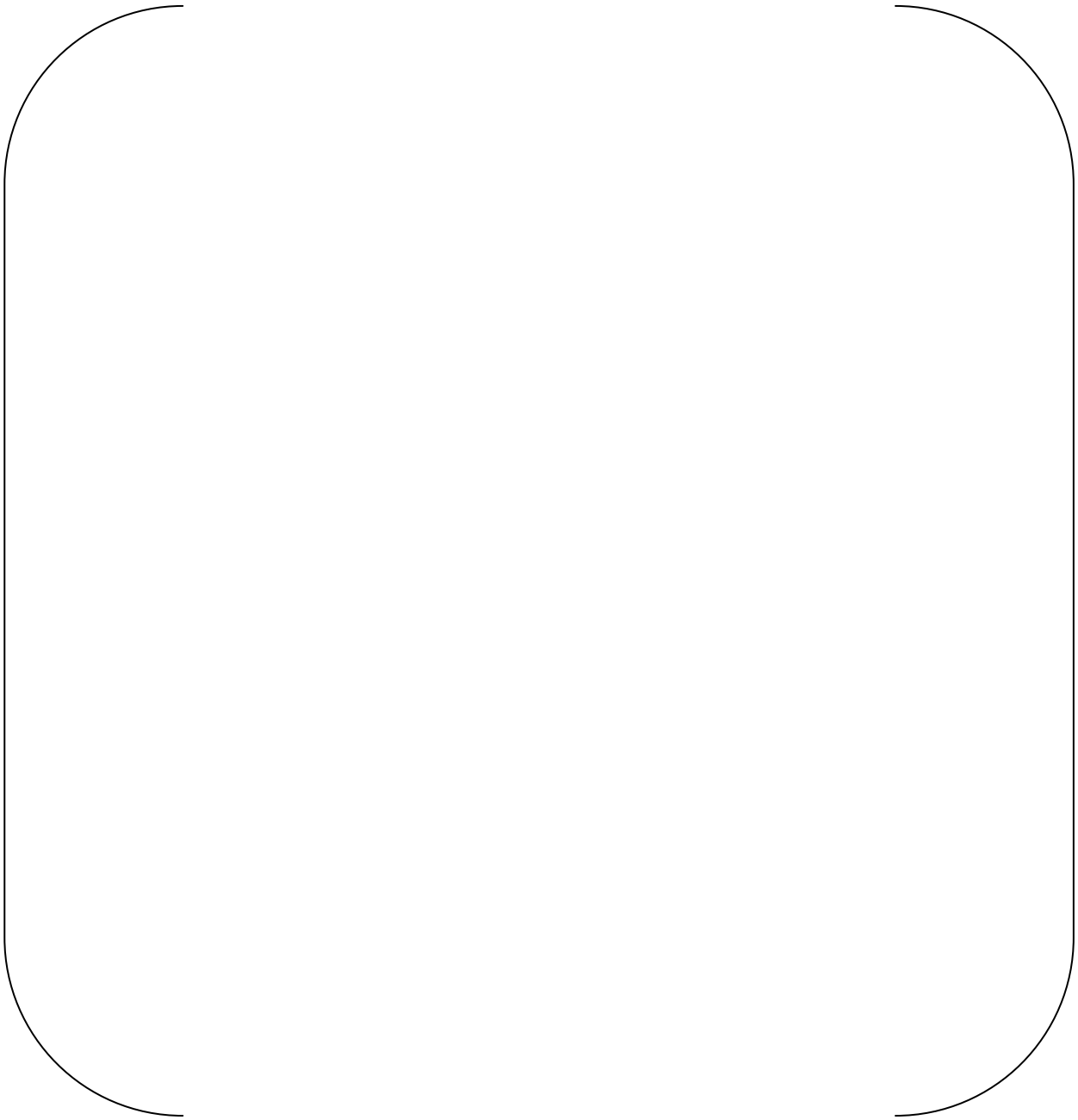

Figure. B-3 Mapping of Downcomer Forcing Functions

Appendix-C Substituting the downcomer turbulent forcing function with updated data

1. Introduction

In MUAP-07027-P, Revision 1, the downcomer turbulent forcing functions from the data measured in the J-APWR 1/5 scale model test (J-APWR SMT) were substituted with those measured in the US-APWR 1/7 scale model lower plenum test (US-APWR LPT). This document explains the reason of this substitution and its impact on the evaluation results.

2. Background

The US-APWR LPT was performed in 2008 after the DCD and MUAP-07027-P, Revision 0, were submitted to NRC. MHI performed a sensibility analysis with the new forcing function replacing that derived from the J-APWR SMT data. As a result, it was confirmed that the new downcomer forcing functions were similar to those derived from J-APWR SMT. On the other hand, re-analyses of the reactor internals vibration were needed to obtain input to the stress analyses of the core support structures in 2009.

3. Discussions

It was decided to replace the downcomer forcing functions with the new one from the US-APWR LPT for the following reasons.

(1) In general, data from the US-APWR scale model test is more appropriate for analyzing the response of the US-APWR. If the data is available there is no special reason to select other data sets.

(2) Comparing the pressure fluctuation PSDs, the difference between the two test data sets was not large as shown in Figures C-1 and C-2, although a more smooth spectrum was obtained in the US-APWR LPT in Figure C-2. A possible reason for the difference was the effect of wiring for the data acquisition system, which was on the outside surface of the core barrel in the J-APWR SMT. This was necessary because there was little free space between the fuel assemblies and the neutron reflector. In the US-APWR LPT, wiring for the data acquisition system was able to be set inside of the core barrel because the fuel assembly and the radial reflector were not included in the scale model.

4. Impact on the stress analysis results and the measuring plan

The effects of substituting the downcomer forcing function with that derived from the US-APWR LPT on the vibration responses were summarized in Table C-1. The impacts are around [ ]% on both the core barrel and the neutron reflector. So there is little impact on the prediction results for the stress analysis and the measurement plan.

Table C-1 Effect of the difference of downcomer forcing function on the CB / NR Response (J-APWR 1/5 SMT benchmark scaled to actual dimensions)

Components	RMS Response 、mil （Ratio to measured results）			Effect of down comer force change
	Measured*	Analysis* based on J-APWR SMT data	Analysis* based on US-APWR-LPT data	
CB bottom –RV relative displacement				
NR top –CB relative displacement				

*Converted to actual plant scale.

Figure C-1 Down comer pressure PSD measured in J-APWR 1/5 scale model test

Figure C-2 Down comer pressure PSD measured in US-APWR 1/7 scale lower plenum test

Appendix-D RCP Pulsation Forcing Functions

1. Introduction

The forcing functions of the RCP-induced pressure pulsations for the US-APWR reactor internals were determined from the scale model tests of the both generic and the APWR-specific RCPs.

2. Studies based on the RCP model tests data

The RCP scale model flow tests of the generic and the APWR-specific types (J-APWR/ US-APWR) were performed. In each test, the measured pressure fluctuations were normalized with the total hydraulic head of the RCP. In Table D-1, the measured pressure fluctuation data are summarized.

(1) Total Pressure fluctuations at the RCP outlet
The pressure fluctuations at the RCP outlet including the local turbulence were obtained in all of the tests. The value for the APWR ([ ]% of hydraulic head) was the same or lower than that for the generic RCP ([ ]%).

(2) RCP pulsations related to the rotation speed
In the generic RCP test, amplitudes of the pressure pulsations generated by the RCP shaft rotation and the blade passing frequency were confirmed with the spectral analysis as shown in Figure D-1. The largest amplitude was about [ ]% of the total head at the first blade passing frequency NZ. At the RCP shaft rotational (N) and the 2nd harmonic of the blade passing frequencies the amplitudes were about 1/5 of that at NZ.

3. Forcing functions for the US-APWR

The amplitude of the RCP pulsation in the US-APWR were assumed to be the same as that generated by the generic RCPs, rationed by the total hydraulic heads to be conservative. The absolute amplitude is defined with the total head of the US-APWR RCP as shown in Table D-2.

Table D-1 Measured RCP pulsation amplitudes in 1/2 scale model tests (ratio to Hydraulic Head)

	Over-all fluctuation	Shaft Rotational Speed	Blade Passing Frequency	2nd Harmonic of Blade Passing Frequency
Generic RCP				
APWR				

Table D-2 US-APWR RCP pulsation amplitude for the vibration Analysis

	Shaft Rotational Speed	Blade Passing Frequency	2nd Harmonic of Blade Passing Frequency
Frequency(Hz)			
ΔH 0-peak / H			
Amplitude(Pa 0-peak)			

Figure D-1 The pressure pulsation spectrum of generic RCP.

Appendix-E A study of the pressure fluctuation for the vertical forcing function

(Related to RAI#272-1585 Question 03.09.02-21)

MHI applied the same measured pressure data in the downcomer to the lower core support and the upper core plate flow holes. The justification for this was based on the assumption that the pressure fluctuation close to the RPV inlet nozzle was caused by the jet flow turbulence exiting from the inlet nozzle and, therefore it was assumed to be similar to the jet flow turbulence through the lower core support plate and the upper core plate flow holes.

An example of the measured pressure PSD in a circular jet is shown in Figure E-1, compared with the US-APWR forcing function based on the downcomer data shown in Figure E-2 (Reference (E1)). Both PSDs are similar in shapes and absolute values. From this, it is justifiable that the downcomer PSD close to the inlet nozzle was used for the flow hole forcing function.

The joint acceptance or the correlation length was not defined. The total force on the plate was calculated as the SRSS of all flow holes in the plate, because the jet flow turbulence in each flow hole is independent of the others.

Reference

(E1) “Pressure spectra in turbulent free shear flows”, Journal of Fluid Mechanics, 1984, vol. 148, pp. 155-191

Figure E-1 Normalized pressure PSD for US-APWR UCP/CSP

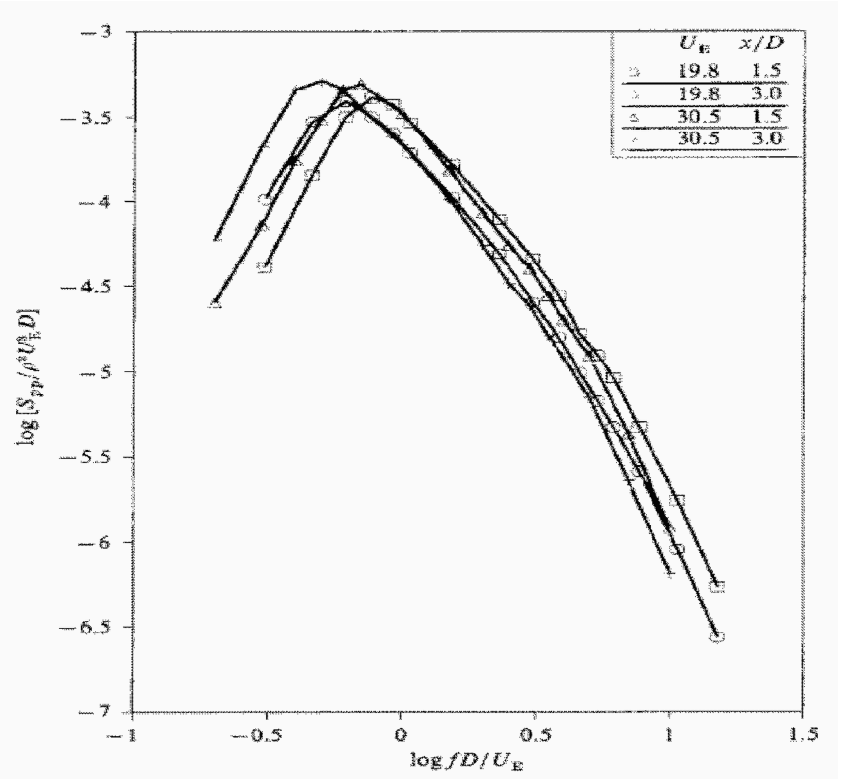

Figure E-2 Normalized pressure PSD measured in a jet flow (Reference E1)

Appendix-F Reactor Internals difference between J-APWR and US-APWR and its effects on the test results

(Related to RAI#498-3782 Question 03.09.02-65,82)

The US-APWR is a 14 ft-core version derived from the J-APWR design, which has a 12 ft core. Specifications of the reactor internals of the J-APWR and the US-APWR are compared in Table F-1. Comparisons of the schematic drawings are shown in Fig. F-1 to F-6.

Although the core length of the US-APWR is extended from that of the J-APWR, the dimensions of the reactor vessel and the core barrel are not changed as shown in rows 1 and 2 in Table F-1. This is obtained by eliminating the space between the lower support plate and the lower core plate, and replaced these two plates with an integrated LCSP design. Therefore, the vibration characteristics of the core barrel can be simulated by integrating the LCP and the LSP as stated in row of 4 in Table F-1.

The neutron reflector of the US-APWR is longer than that of the J-APWR. The fundamental natural frequency is reduced from [ ] Hz (in the J-APWR) to [ ] Hz (in the US-APWR). But the flow-induced vibration response obtained from the analysis is still sufficiently small as stated in MUAP-07027-P(R1).

The secondary core support assemblies in the lower plenum of the US-APWR are simplified in the number of columns from those in the J-APWR because of the elimination of the columns for the bottom-mounted ICIS. By optimization of the diameters of the support columns, the fundamental modal frequencies of the assemblies are maintained to be the same as those in the J-APWR.

For the upper plenum structures such as the lower part of the RCCA guide tube or the upper support column, specifications are not changed from those of the J-APWR.

In the US-APWR, the in-core instrumentation system (ICIS) is inserted from the top of the vessel, instead of from the bottom of the vessel as in the J-APWR. In both designs, the ICIS is guided and protected from the cross flow loads by the guide tubes and the support columns. This function is also replaced from the BMI columns in the lower plenum to the upper support columns in the upper plenum.

The information of this RAI response will be included in revised version of the Vibration Assessment Program Report MUAP-07027-P (not J-APWR SMT Report MUAP-07023-P).

Table F-1 (1/2) J-APWR&US-APWR Comparison of Reactor Internals

	J－APWR	US-APWR	Effects on FIV
1. Reactor Vessel (Fig. 1) Inlet dia. Inside diameter Outlet dia.			Unchanged
2. Core barrel (Fig. 1) Length[*1] × outer dia Thickness(upper/lower)			Unchanged *1: From lower surface of Flange to LSP bottom *2: in SMT
3 . Secondary Core Support assembly (Fig 3)			
Upper Assembly OD × ID × t Column dia.x number Column length			Unchanged because Fundamental frequency is about [ ] Hz in both designs.
Lower Assembly OD × t Column dia SCS dia Column length			Unchanged because Fundamental frequency is about [ ] Hz in both designs.
4.LCP/LSP(Fig. 2)			
4.1. LSP/LCSP Thickness Flow Hole			Unchanged as core barrel assembly. In spite of the extended core in US-APWR, core barrel length is identical to that of the J-APWR by means of the integrated LCSP design.
4.2 LSC Height x dia. x n			
4.3 LCP Thickness Flow hole			
5. Fuel Assembly UCP-LCSP height Number of assembly			Little impact on reactor internals vibration although fundamental mode frequency of fuel is reduced.
6 Nuetron Reflector (Fig. 4) Height x diameter Number of blocks	 8	 10	Natural frequency of fundamental beam mode is reduced from [ ]Hz to [ ] Hz.

Table F-1(2/2) J-APWR&US-APWR Comparison of Reactor Internals

	J－APWR	US-APWR	Effects on FIV
7.Upper Internals (Fig 5)	[ ]	[ ]	
7.1 UCP OD x t			Identical
7.2 UCS OD x t Skirt thickness Height			Identical
7.3 USC			
Height x OD			Identical
7.4 TSC			
Height x OD			Identical
7.5 RCC Guide Tube			
Lower Height x width Guide plates			Unchanged
Upper Height x dia Guide plates			Natural frequency is reduced from approximately [ ]Hz to [ ]Hz. There is no impact because flow velocity is lower in one order than upper plenum.
8. ICIS guide and protection from flow (Fig. 6)	(Lower plenum) Guide and flow protection by BMI Column	(Upper plenum) Guide and flow protection by USC	In both design, ICIS are guided and protected from cross flow.

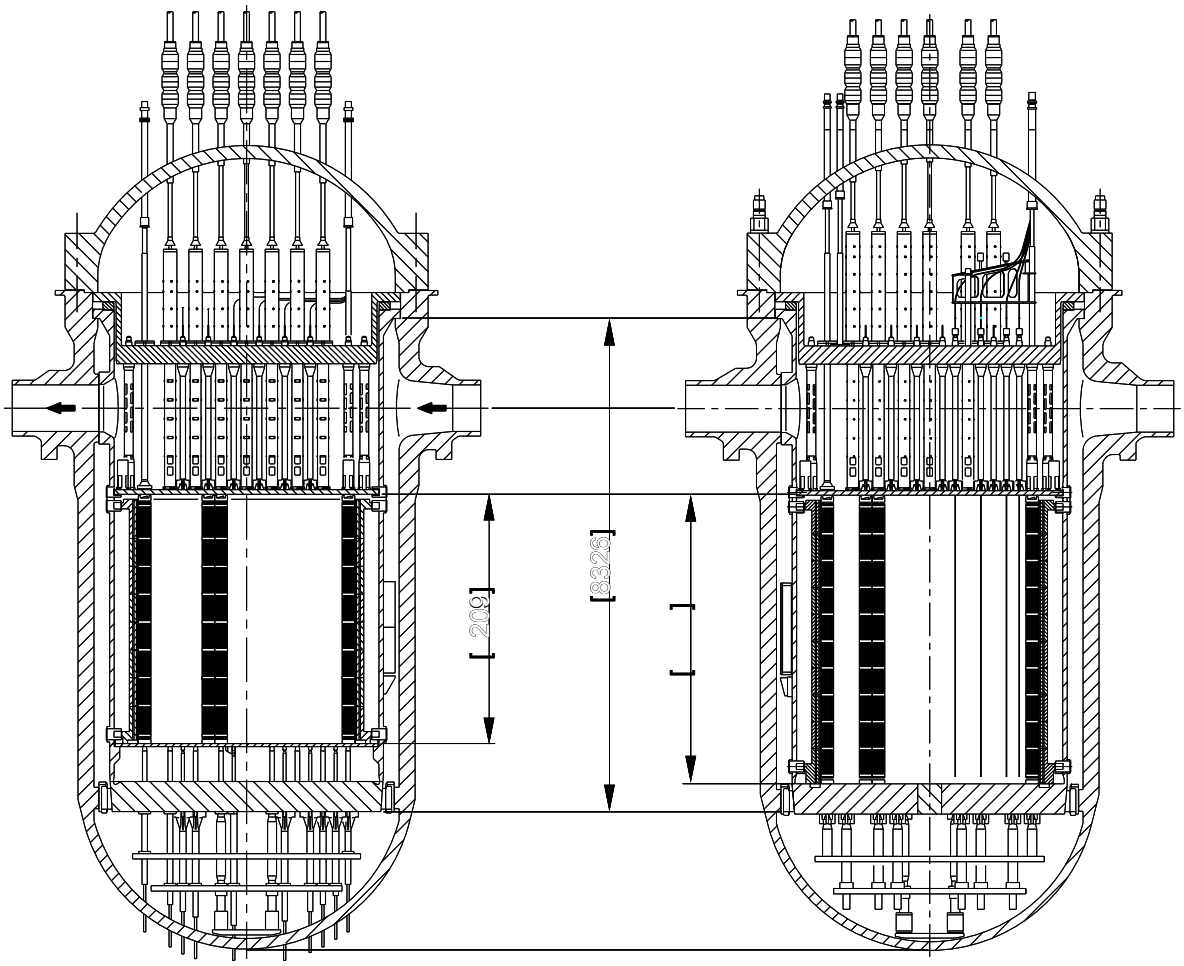

Figure F-1 Reactor General Assembly

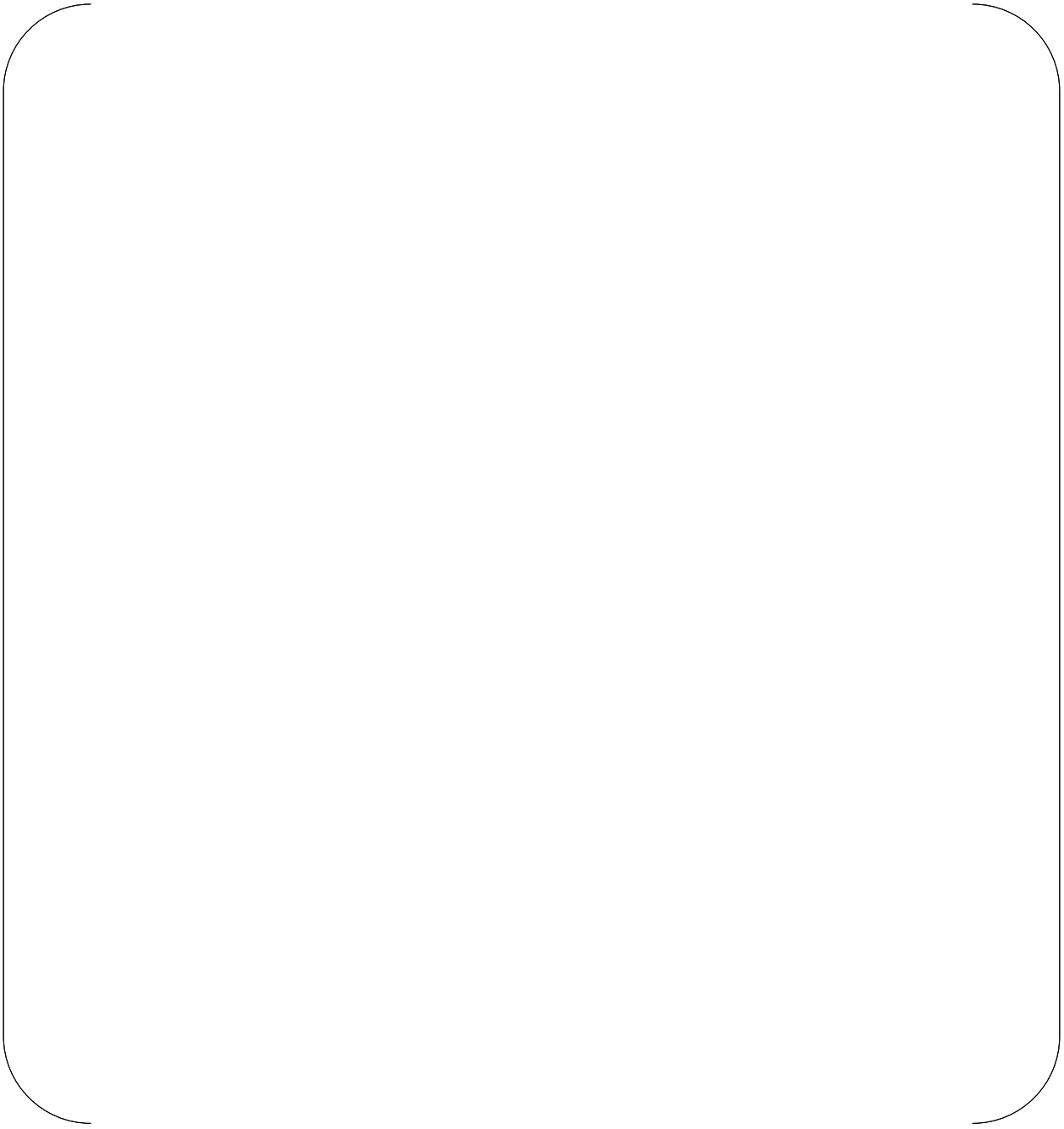

J-APWR US-APWR

Figure F-2 Lower Core Support Plate

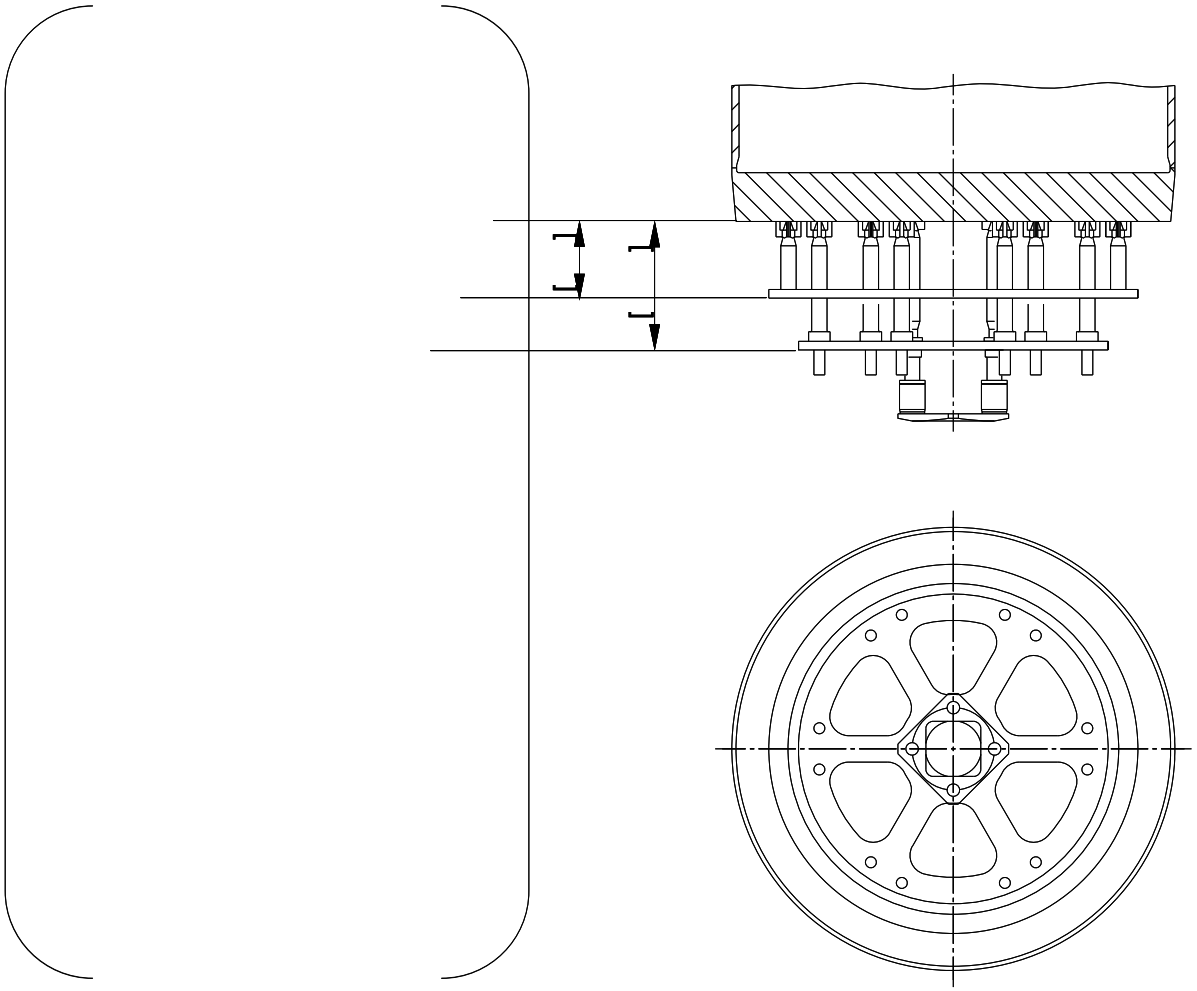

J-APWR US-APWR

Figure F-3 Secondary Core Support Assembly

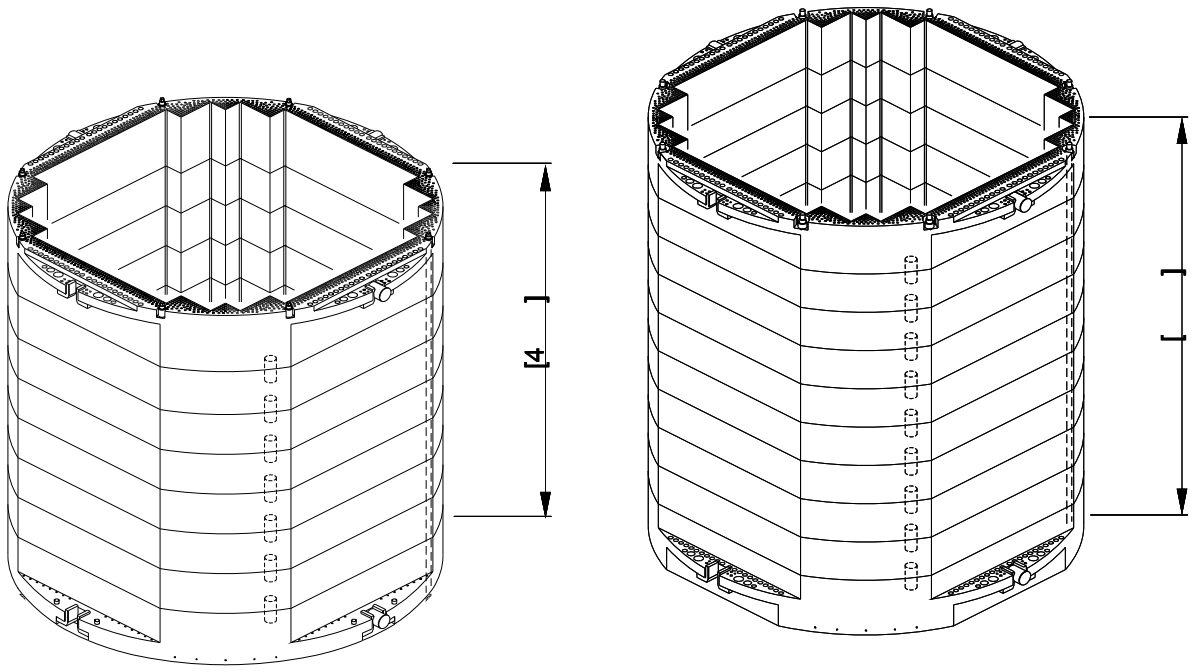

J-APWR US-APWR

Figure F-4 Neutron Reflector

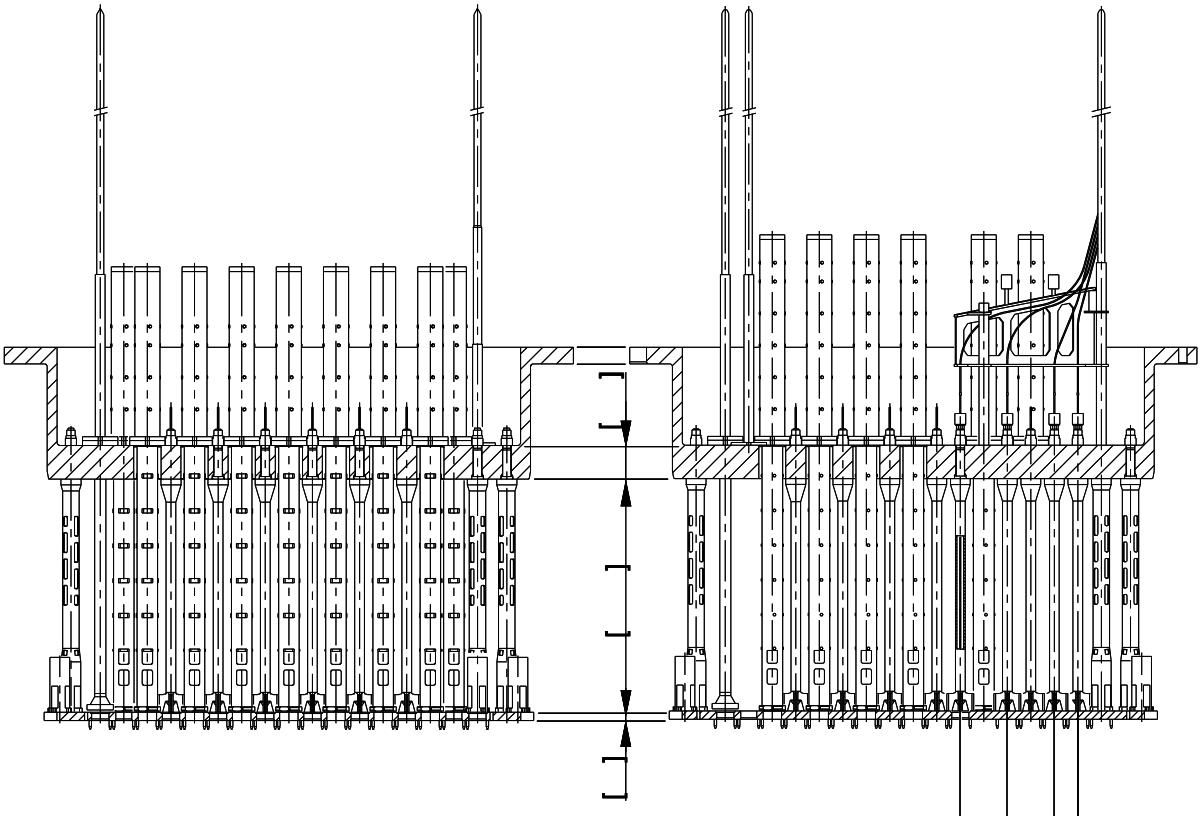

J-APWR US-APWR

Figure F-5 Upper Reactor Internals

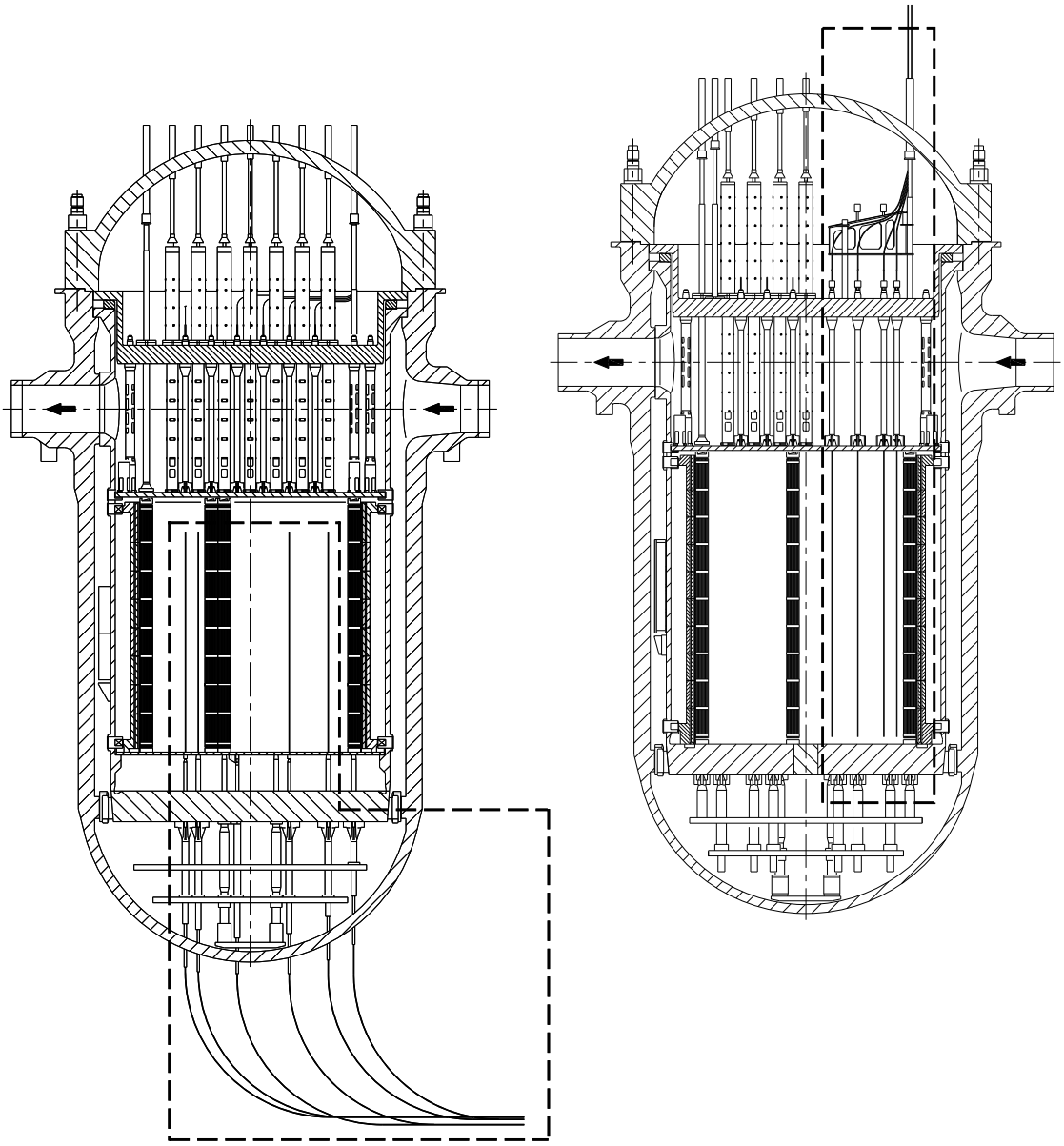

Figure F-6 ICIS Routing

Appendix-G Bias Error and Uncertainties of the Analysis Model

(Related to RAI No. 498-3782 QUESTION 03.09.02-66)

1. Validation of the structural modeling approach

(1) Procedure and Referenced data

The vibration analysis of the US-APWR reactor internals consists of the following two Tasks.

Task1: Verification of the analysis model and forcing functions

Task2: Prediction of the US-APWR reactor internals vibrations

In Task 2, as stated in the question, MHI does not use existing plant data as reference. Instead, MHI uses the J-APWR 1/5 scale model test data as reference, for the following reasons:

- The US-APWR reactor internals are more similar to those of the J-APWR than those of the existing plants.
- MHI dose not have the measured data from the existing plants for use as reference.

Finally, the adequacy of the analysis will be verified with the measured data in the preoperational test of the US-APWR, based on the acceptance criteria described in Subsection 3.5 of MUAP-07027-P(R1)

(2) Acceptance Criteria due to analysis model uncertainty

Based on past experience, MHI assumed a factor of [ ] for the uncertainty in the flow-induced vibration responses and a factor of [ ] for the uncertainty in the flow-induced loads. Therefore the uncertainty of the analysis model itself is expected to be no larger than a factor of [ ] in the response. To achieve this, the uncertainty in the fundamental modal frequency was limited to be less than 10 percent, which corresponds to 20 percent in the response considering the frequency transfer function as explained below.

a. The vibration characteristic of the model can be represented by the natural frequency and the frequency transfer function (FTF). In modal analysis, the FTF of each mode is similar to that of a single spring-mass system, in which a force with a frequency much lower than the structural natural frequency would act like a static force. When the force frequency is close to the natural frequency, the response is amplified with an amplification factor depending on the damping ratio. When the force frequency is higher than [ ] % of the natural frequency, the vibration response is reduced from that caused by the static force of the same magnitude.

b. For the core barrel or the neutron reflector, the flow-induced responses depend on the downcomer flow turbulence. Because a turbulence forcing function have a broad-band spectrum, the response is insensitive to small changes in the structural natural frequency. Therefore the impact of uncertainties in the natural frequency on the response can be estimated by the changes in quasi-static response due to the changes in the stiffness. For example, a [ ] percent change in the natural frequency can be represented by a [ ] % change in the stiffness or vibration response.

c. For structures in the upper plenum or the lower plenum, both the cross flow turbulence and vortex shedding load were considered. Because the vortex shedding frequency will be locked in with the natural frequency of structures if it is within 70-130 percent of the vortex shedding frequency, the uncertainty in the natural frequency should be checked to avoid lock-in with the vortex shedding. As shown in Table 3.4.1-1 of MUAP-07023-P(R1), the best estimated natural frequencies in the upper or lower plenum structures are sufficiently high to avoid lock-in with the vortex shedding even with 10 % uncertainty. Therefore the sensitivity on the response can be represented by the same discussion as in the case of the core barrel.

2. Bias errors and uncertainties on the vibration analysis model of reactor internals

For the reactor internals models, the model dimensions and the relating properties (length, area and section modulus etc.), were determined based on the design drawings of the actual plant. Because the dimensions in the drawings are given under the room temperature conditions, the thermal expansion under operating condition is one of the bias errors. In general, the effects of thermal expansions are negligibly small for the base dimensions, but not for the small clearances such as the key supports. Therefore the clearance properties in the key supports are specified under plant operating temperature, taking into account thermal expansions. Uncertainties with the tolerance in manufacturing or alignment are not considered because they are smaller than the thermal expansions.

The material properties such as the mass density and Young modulus are specified under the temperature during plant operating conditions. Because the coolant temperatures are precisely controlled during plant operations, both the bias and uncertainties of the material properties can be neglected.

For support conditions at the mating surface with friction such as the bottom of the neutron reflector, or close fitting like key supports, the realistic analysis conditions depend on the magnitude of the displacement or the acting loads at that point. The damping ratio to the critical damping is also depends on the vibration magnitude. Therefore, two kinds of models are made based on the same basic dimensions and the material properties. One is used for the flow-induced vibration with the small responses and the another is used for seismic / LOCA analysis with the larger responses. Bias error and uncertainties on the FIV analysis model are summarized in Table G-1 and those for the Seismic/ LOCA analysis model are shown in Table G-2.

Table G-1 Bias errors and uncertainties on the Vibration analysis model of Reactor Internals(FIV)

	Bias	Uncertainty	Validation
Structure dimensions			
Clearance of closed fitting parts			
Friction on mating surface	• •		
Material • Mass density • Young modulus			
Damping ratio			

Table G-2 Bias errors and uncertainties on the Vibration model of Reactor Internals (Seismic and LOCA)

	Bias	Uncertainty	Validation
Structure dimensions			
Clearance of closed fitting parts such as radial key			
Friction on mating surface			
Material • Mass density • Young modulus			
Damping ratio			

Appendix-H Uncertainty of the RCP Related Forcing Function

(Related to RAI#498-3782 Question 03.09.02-68)

An acoustic analysis code, SYSNOISE, was used in the assessment of the US-APWR reactor internals. MHI performed the verification of SYSNOISE by benchmark analysis of a simple cylindrical annulus system. The model dimensions were selected to represent the downcomer or the upper plenum of the actual reactor respectively. As stated in the question, the upper plenum of an actual reactor is more complicated because of the many components, such as the RCCA Guide tubes, inside. MHI assumed that these internal components may act as an acoustic resistance (damper of pressure) but do not have significant effects on the basic acoustic modes, because the diameters and their pitches (0.1-0.2m) are much smaller than the wave lengths of the RCP pulsation ([ ]m for [ ] Hz and [ ]m for [ ] Hz), although it is difficult to verify this estimation. The 1/5 SMT test data also provided no information on this issue because the RCP characteristics were not simulated in this test. Therefore MHI used the simple models without internal structures for the benchmark problem, where theoretical values of acoustic resonance modes can be calculated.

To allow for the above small uncertainty, it is assured that the analysis results with the SYSNOISE code will have the sufficient conservatism by neglecting the acoustic damping effects due to the structural flexibility. MHI performed a sensitivity study using the ANSYS code and a scaled vessel model filled with water as shown in Figure H-1. Case1 is an analysis with a rigid wall like in the SYSNOISE model and case 2 with the actual flexible reactor vessel wall. With the flexible wall, the resonance peak is about one order of magnitude smaller than that with a rigid wall. This is the uncertainty in the analysis but the bias is on the conservative side.

From the above discussions, we assumed a factor of [ ] for the uncertainty in the RCP pulsation loads and with the same magnitude of bias error on the conservative side. In other words, the RCP pulsation loads may be 10 times larger than the actual value, but not smaller than that.

Figure H-1 Effect of vessel wall flexibility on the acoustic resonance

Appendix-I Cross Flow Forcing Functions for Upper Plenum Structure

Along the structures in the upper plenum (between the upper core plate and the upper core support plate), several segments are defined. For the each segments cross flow force is determined based on the local cross flow velocity.

Time histories of the RCCA GT forcing function for 4 elevations from the total 9 segments are shown in the next page as samples. Forcing function has a peak around the center of the out let nozzle corresponding to the cross flow velocity distribution.

Note: Both of the scale of force and time are for the US-APWR actual plant. The same time histories are applied for the J-APWR SMT benchmark analysis except the modification of scaling.

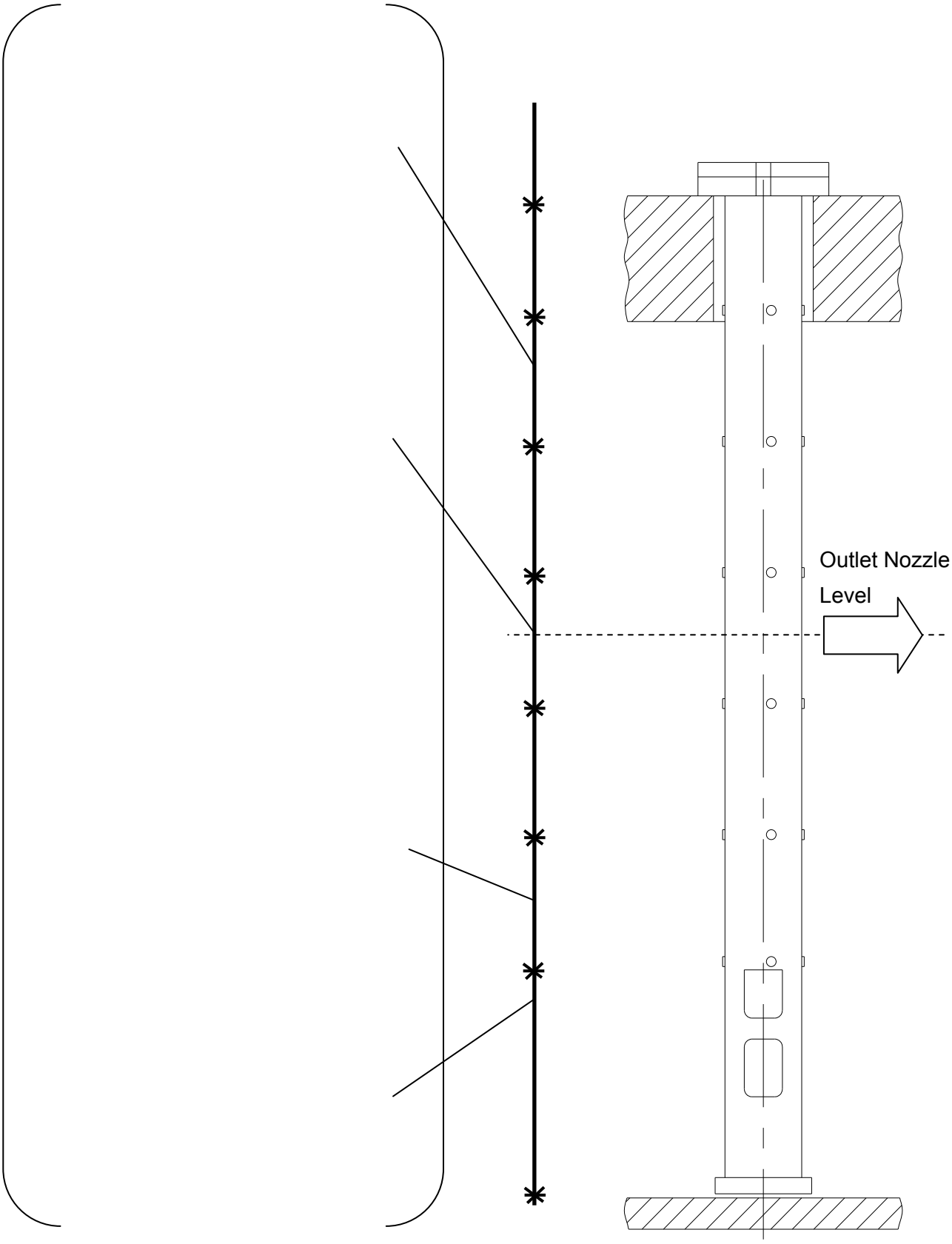

Figure I-1 Distribution of Cross Flow Forcing Functions along the RCCA GT

Appendix-J Previous Discussions about Minimum Margin of Safety in R1 Report

In this appendix, previous RAI responses are attached about discussions of the margin of safety on the high cycle fatigue evaluation results in MUAP-07027-R1. In these discussions, the minimum margin of safety [ ] on the upper plenum structures was judged to be acceptable because a sufficient conservative bias had been identified in the cross flow loads based on the assumption of the uniform cross flow velocity distributions.

After the above RAI response, in-adequate uses of dashpot elements were found out in the beam model for the US-APWR analysis in Revision 1. By the impact analysis, corrected damping model derive [ ]% larger response in typical. For the upper internals, the high cycle fatigue stress may be satisfied the design limit with the original cross flow loads based on the uniform flow velocity.
So MHI decided to precise the cross flow loads in the upper plenum by considering the practical cross flow velocity distribution.

In this Revision 2, both of the damping correction and the precise upper plenum cross flow loads. As the results the margin of safety of the upper plenum structures were improved from [ ] to [ ]. For the lower plenum structures without the cross flow load modification, the margins of safety were reduced by the effect of the corrected damping.

1. Response to RAI 498-3782 Question 03.09.02-75

RESPONSE TO REQUEST FOR ADDITIONAL INFORMATION

2/3/2010

US-APWR Design Certification

Mitsubishi Heavy Industries

Docket No. 52-021

RAI NO.: **NO. 498-3782 REVISION 0**

SRP SECTION: **03.09.02 - Dynamic Testing and Analysis of Systems Structures and Components**

APPLICATION SECTION: 3.9.2

DATE OF RAI ISSUE: **12/01/2009**

QUESTION NO. RAI 03.09.02-75:

In the response to RAI 3.9.2-33, several issues are still unclear. Report No. MUAP-07027-P (R1) indicates that substantial uncertainties exist in the dynamic analysis. For example, in the revised SYSNOISE analysis, the RCP pulsation amplitude is reduced by a factor of 5, and the response of the reactor internals to this RCP pulsation increases by a factor of 5 when the simulation time step is refined. Moreover, when comparing the SMT random response with the response obtained from the dynamic analysis, a ratio of 3 between the measured and predicted values is considered acceptable.

Despite these substantial uncertainties indicated above, the applicant considers a margin of safety of 30 percent acceptable for the high cycle fatigue analysis as indicated in Table 3.3.3-4 of the above mentioned report. The applicant is requested to explain why this margin of safety (30 percent) is considered conservative despite the existing much wider range of uncertainty.

Answer:

The uncertainty of the analysis is determined as the ratio to the best-estimated value without bias errors if they are identified.

Through the results of the high cycle fatigue analysis for the US-APWR reactor internals, minimum margins of safety [ ] were predicted for the components in the upper plenum, the RCC guide tube (GT), upper support column (USC) and top slotted column (TSC) as shown in Table 1. (Table 3.3.3-4 of MUAP-07027-P(R1). Both cross flow and RCP pulsation were taken into account in these results. MHI has verified that these results are acceptable based on the following considerations.

1. The alternating stresses due to the RCP pulsation have large uncertainty ([ ]) but the absolute value of these ([ ] ksi) are lower than those due to the cross flow ([ ]ksi) by one order of magnitude.

2. The RCP pulsation loads include a conservative bias by neglecting the acoustic damping due to structural flexibility as discussed in the response to RAI 03.09.02-68. Because this effect is also the main part of the uncertainty in the acoustic resonance analysis, the magnitude of bias error is approximately the same as the uncertainty (factor of [ ]). Therefore, the analysis results due to RCP pulsation may be 10 times larger than the actual values, but not smaller.

3. The cross flow loads on the upper and lower plenum structures are determined with peak cross flow velocity along the entire length of structures. The bias due to neglecting the cross flow distribution is estimated to be around a factor of 2, which is comparable to the assumed uncertainty in the flow-induced loads.

4. From the above discussions, the minimum margin of safety of [ ] for the upper plenum structures due to cross flow loads includes a conservative bias of around 2 due to non-uniform cross flow distribution. Because this bias is comparable to the assumed uncertainty in the flow induced loads (factor of 2), the margin of safety [ ] was considered acceptable.

Table J-1 High Cycle Fatigue Evaluation Based on Analysis Responses (Table 3.3.3-4 of MUAP-07027-P(R1))

Components	Locations or parts	Alternating Stress (ksi)			Limit	Margin of Safety [1)]
		Flow	RCP	Total		
Core Barrel	Flange				13.6 ksi	
Neutron Reflector	Block Alignment Pin					
Diffuser Plate Assembly	Support Column Upper Assembly Lower Assembly					
UCS	Flange Skirt					
RCCA GT	Top of Lower GT					
USC						
TSC						

Note
1) Margin of safety = (Allowable Stress Limit) / (Alternating Stress) - 1

Impact on DCD
There is no impact on the DCD.

Impact on COLA

There is no impact on the COLA.

Impact on PRA

There is no impact on the PRA.

2. Response to RAI 614-4853 Question 03.09.02-90

RESPONSE TO REQUEST FOR ADDITIONAL INFORMATION

09/27/2010

US-APWR Design Certification

Mitsubishi Heavy Industries

Docket No. 52-021

RAI NO.: NO. 614-4853

SRP Section: 03.09.02 – Dynamic Testing and Analysis of Systems Structures and Components

APPLICATION SECTION: 3.9.2

DATE OF RAI ISSUE: 08/13/2010

QUESTION NO.: RAI 03.09.02-90

In the response to the US-APWR DCD RAI 498-3782, Question 03.09.02-75, the applicant explained in detail why, despite the existing high degree of uncertainty, a margin of safety of 30 percent is considered conservative for the high cycle fatigue analysis as indicated in Table 3.3.3-4 of the revised vibration assessment report MUAP07027-P-R1. The staff reviewed the applicant's response and found it acceptable because the margin of safety already covers conservatively estimated bias errors and uncertainties associated with determining the loading functions due to cross flow and RCP pulsation. However, this information should be included in MHI report MUAP07027-P-R1.

Therefore, the applicant is requested to indicate clearly in the Technical Report MUAP07027-P(R1) that the safety margin of 0.3 covers all the uncertainties and bias errors which are associated with determining the loading functions.

Reference: MHI's Response to US-APWR DCD RAI No. 498-3782; MHI Ref: UAP-HF10031; dated February 3, 2010; ML100470583.

answer:

As requested, the technical report MUAP-07027-P (R1) will be modified to include the information provided in the response to RAI 03.09.02-75, as shown in the attachment.

Impact on DCD

1. DCD document
The revision to the technical report MUAP-07027-P will be reflected in Reference 3.9-22 in DCD Subsection 3.9.10 References.

2. Technical Report MUAP-07027-P

The first paragraph of 'b. Evaluation Results' in 'Subsection 3.3.3.2 (2) High Cycle Fatigue', on Page 89, will be replaced with the following.

Through the results of the high cycle fatigue analysis for the US-APWR reactor internals, minimum margins of safety were predicted for the components in the upper plenum, the RCC guide tube (GT), the upper support column (USC), and the top slotted column (TSC). Both cross flow and RCP pulsation were taken into account in these results. MHI has verified that these results are acceptable based on the following considerations:

1. The uncertainty of the analysis is determined by the ratio to the best estimated value without bias errors if identified.
2. The alternating stresses due to the RCP pulsation have large uncertainty, but the absolute values of these are lower than those due to the cross flow by one order of magnitude.
3. The RCP pulsation loads include a conservative bias by neglecting the acoustic damping due to structural flexibility. Because this effect is also the main part of the uncertainty in the acoustic resonance analysis, the magnitude of bias error is approximately the same as the uncertainty (by a factor of 5). Therefore, the analysis results due to RCP pulsation may be 10 times larger than the actual values, but not smaller.
4. The cross flow loads on the upper and lower plenum structures are determined with peak cross flow velocity along the entire length of structures. The bias due to neglecting the cross flow distribution is approximately a factor of 2, which is comparable to the assumed uncertainty in the flow-induced loads.

From the above discussions, the minimum margin of safety 0.3 for the upper plenum structures due to cross flow loads includes a conservative bias of approximately 2 due to non-uniform cross flow distribution. Because this bias is comparable to the assumed uncertainty in the flow-induced loads (a factor of 2), the margin of safety 0.3 is considered acceptable.

Impact on COLA

There is no impact on the COLA.

Impact on PRA

There is no impact on the PRA.

Appendix-K Impact of Outlet Nozzle Leakage Flow on Core Barrel Vibration

(Related to RAI #646-5065 Question 03.09.02-92)

In this appendix, MHI will discuss 3 points of view on the potential core barrel vibration due to the outlet nozzle bypass flow. The first one is the forced vibration due to the flow turbulence, in which we have estimated the turbulence force due to the outlet nozzle in comparison with that due to the inlet nozzle. The 2nd is the potential of instability vibration due to the leakage flow. At the last, the related parameters are discussed by comparison with existing PWR plants.

1. Forced vibration due to the flow turbulence

This section addresses the potential core barrel vibration due to the outlet nozzle bypass flow by making a comparison to the potential vibration due to the reactor vessel inlet nozzle flow.

The core barrel flange stress due to the flow vibration depends both on the magnitude of the flow-induced force on the core barrel and the distance from the forced point to the core barrel flange. The reactor vessel inlet nozzle and outlet nozzle are located at the same elevation, in which the distances from the inlet and the outlet nozzle centers to the core barrel flange are the same. Therefore, insights into the effects on the core barrel flange stress by the outlet nozzle bypass flow can be based on a comparison of the vibration forces by the inlet flow to the forces associated with the outlet nozzle bypass flow.

Table K-1 summarizes the key parameters of the comparison, such as the flow rate, flow velocity and forced area on the core barrel. It is noted that, in the US-APWR reactor design, the outlet nozzle bypass flow velocity at the mating surface gap is approximately the same as the inlet nozzle flow velocity. Because the turbulent pressure fluctuation is generally proportional to the square of flow velocity, the pressure fluctuation amplitude of the outlet nozzle bypass flow has the same magnitude as the inlet nozzle flow.

The flow entering through the inlet nozzle is spread into the reactor vessel downcomer after impingement on the core barrel wall. Therefore, the vibration force of the inlet nozzle flow is applied to the upper portion of the core barrel. On the other hand, the forced area for the outlet nozzle bypass flow is applied only to the mating surface of the core barrel outlet nozzle. The forced area for an inlet nozzle flow is much larger and can be approximated by a [ ] sector of the upper half of the core barrel excluding the outlet nozzle. The [ ] sector is simply derived from the four equally-positioned inlets. As a result, as shown in Table K-1, the forced area for the outlet nozzle bypass flow is only [ ]% of that for the inlet nozzle flow.

The flow-induced force is proportional to the multiple of the forced area and the amplitude of pressure fluctuation. As shown in Table K-1, the effective vibration force due the outlet nozzle bypass flow is evaluated as [ ]% of that by the inlet flow. The combined effects of inlet flow and outlet nozzle bypass is derived using Square Root Sum of Squares (SRSS) as [ ]. Therefore, the relative effect of the outlet nozzle bypass flow is evaluated as [ ] %.

2. Potential instability vibration due to the leakage flow

Potential for instability is discussed with a simple theoretical model which describes the interaction between the oscillation of the nozzle gap flow and the mechanical vibration of the core barrel with following assumptions.

(1) The gap width on the outlet nozzle is oscillating with the core barrel vibration.

(2) Total pressure difference across the outlet nozzle gap is not depend on the nozzle gap width because the total pressure loss of the vessel is not affected with nozzle bypass flow.

(3) The flow velocity in the outlet nozzle gap is a function of the gap width because the friction loss coefficient is depend on the gap width. As the result, the higher velocity is expected with the larger gap width.

(4) The static pressure inside the gap is depend on the gap flow velocity based on the Bernoullii's theory.

(5) The static pressure force change on the nozzle mating surface effects on the mechanical vibration of the core barrel.

Above feedback loop model derives a principal conclusion about the possibility of self–excited vibration as follows.

a. In the timing of gap increasing, the gap flow velocity also increases with the reduction of hydraulic friction loss coefficient of the gap flow path. As the result, the static pressure in the gap is reduced as explained by Bernoullii's theory. This negative pressure force acts to damp the gap increase motion.

b. In the timing of gap decreasing, the pressure force increases in the gap and acts to damp the gap width decreasing motion in the same manner.

It is noted that the pressure force change in the outlet nozzle gap due to the core barrel vibration acts to reduce the core barrel motion both in the gap increasing and decreasing. As the conclusion, the outlet nozzle leakage flow may act as a damping mechanism on the core barrel vibration rather than an additional vibration source.

Thus, there is no need to consider the outlet nozzle leakage flow effect on the core barrel vibration analysis and stress evaluation.

3. Comparison with the existing plants

In addition to the discussion above, quantitative insights are also available by comparison of the key parameters with the existing plants.

The key non-dimensional parameter for the flow-induced vibration is the “reduced velocity” defined as U/(fn D), where “U” is the flow velocity, “fn” is the natural frequency of structures and “D” is the representative dimension. In general, a larger reduced velocity provides greater potential for the flow instability. In this comparison, the outlet nozzle gap flow velocity was represented by the pressure drop of the reactor vessel. As shown in Table K-2, the pressure drop of the US-APWR reactor vessel is equivalent to the 12-ft core 4-loop PWR or approximately [ ] % of the 14-ft core 4-loop PWR design.

As for the vibration characteristics, the oval (n=2) mode natural frequency of the core barrel was considered as the most likely mode to interact with the outlet nozzle gap. An evaluation was conducted with the core barrel diameter, length and wall thickness. The result is that the shell mode natural frequency of the US-APWR core barrel is approximately [ ]% higher than that of the current 12-ft core 4-loop PWR design, as shown in Table K-2.

Based on the comparison of both the vessel pressure drop and the core barrel natural frequency, the potential vibration instability due to the outlet nozzle flow for the US-APWR is not greater than the existing PWR plants.

4. Conclusion

Based on the aforementioned discussions, MHI concludes that there is no concern for the core barrel vibration due to the outlet nozzle gap flow for the US-APWR.

Table K-1 Comparison of Vibration Forces Associated with Inlet Nozzle and Outlet Nozzle Bypass Flows

	Main Flow from Inlet Nozzle	Outlet Nozzle Bypass
Flow rate: Q(ratio)	1.0	
Flow Velocity: V (ratio)	1.0	
Pressure fluctuation: Prms $\propto \rho V^2$(ratio)	1.0	
Forced Area per one nozzle: A (ratio)	1.0 (upper core barrel 1/4 sector excluding the outlet nozzle)	
Effective Vibration Force $\propto$ Prms A (ratio)	1.0	
Effect on Core Barrel Vibration (ratio)	1.0	

Notes ρ: fluid mass density (same for both flows)
Prms : root mean square of the pressure fluctuation amplitude

Table K-2 Comparison between US-APWR and Existing PWR Designs

	US-APWR	Typical 12-ft core 4-loop PWR	Typical 14-ft core 4-loop PWR
Pressure Drops (psi)(1)			
Core	32.1±3.2	25.8±2.6	39.78±4.0
Reactor Vessel	48.2±4.8	48.5±4.9	62.68±8.9
Core Barrel Vibration Characteristics			
Outside diameter (in)			-
Wall thickness (in)			-
Axial length of shell portion (in)			-
Oval mode natural frequency (n=2) (relative ratio of the theoretical values)	1.1	1.0	-

(1) From Table 4.4-1 of US-APWR DCD